

Title: Durable immunity to SARS-CoV-2 in both lower and upper airways achieved with a gorilla adenovirus (GRAd) S-2P vaccine in non-human primates

Authors:

Juan I. Moliva^{1,8}, Shayne F. Andrew¹, Barbara J. Flynn¹, Danielle A. Wagner¹, Kathryn E. Foulds¹, Matthew Gagne¹, Dillon R. Flebbe¹, Evan Lamb¹, Samantha Provost¹, Josue Marquez¹, Anna Mychalowych¹, Cynthia G. Lorag¹, Christopher Cole Honeycutt¹, Matthew R. Burnett¹, Lauren McCormick¹, Amy R. Henry¹, Sucheta Godbole¹, Meredith E. Davis-Gardner², Mahnaz Minai³, Kevin W. Bock³, Bianca M. Nagata³, John-Paul M. Todd¹, Elizabeth McCarthy¹, Alan Dodson⁴, Katelyn Kouneski⁴, Anthony Cook⁴, Laurent Pessaint⁴, Alex Van Ry⁴, Daniel Valentin⁴, Steve Young¹, Yoav Littman¹, Adrianus C. M. Boon⁵, Mehul S. Suthar², Mark G. Lewis⁴, Hanne Andersen⁴, Derron A. Alves³, Ruth Woodward¹, Adriano Leuzzi⁶, Alessandra Vitelli⁶, Stefano Colloca⁶, Antonella Folgori⁶, Angelo Raggioli⁶, Stefania Capone⁶, Martha C. Nason⁷, Daniel C. Douek¹, Mario Roederer¹, Robert A. Seder^{1,9}, Nancy J. Sullivan^{8,9,10}

Affiliations:

¹ Vaccine Research Center, National Institute of Allergy and Infectious Diseases, National Institutes of Health, Bethesda, Maryland, 20892, United States of America

² Department of Pediatrics, Emory Vaccine Center, Yerkes National Primate Research Center, Emory University School of Medicine, Atlanta, Georgia, 30322, United States of America

³ Infectious Disease Pathogenesis Section, Comparative Medicine Branch, National Institute of Allergy and Infectious Diseases, National Institutes of Health, Rockville, Maryland, 20892, United States of America

⁴ Bioqual, Inc., Rockville, Maryland, 20850, United States of America

⁵ Department of Medicine, Washington University School of Medicine, St. Louis, Missouri, 63110, United States of America

⁶ ReiThera Srl, 00128 Rome, Republic of Italy

⁷ Biostatistics Research Branch, Division of Clinical Research, National Institute of Allergy and Infectious Diseases, National Institutes of Health, Bethesda, Maryland, 20892, United States of America

⁸ National Emerging Infectious Diseases Laboratories, Boston University, Boston, Massachusetts, United States of America

⁹ Correspondence: rseder@mail.nih.gov and njsull@bu.edu

¹⁰ Lead contact

1 **Summary**

2 SARS-CoV-2 continues to pose a global threat, and current vaccines, while effective against
3 severe illness, fall short in preventing transmission. To address this challenge, there's a need for
4 vaccines that induce mucosal immunity and can rapidly control the virus. In this study, we
5 demonstrate that a single immunization with a novel gorilla adenovirus-based vaccine (GRAd)
6 carrying the pre-fusion stabilized Spike protein (S-2P) in non-human primates provided
7 protective immunity for over one year against the BA.5 variant of SARS-CoV-2. A prime-boost
8 regimen using GRAd followed by adjuvanted S-2P (GRAd+S-2P) accelerated viral clearance in
9 both the lower and upper airways. GRAd delivered via aerosol (GRAd(AE)+S-2P) modestly
10 improved protection compared to its matched intramuscular regimen, but showed dramatically
11 superior boosting by mRNA and, importantly, total virus clearance in the upper airway by day 4
12 post infection. GrAd vaccination regimens elicited robust and durable systemic and mucosal
13 antibody responses to multiple SARS-CoV-2 variants, but only GRAd(AE)+S-2P generated
14 long-lasting T cell responses in the lung. This research underscores the flexibility of the GRAd
15 vaccine platform to provide durable immunity against SARS-CoV-2 in both the lower and upper
16 airways.

17 18 **Keywords**

19 SARS-CoV-2; viral-vector; GRAd; Omicron; BA.5; COVID-19; mRNA vaccine; antibody; B
20 cells; T cells; immune memory

21 22 **Introduction**

23 Severe acute respiratory syndrome coronavirus-2 (SARS-CoV-2) is an infectious respiratory
24 human coronavirus and the causative agent of COVID-19. At the time of writing, COVID-19 has
25 been responsible for more than 676 million cases and 6.8 million deaths worldwide.¹ In response
26 to its rapid spread, vaccine development was substantially accelerated, resulting in the evaluation
27 and approval of numerous novel vaccine technologies, namely the mRNA encapsulated (*e.g.*,
28 mRNA-1273 and BNT162b2) and viral-vectored (*e.g.*, ChAdOx nCoV-19/AZD1222 and
29 Ad26.COV2.S) platforms.² Initially, and for much of the pandemic, the vaccines approved for
30 human use were based on the ancestral Wuhan-Hu-1/USA-WA1/2020 (WA-1) isolate and
31 proved remarkably effective against severe disease.³ However, the high transmissibility of
32 SARS-CoV-2 facilitated the rise of mutations, deletions and insertions in the Spike (S) protein,
33 the S receptor-binding domain (RBD) and the S N-terminal domain (NTD) leading to the
34 emergence of numerous subvariants with progressive resistance to vaccine-elicited immunity,
35 diminishing the durable efficacy of the vaccines and increasing transmissibility.⁴⁻⁷

36

37 One significant limitation of most SARS-CoV-2 vaccines, including all mRNA-based vaccines
38 approved for human use to date, is that they do not directly stimulate immune responses in the
39 mucosal surfaces of the upper and lower airway, the major site of SARS-CoV-2 entry,
40 replication, pathology, and shedding.⁸ Despite this, intramuscular mRNA-based vaccines induce
41 robust humoral and cellular immunity and are effective against severe disease caused by SARS-
42 CoV-2.⁹ However, the ability of intramuscularly delivered mRNA-based vaccines to prevent
43 transmission is limited,^{10,11} and efficacy against severe disease wanes,¹² possibly due to the
44 failure of properly priming the respiratory mucosa. Since the respiratory tract serves as the first
45 line of defense against SARS-CoV-2, robust and durable immunity in the mucosa could provide

46 systemic durable immunity and prevent initial infection and subsequent transmission as tissue-
47 resident memory T and B cells are likely among the early responders.¹³ Indeed, pre-clinical
48 studies have demonstrated that mucosal immunity can protect against SARS-CoV-2.¹⁴⁻¹⁶
49 Therefore, it is important to evaluate additional vaccine approaches and candidates that can
50 prime or boost mucosal immunity.
51
52 GRAd32 is a novel replication-defective simian adenoviral vector that was isolated from a
53 captive gorilla.¹⁷ Simian adenoviruses do not cause disease in humans, and consequently, have
54 low or no seroprevalence in the human population making them suitable vaccine candidates.¹⁸
55 Additionally, simian-based adenoviral vaccine vectors have been proven safe in humans,
56 generate potent and durable immune responses, and have been shown to stimulate humoral and
57 cellular responses across a plethora of antigens (*e.g.*, Ebola, malaria, hepatitis C, human
58 immunodeficiency virus, and respiratory syncytial virus, SARS-CoV-2).¹⁹⁻²² When combined
59 with other vaccine platforms (*e.g.*, mRNA or subunit protein), called heterologous immunization
60 strategies, the inclusion of a viral-vectored vaccine can confer superior durability and efficacy
61 compared to homologous vaccination.²³⁻²⁶ In this study, we used the GRAd32 vector backbone
62 encoding the WA-1 SARS-CoV-2 pre-fusion stabilized S (henceforth abbreviated GRAd in this
63 manuscript) to assess the durability of immune responses in a combination of prime and prime
64 and boost homologous and heterologous immunization strategies to evaluate the protective
65 efficacy to SARS-CoV-2.
66
67 Using non-human primates (NHP), a model that has faithfully predicted protective efficacy of
68 SARS-CoV-2 vaccines in humans,^{27,28} herein we demonstrate efficacy of the GRAd vaccine

69 platform encoding WA-1 against mismatch challenge with BA.5. Groups of eight NHP were
70 primed with intramuscular (IM) GRAd, primed and boosted with a combination of IM GRAd
71 and adjuvanted S-2P (GRAd+S-2P), primed and boosted with IM adjuvanted S-2P (S-2P+S-2P),
72 or primed with aerosolized (AE) GRAd and boosted with IM adjuvanted S-2P (GRAd(AE)+S-
73 2P). The NHP were followed for 48 weeks, at which point four of the eight NHP were boosted
74 with mRNA BNT162b2 (S-2P encoded in mRNA). At week 64, all NHP were challenged with
75 SARS-CoV-2 BA.5. For the duration of the 64 weeks, we collected blood, bronchoalveolar
76 lavage (BAL) and nasal washes to analyze systemic and mucosal antibody kinetics and B and T
77 cell responses. Following BA.5 challenge, viral replication in the lung and nose was quantified to
78 assess the efficacy of these vaccine regimens. We found that GRAd in any combination
79 conferred year-long protection in the lower airway, but heterologous GRAd vaccine regimens
80 were superior. Priming with AE GRAd provided an advantage to IM GRAd in control of BA.5 in
81 the upper airway.

82

83 **Results**

84 GRAd confers durable protection against BA.5 in the lower airway

85 To quantify the durable protective effect of GRAd or adjuvanted protein subunit-based
86 immunogens against SARS-CoV-2, Indian-origin rhesus NHP were stratified into groups of eight
87 and immunized according to the experimental schema (**Fig. S1A**). At week 48, all groups (except
88 control) were further subdivided, and four of the eight NHP were boosted with BNT162b2
89 (henceforth abbreviated mRNA in this manuscript). At week 64, each NHP was challenged with
90 a dose of 8×10^5 PFU of sequence-confirmed Omicron sub-lineage BA.5 (**Fig. S2A-D**). BAL
91 was collected on days 2, 4, and 8 (**Fig. S1B**). SARS-CoV-2 subgenomic RNA (sgRNA) in BAL

92 was quantified to assess the extent of viral burden in the lower airway. Specifically, we relied
93 primarily on the sgRNA encoding for the N gene (sgRNA_N) as it is the most abundant
94 transcript produced due to the viral discontinuous transcription process, and thus provides the
95 most sensitive way to detect SARS-CoV-2.²⁹

96
97 Two days following challenge, control NHP had a geometric mean copy number of 168261
98 sgRNA_N per mL (**Fig. 1A**), whereas GRAd, S-2P+S-2P, GRAd+S-2P and GRAd(AE)+S-2P
99 had 3091, 4690, 138 and 81, respectively, representing statistically significant decreases except
100 in the S-2P+S2P group (**Fig. 1B**). By day 4, the copy number in the control NHP was 102535,
101 and significantly lower in all immunized groups except for S-2P+S-2P (GRAd - 144; S-2P+S-2P
102 - 1111; GRAd+S-2P - 135; GRAd(AE)+S-2P - 77). By day 8, copy number in the control NHP
103 was 2244, below 100 in the GRAd and S-2P+S-2P groups, and below 50 (limit of detection) in
104 the GRAd+S-2P and GRAd(AE)+S-2P groups. Altogether, the data suggest year-long and rapid
105 protection can be achieved in the lower airway with a prime and boost strategy that includes one
106 dose of GRAd.

107
108 We next asked whether the mRNA boost amplified the observed protection. The mRNA boost
109 had its greatest impact on the GRAd and S-2P+S-2P groups, reducing the day 2 geometric mean
110 sgRNA copy number from 3091 to 57 and 4690 to 264, respectively, while the sgRNA_N copy
111 number remained approximately equal in the GRAd+S-2P and GRAd(AE)+S-2P groups at day
112 2. By day 4, all mRNA-boosted NHP had a nearly undetectable virus in the lower airway, and no
113 sgRNA_N was detected in any group at day 8 (**Fig. 1C**). This data suggests a limited benefit of
114 additional mRNA boost if the priming immunization is adequate.

115

116 In addition to measuring the sgRNA_N, we quantified the amount of culturable virus in the BAL
117 using a tissue culture infectious dose assay (TCID₅₀). While BA.5 was recovered from 7/8, 6/8,
118 and 2/8 control NHP at days 2, 4 and 8, respectively (**Fig. S3A**), hardly any virus was recovered
119 from the immunized groups, irrespective of whether they received the mRNA boost (**Fig. S3B**,
120 **C**). Of note, the only group with no recoverable virus at any timepoint in the BAL were the NHP
121 that received GRAd(AE)+S-2P as the primary immunization series.

122

123 Finally, to assess pathology caused by SARS-CoV-2 BA.5 to the lung, two NHP from each
124 group were euthanized on days 8 or 9 following challenge, and the extent of viral antigen and
125 inflammation were quantified. SARS-CoV-2 antigen was detected in variable amounts in the
126 lung of 3/4 control NHP and only associated with the alveolar septa lining in areas of interstitial
127 inflammation and thickening. No antigen was detected in the lung of any of the immunized NHP
128 on days 8 or 9, nor in any of the NHP on days 14 or 15 (**Fig. S4A**). Histopathologic lesions were
129 observed in one or more lung lobes in one or more NHP from each group on days 8 or 9 and 14
130 or 15. Generally, the inflammatory lesion severity in immunized NHP ranged from minimal to
131 moderate, although more severe changes were occasionally observed, while that of control NHP
132 ranged from moderate to severe. Mild to moderate inflammation was characterized by few foci
133 of perivascular inflammation or cuffing without other changes. Increases in severity were
134 marked as foci of perivascular inflammation accompanied by mild alveolar interstitial thickening
135 by mononuclear cells, protein-rich edema accumulation in the alveolar lumina, minimal type II
136 pneumocyte hyperplasia, and mild histiocytic and neutrophilic inflammation to the alveolar
137 lumina. Further increases in severity had a more widespread distribution of the listed lesions.

138 Moderate to marked neutrophilic peribronchial infiltrates were also observed in the highly
139 affected lobes (**Fig. S4B**).

140

141 Aerosol delivery of GRAd rapidly protects against BA.5 in the upper airway

142 Nasal swabs (NS) were collected from each NHP on days 2, 4 and 8 (**Fig. S1B**) to assess viral
143 burden in the upper airway, the primary source of transmission for SARS-CoV-2.³⁰ Two days
144 following challenge, control NHP had geometric mean copy number of 41186 sgRNA_N per
145 swab (**Fig. 2A**), with 1/8 NHP having no detectable virus, whereas GRAd, S-2P+S-2P,
146 GRAd+S-2P and GRAd(AE)+S-2P had 66251, 21952, 7541 and 1151, respectively (**Fig. 2B**).
147 Though not significant, GRAd(AE)+S-2P NHP had a median sgRNA_N copy number 35-fold
148 lower than control NHP on day 2. By day 4, the copy number in the control NHP was 22960 and
149 had decreased substantially, albeit non-significantly, in the GRAd+S2P and GRAd(AE)+S-2P
150 immunized groups (GRAd - 91560; S-2P+S-2P - 32276; GRAd+S-2P - 2738; GRAd(AE)+S-2P
151 - 335). Furthermore, on day 4, 2/4 GRAd+S-2P NHP and 3/4 GRAd(AE)+S-2P had undetectable
152 sgRNA_N in the nose. By day 8, copy number in the control NHP was 12820 but was
153 significantly lower in the GRAd+S-2P and GRAd(AE)+S-2P groups (GRAd - 2491; S-2P+S-2P
154 - 1918; GRAd+S-2P - 122; GRAd(AE)+S-2P - 71). Together, the data suggest that a prime and
155 boost immunization strategy with GRAd can rapidly reduce the viral load in the nose (**Fig. 2B**).

156

157 Next, we asked whether an mRNA boost could improve the observed protection in the upper
158 airway. Boosting with mRNA significantly decreased the sgRNA_N copy number on day 2 in
159 the GRAd and GRAd(AE)+S-2P groups, reducing the geometric mean copy number from 66251
160 to 324 and 1151 to 125, respectively. The mRNA boost had no significant impact on the

161 sgRNA_N copy number in the S-2P+S-2P and GRAd+S-2P groups on day 2. By day 4, the
162 GRAd, S-2P+S-2P and the GRAd+S-2P group had detectable virus in the nose, while 4/4 NHP
163 in the GRAd(AE)+S-2P group had cleared the virus. By day 8, BA.5 virus remained detectable
164 in all groups except in the GRAd(AE)+S-2P NHP (**Fig. 2C**). The TCID₅₀ assay confirmed these
165 findings (**Fig. S3D-F**). Together, the data suggest that rapid clearance of SARS-CoV-2 from the
166 nasal passage can be achieved with a vaccine regimen that includes AE delivery of GRAd.

167

168 GRAd immunization strategies generate durable antibody responses to SARS-CoV-2 variants
169 that can be boosted with mRNA

170 Antibody responses were assessed over the period of 63 weeks. Sera was collected at week 8
171 (approx. peak), week 46 (memory; before mRNA boost), week 50 (peak after the mRNA boost),
172 and week 63 (before challenge) to measure immunoglobulin G (IgG) binding to WA-1 (ancestral
173 SARS-CoV-2 and the vaccine insert), BA.1 (ancestral Omicron) and BA.5 (**Fig. 3A-C, Fig.**
174 **S5A**). At week 8, the geometric mean titer (GMT) to WA-1 in arbitrary units/mL (AU/mL) was
175 the highest in the S-2P+S-2P group, followed by GRAd(AE)+S-2P, GRAd+S-2P and GRAd at
176 432740, 267183, 250180 and 79109, respectively (**Fig. 3B**). Antibody titers waned by week 46
177 in all groups, decreasing by 3.3-, 6.7-, 5.3- and 25.8-fold in the GRAd, GRAd+S-2P,
178 GRAd(AE)+S-2P and S-2P+S-2P groups, respectively. The WA-1 GMT remained relatively
179 unchanged from week 46 through week 63 in the NHP not boosted with mRNA (closed circles),
180 while increasing significantly in NHP that did receive the mRNA boost (open circles). By week
181 63, the WA-1 GMT remained significantly higher in the GRAd, S-2P+S-2P and GRAd(AE)+S-
182 2P NHP that were boosted with mRNA (GRAd: 21170 v. 107163; S-2P+S-2P: 17034 v. 155299;
183 GRAd+S-2P: 64166 v. 48979; GRAd(AE)+S-2P: 50888 v. 131716). Antibody binding kinetics

184 and potency to BA.5 mirrored those of WA-1, albeit on average approximately 4-fold lower
185 (**Fig. 3C**).

186

187 Neutralizing antibody (nAb) titers to D614G, BA.1, and BA.5 were quantified using a lentiviral
188 pseudovirus neutralization assay (**Fig. 3D-E, Fig. S5C**). At week 8, nAb titers to D614G were
189 highest in the S-2P+S-2P NHP with a GMT of 3150 reciprocal 50% inhibitory dilution (ID₅₀),
190 followed by GRAd(AE)+S-2P, GRAd+S-2P and GRAd at 3097, 2162 and 502, respectively
191 (**Fig. 3D**). Week 8 nAb titers to BA.1 and BA.5 decreased significantly (**Fig. 3E, Fig. S5C**),
192 dropping to 20 (limit of detection), 153, 94 and 197 in the GRAd, S-2P+S-2P, GRAd+S-2P and
193 GRAd(AE)+S-2P against BA.5. The nAb titers at week 46 to D614G, BA.1 and BA.5 decreased
194 from the week 8 peak but remained highest in the GRAd(AE)+S-2P group. Similar to the
195 binding titers, nAb titers remained relatively stable from week 46 through 63 in NHP not boosted
196 with mRNA, while the mRNA boost significantly increased them across all groups to levels
197 above those of week 8 across all variants tested. By week 63, the D614G nAb GMT in the non-
198 mRNA boosted NHP were 360, 226, 1172 and 2040 for GRAd, S-2P+S-2P, GRAd+S-2P, and
199 GRAd(AE)+S-2P, respectively, significantly lower than in the mRNA boosted cohorts (4973,
200 4016, 4458 and 3662, respectively). The mRNA boost had the greatest impact on the GRAd and
201 S-2P+S2P group nAb titers to BA.5 at week 63 (GRAd: 44 v. 173; S-2P+S-2P: 40 v. 345;
202 GRAd+S-2P: 97 v. 166; GRAd(AE)+S-2P: 249 v. 301). Together, the data suggest that AE
203 delivery of GRAd may stimulate superior durable humoral immunity to SARS-CoV-2.

204

205 We wondered whether the delivery of the first GRAd immunization had an impact on the initial
206 humoral response as it has been suggested that viral vectors delivered mucosally could be less

207 immunogenic compared to parenteral routes.³¹ The nAb titers to D614G at week 2 and week 4
208 were approximately equal after the first dose of GRAd in all the groups that received one dose of
209 GRAd, irrespective of whether it was given IM or AE (**Fig. S6**). Only in the case of a single S-2P
210 immunization did we observe significantly lower titers. Notably, nAb titers to BA.5 at week 2
211 and week 4 were below the limit of detection, highlighting the benefit of a boost and the advantage
212 of heterologous boosting.

213

214 Antibody binding and nAb titers were also quantified immediately following BA.5 challenge, at
215 days 2, 4, 8 and 14 to assess the extent of secondary responses in immunized NHP and primary
216 responses to BA.5 in control NHP (**Fig S5B,D, Fig. S7A-D**). In general, the primary binding and
217 nAb response to BA.5 was more robust than that to WA-1/D614G or BA.1 and was detectable in
218 some of the control NHP as early as day 2. All control NHP had a measurable binding and nAb
219 titer to BA.5 by day 14. In contrast, secondary responses following challenge in the immunized
220 animals were primarily observed in non-mRNA boosted NHP and were not evident until after
221 day 8 following challenge.

222

223 GRAd immunization strategies generate durable IgG and IgA responses to BA.5 in the lower and
224 upper airway mucosa.

225 Antibody responses to SARS-CoV-2 infection are critical for mediating protection.²⁸ BAL fluid
226 was collected at weeks 6, 46, 50 and 61, while nasal washes (NW) were collected at weeks 46,
227 50, and 61 to quantify antigen-specific IgG and IgA responses in the lung and nose to WA-1,
228 BA.1 and BA.5 (**Fig. 4, Fig. S8-10**). At week 6, the BA.5 IgG GMT in the BAL was the highest
229 in the S-2P+S-2P group at 426 AU/mL, followed by GRAd+S-2P, GRAd(AE)+S-2P and GRAd

230 at 398, 361 and 76, respectively (**Fig. 4B**). The IgG titers waned by week 46, but remained
231 highest in the GRAd(AE)+S-2P group. The mRNA boost significantly increased the IgG titers in
232 all groups (week 50, closed *v.* open circles), but the responses mostly waned by week 61.
233 However, IgG titer in the BAL remained elevated in the mRNA-boosted NHP (GRAd: 30 *v.* 105;
234 S-2P+S-2P: 33 *v.* 227; GRAd+S-2P: 44 *v.* 130 and GRAd(AE)+S-2P: 47 *v.* 151). In contrast,
235 antigen-specific IgA responses in BAL to BA.5 were almost exclusively detected in the
236 GRAd(AE)+S-2P NHP, with a BA.5 IgA GMT of 150 at week 8 in this group, while below 30 in
237 all the other groups (**Fig. 4C**). Responses waned by week 46, but the mRNA boost increased the
238 IgA GMT in the GRAd(AE)+S-2P group from 69 to 117 at week 50, albeit non-significantly.
239 The mRNA boost did not increase the BAL IgA GMT in any of the other groups. By week 61,
240 antigen-specific IgA had mostly waned in all groups except in the GRAd(AE)+S-2P NHP.
241 Together, this data suggest that AE delivery of GRAd stimulates antigen-specific IgA responses
242 in the lung.

243
244 In the NW, antigen-specific IgG titers to BA.5 at week 46 were approximately equal across all
245 groups (**Fig. 4D**). The mRNA boost increased the IgG titer significantly in most groups (week 50
246 GMT: GRAd: 15 *v.* 221; S-2P+S-2P: 7 *v.* 399; GRAd+S-2P: 43 *v.* 302 and GRAd(AE)+S-2P: 22
247 *v.* 349). At week 61, the IgG titers had waned, but remained significantly elevated in the GRAd
248 NHP that received an mRNA boost (week 61 GMT: GRAd: 8 *v.* 201; S-2P+S-2P: 58 *v.* 100;
249 GRAd+S-2P: 44 *v.* 143 and GRAd(AE)+S-2P: 19 *v.* 79). We also detected antigen-specific IgA
250 responses in the NW in all groups (**Fig. 4E**). At week 46, the IgA GMT was 6, 11, 8, and 18 in
251 the GRAd, S-2P+S-2P, GRAd+S-2P and GRAd(AE)+S-2P groups, respectively. In contrast to
252 the IgA measured in the BAL, the IgA in the NW was boosted after administration of the mRNA

253 in most groups. Notably, however, the mRNA boost did not significantly increase the IgA titer in
254 the NW of GRAd(AE)+S-2P NHP (week 50: GRAd: 2 v. 14; S-2P+S-2P: 11 v. 38; GRAd+S-2P:
255 4 v. 70; GRAd(AE)+S-2P: 16 v. 51). By week 61, NW IgA titers had waned, but generally
256 remained elevated in NHP boosted with mRNA across the groups except in the S-2P+S-2P NHP.

257

258 We also quantified antigen-specific IgG and IgA titers against WA-1 and BA.1 in the BAL and
259 NW (**Fig. S8**). In general, the titers and kinetics to WA-1 and BA.1 mirrored those to BA.5 but
260 were expectedly higher. This suggests that despite having the ancestral WA-1 insert, GRAd can
261 generate antigen-specific humoral responses in the upper and lower airway mucosa to newly
262 emerging SARS-CoV-2 variants that have high levels of neutralization escape.³² Finally, we
263 quantified IgG and IgA titers in the BAL and NW immediately following challenge (**Fig. S9**,
264 **Fig. S10**). IgG primary responses in the control NHP were predominantly detected against BA.5,
265 appearing after day 8 following challenge (**Fig. S9-10A-C**). In immunized NHP, evidence of a
266 secondary antigen-specific IgG response was observed, appearing as early as 2 days following
267 challenge in many of the groups in both the BAL and NW. As for IgA, we also observed
268 evidence for a primary response in the control NHP and a secondary response in the immunized
269 groups (**Fig. S9-10D-F**). Together, our mucosal antibody data suggest robust antigen-specific
270 IgG and IgA responses are generated following immunization with GRAd.

271

272 GRAd(AE)+S-2P generates potent year-long S-specific T cell responses in the lung

273 While SARS-CoV-2-specific mRNA-based vaccines elicit S-specific T_h1, T_h, and CD8⁺ T cell
274 responses in NHP and humans, their frequencies are relatively low.^{33,34} Furthermore, rapid
275 control of SARS-CoV-2 may depend on fast localized T cell responses in the lung. This could be

276 achieved by establishing a large population of SARS-CoV-2-specific T cells at the sites of
277 infection. With some notable exceptions, all our primary immunization strategies generated T_h1,
278 T_{fh}, and CD8⁺ S-specific T cell responses in the lung (**Fig. 5, Fig. S11**). The percentage of
279 memory CD4⁺ T cells with a T_h1 phenotype (IL-2, TNF and IFN γ) peaked in all groups at week
280 6, with GRAd, S-2P+S-2P, GRAd+S-2P, and GRAd(AE)+S-2P having 0.82, 0.65, 0.84 and
281 14.26, respectively, of their CD4⁺ T_h1 cells positive for WA-1 S (**Fig. 5A**). Thus, on average the
282 GRAd(AE)+S-2P NHP had approximately 17-20 times as many T_h1 cells than the other groups
283 at week 6. The CD4⁺ T_h1 cells contracted after week 6, remaining below one percent through
284 week 61, even after the mRNA boost, in the GRAd, S-2P+S-2P and GRAd+S-2P groups.
285 Despite a contraction, the GRAd(AE)+S-2P NHP maintained high percentages of S-specific
286 CD4⁺ T_h1 cells, even in the absence of the mRNA boost (week 46: 7.41%; week 50: 6.87%;
287 week 61: 6.90%). The mRNA boost did not significantly increase the percentage of S-specific
288 CD4⁺ T_h1 cells in this group (week 50: 8.35%; week 61: 4.39%). On the opposite side of the
289 spectrum, the percentage of S-specific memory CD4⁺ T_h2 cells (IL-4 and IL-13) was below
290 0.2% before challenge in most NHP (**Fig. S12A**).

291

292 Next, we quantified the percentage of CD40L⁺ T_{fh} cells, which could participate in the S-specific
293 memory B cell response.³⁵⁻³⁷ Much like the memory CD4⁺ T_h1 cells, lung CD40L⁺ T_{fh} cells
294 peaked at week 6 in all groups, though in many NHP a response was not detected (**Fig. 5B**). On
295 average, the percent of lung CD40L⁺ T_{fh} cells at week 6 was 2.52%, 3.72%, 4.99% and 26.65%
296 in the GRAd, S-2P+S-2P, GRAd+S-2P, and GRAd(AE)+S-2P groups, respectively. Lung
297 CD40L⁺ T_{fh} cells contracted dramatically in the GRAd, S-2P+S-2P and GRAd+S-2P, with these
298 groups having less than one percent CD40L⁺ T_{fh} positive cells at week 61, even after an mRNA

299 boost. In contrast, at week 61, the GRAd(AE)+S-2P group had 26.51% CD40L+ T_{fh} cells in the
300 lung. IL-21+ T_{fh} cells mirrored CD40L+ T_{fh} responses, displaying similar kinetics, but with
301 lower overall frequency (**Fig. S12B**).

302

303 Antigen-specific memory CD8+ T cells with a T_h1 phenotype were induced by our immunization
304 strategies in all groups except the S-2P+S-2P group (**Fig. 5C**). This was not surprising given the
305 inability of subunit vaccine regimens to stimulate CD8+ T cell responses.³⁸ At week 6, 3.77%,
306 1.72% and 11.12% were S-specific memory CD8+ T cells in the GRAd, GRAd+S-2P, and
307 GRAd(AE)+S-2P groups, respectively. The mRNA dose boosted CD8+ T cell responses in the
308 GRAd group, but not the others, although this was not statistically significant. The CD8+ T cell
309 responses contracted in all groups through week 61, but remained on average above 1% in the
310 GRAd(AE)+S-2P NHP and below 1% in the other groups, regardless of whether NHP were
311 boosted with mRNA or not.

312

313 We also quantified the S-specific T_h1 and T_h2, T_{fh}, and CD8+ T cells following challenge (**Fig.**
314 **S12C,D, Fig. S13**). Primary CD4+ T_h1 and CD40L+ T_{fh} responses in the controls were evident
315 at day 8, and secondary responses were also observed at day 8 in the immunized groups,
316 particularly in the GRAd, S-2P+S-2P and GRAd+S-2P NHP that were not boosted with mRNA.
317 Memory CD4+ T_h1 and CD40L+ T_{fh} remained relatively unchanged from day 2 through day 14
318 in the GRAd(AE)+S-2P NHP. CD8+ T cells remained relatively unchanged through the
319 challenge phase across all groups.

320

321 Finally, we asked whether the induction of potent year-long memory CD4⁺ T cell responses
322 observed in the lung of GRAd(AE)+S-2P group was also present in blood. The percentage of S-
323 specific CD4⁺ T_h1 cells in blood of GRAd(AE)+S-2P NHP never rose above 1% from week 8
324 through week 63 (**Fig. S14A**). This observation was in sharp contrast to our observations in the
325 lung, in which at the week 8 peak approximately 14% of the CD4⁺ T cells were S-specific.
326 Despite the contraction, 3-7% of the CD4⁺ T cells in the lung were S-specific at week 63, in
327 contrast to the less than 0.2% in the blood. This finding highlights the impact of AE delivery of a
328 viral-vector on the ability to stimulate and retain antigen-specific T cells in the lung. We
329 observed a very similar discrepancy in lung v. blood in the CD40L⁺ and IL-21⁺ T_h cells (**Fig.**
330 **S14B, E**) and S-specific memory CD8⁺ T cells (**Fig. S14C**), while CD4⁺ T_h2 cells in the blood
331 were undetectable in most NHP (**Fig. S14D**). Overall, our T cell data indicate potent and durable
332 S-specific T cells are induced in the lung mucosa by GRAd(AE)+S-2P.

333

334 Cross-reactive S-specific memory B cells are generated following immunization

335 Our observations of durable binding and neutralizing antibody titers in the serum and mucosa
336 suggested an active involvement of SARS-CoV-2 S-specific cross-reactive memory B cells. To
337 address this, we quantified the frequency of B cells in the blood specific to pairs of
338 fluorochrome-labeled S-2P probes (**Fig. S15**), including WA-1 and BA.5 (**Fig. 6**) and WA-1 and
339 BQ.1.1 (**Fig. S16**) before challenge at weeks 8, 46, 50, 63, and days 8 and 14 following
340 challenge.

341

342 At week 8 the B cell frequency (total S-2P specific memory B cells) was 0.72, 0.36, 1.12 and
343 0.39 percent in the GRAd, S-2P+S-2P, GRAd+S-2P, and GRAd(AE)+S-2P groups, respectively

344 **(Fig. 6)**. At week 8, the relative proportion of dual specific B cells capable of binding both WA-1
345 and BA.5 was approximately equal across all groups and accounted for ~50% of the total (dark
346 grey), while WA-1 only specific B cells (black) accounted for most of the remainder (~45%).
347 Only a very small percentage of the B cells were exclusively BA.5 specific (<5%; light grey). By
348 week 46, the frequency of S-specific memory B cells had declined uniformly across the groups,
349 decreasing on average by ~80% from the week 8 peak, while the relative proportion of probe-
350 specific B cells remained approximately the same.

351

352 In contrast to our T cell data, the mRNA boost had a pronounced effect on the expansion of the
353 S-specific B cell compartment, particularly in the GRAd and GRAd+S-2P groups. At week 50,
354 the B cell frequency was 6.47, 1.29, 5.94 and 1.05 percent in the GRAd, S-2P+S-2P, GRAd+S-
355 2P, and GRAd(AE)+S-2P groups boosted with mRNA, respectively **(Fig. 6)**, representing
356 3944%, 1743%, 3613% and 1650% increases from week 46. Except for the GRAd+S-2P group,
357 the mRNA boost may have expanded the dual-specific B cell population. However, by week 63
358 the frequency of S-specific memory B cells had declined on average by ~80% across all groups
359 from week 50. Nevertheless, at week 63 the mRNA-boosted cohorts in the GRAd, S-2P+S-2P,
360 GRAd+S-2P, and GRAd(AE)+S-2P groups had approximately 20-, 4-, 4- and 10-fold higher S-
361 specific B cells in blood, respectively, compared to non-boosted counterparts.

362

363 Lastly, we measured the S-specific B cell response on days 8 and 14 following challenge to
364 assess whether BA.5 challenge had expanded the B cell compartment. In control NHP, the
365 frequency of S-specific B cells at day 14 was low, but ~90% of the response was BA.5 specific.
366 Evidence of a secondary response was not uniform across the groups. In the GRAd group, the B

367 cell frequencies in the non-boosted cohort rose from 0.05 at week 63 to 0.07 on day 8 and to 0.19
368 on day 14, suggesting an expansion due to the challenge. A similar phenomenon was observed in
369 the mRNA-boosted GRAd cohort, and in the S-2P+S-2P and GRAd+S-2P cohorts, regardless of
370 whether they were boosted or not. In contrast, we did not observe an expansion in the non-
371 boosted GRAd(AE)+S-2P cohort, going from 0.03 at week 63 to 0.09 on day 8 and 0.05 on day
372 14, nor in the presence of the mRNA boost, going from 0.31 at week 63 to 0.30 on day 8 to 0.23
373 on day 14. Additionally, this was the only group we observed a decline in the proportion of dual-
374 specific B cells and an increase in WA-1 only specific B cells over time. Similar kinetics were
375 observed when WA-1 and BQ.1.1 probes were used, albeit the relative proportion of dual
376 specific B cells was lower (**Fig. S16**). Overall, all our immunizations generated durable S-
377 specific B cell responses in blood that could be boosted, but in the absence of a boost they
378 contracted over time.

379

380 Priming with IM or AE GRAd alters serum antibody epitope profile in presence or absence of
381 mRNA boost

382 To evaluate the impact of GRAd- or adjuvanted protein subunit-based immunogens and the
383 impact of mRNA boosting on epitope targeting of serum antibodies to SARS-CoV-2 Spike, we
384 used serum antibody competition assays. We determined the relative serum reactivity (as percent
385 competition) to 18 distinct antigenic sites spanning the S1, S2, NTD and RBD subdomains of the
386 homologous spike protein (WA-1). Serum was evaluated at week 63, immediately before BA.5
387 challenge.

388

389 All primary immunization strategies incorporating GRAd, both in the presence or absence of
390 mRNA boost, showed breadth of reactivity spanning epitopes in the S2, NTD, and RBD
391 subdomains, resembling earlier findings following mRNA-1273 vaccination (**Fig. 7A-B**).³⁹ In
392 contrast, the adjuvanted protein subunit group (S-2P+S-2P) demonstrated a distinct epitope
393 profile characterized primarily by an absence of reactivity to 3 out of 4 antigenic sites in the
394 NTD subdomain, as well as dominant reactivity to RBD antigenic site D (**Fig. 7A**). An average
395 of 38.5% of all serum antibodies targeting WA-1 S were competed by the presence of Site D,
396 defined by monoclonal Ab (mAb) A19-46.1, in this group (**Fig. 7A**).⁴⁰ This antigenic site falls
397 within Class II designation,⁴¹ indicating its ability to block the interaction of S with the human
398 SARS-CoV-2 receptor, hACE2 (angiotensin-converting enzyme 2), and includes 2 mutations in
399 BA.5 (N501Y, Y505H) (**Fig. 7C**). The mRNA boost did not significantly alter the epitope profile
400 or recover reactivity to epitopes not targeted by the primary immunization regimen (**Fig. 7B**).
401
402 No significant differences in epitope targeting were observed between the GRAd and GRAd+S-
403 2P groups, nor did these groups show significantly different epitope reactivity profiles following
404 the mRNA boost (**Fig. 7A,B**). In contrast, NHP that received AE GRAd as the prime
405 (GRAd(AE)+S-2P) demonstrated a remarkably different epitope profile compared to the IM
406 counterparts (GRAd+S-2P). Immediately before challenge (week 63), GRAd(AE)+S-2P NHP
407 had significantly higher proportions of serum reactivity to NTD antigenic site A, defining the
408 NTD supersite, and antigenic site C compared to IM counterpart GRAd+S-2P (**Fig. 7A**). In
409 addition, we observed a significantly higher proportion of serum antibodies targeting RBD
410 antigenic site K (**Fig. 7A**). This site is defined by the Class IV mAb CR3022, which is highly
411 conserved across SARS-CoV and SARS-CoV-2.^{41,42} In BA.5, this footprint contains two

412 mutations located on the periphery of the binding site (S371F, S373P) (**Fig. 7C**). These
413 significant differences in epitope targeting between AE and IM delivery groups were also
414 evident after the mRNA boost (**Fig. 7B**). Together, these data highlight the impact of antigen
415 delivery, the importance of the initial vaccination formulation and route, and the impact of the
416 immunization series on epitope targeting and emphasizes that the initial vaccination is critical in
417 shaping the serum antibody epitope profile following subsequent vaccinations.

418

419 **Discussion**

420 SARS-CoV-2 vaccines that prevent or mitigate infection and transmission are urgently needed.
421 While the currently approved vaccines have successfully curbed morbidity and mortality from
422 SARS-CoV-2, thousands continue to die due to COVID-19 worldwide every week.¹ An obvious
423 tactic to reduce the number of cases, and consequently the number of deaths, would be to reduce
424 person-to-person transmission. One approach may be with vaccines that directly stimulate local
425 respiratory tract immunity in addition to systemic immunity. While pre-clinical research studies
426 with intranasal (IN) vaccines have demonstrated efficacy against SARS-CoV-2, it remains
427 unclear if this delivery method would help curtail transmission.¹⁴⁻¹⁶ It has been reported that AE
428 delivery generates stronger immune responses than IN delivery, leading us to speculate that AE
429 may outperform IN delivery at curtailing transmission.^{43,44} In this study, we evaluated the GRAd
430 viral vector vaccine platform expressing pre-fusion stabilized S as a single dose, and as a
431 heterologous prime and boost regimen that included intramuscular and AE delivery in NHP. A
432 single GRAd dose provided over one-year protective immunity against SARS-CoV-2. Boosting
433 with adjuvanted S-2P (GRAd+S-2P) accelerated viral clearance in the lower and upper airways.
434 Although aerosol-delivered GRAd (GRAd(AE)+S-2P) only modestly improved protection,

435 mRNA boosting proved more effective in this group, achieving total virus clearance in the upper
436 airway by day 4 post-infection. GRAd vaccination triggered strong systemic and mucosal
437 antibody responses to diverse SARS-CoV-2 variants, while GRAd(AE)+S-2P uniquely
438 generated enduring T cell responses in the lung.

439

440 In a first-in-human, dose-escalation phase 1 trial, a single intramuscular dose of the GRAd vector
441 expressing S-2P (abbreviated GRAd-COV2 when used in humans) was shown to be safe and
442 immunogenic in younger (18 to 55 years old) and older (65 to 85 years old) adults.⁴⁵ The
443 observed favorable tolerability was confirmed and extended in a randomized, double-blinded,
444 placebo-controlled phase 2 study, where a two GRAd-COV2 dose regimen with an interval of 21
445 days was also evaluated.⁴⁶ The safety profile was similar to other viral vector vaccines,^{22,47-50} and
446 adverse events were milder than those reported for nanoparticle encapsulated mRNA and
447 adjuvanted subunit/protein vaccines.^{34,51,52} In both phase 1 and 2 studies, the vaccine was
448 immunogenic after a single dose, inducing rapid binding and neutralizing antibodies that were
449 boosted by the administration of a second GRAd-COV2 dose. The vaccine also induced potent,
450 broad, durable cross-reactive T_H1 S-specific CD4⁺ and CD8⁺ T cells with high proliferative
451 capacity, that was not expanded by a homologous boost.^{46,53} When compared in SARS-CoV-2
452 International Units (IU), GRAd-COV2 induced binding and neutralizing antibody levels that
453 were equivalent to those of other single-dose viral vector-based vaccines such as Ad26 and
454 ChAdOx1,^{22,34,54-56} but lower than those reported for the two-dose regimen of mRNA
455 vaccines.^{16,57,58} Despite the human immunogenicity data, GRAd-COV2 has not been formally
456 evaluated for efficacy and it remains unknown how this platform would perform in a
457 heterologous prime and boost immunization strategy, but observations from phase 1 and 2

458 clinical studies revealed compelling immune responses when GRAd-COV2 recipients were
459 boosted with mRNA;^{46,59} or if the initial GRAd-COV2 dose was delivered directly into the upper
460 and lower airway mucosa to stimulate systemic and local mucosal immunity in the respiratory
461 tract.

462
463 In the present study in NHP, a single IM dose of GRAd given 64 weeks before challenge
464 protected against SARS-CoV-2 BA.5 in the lung, while two IM doses of adjuvanted S-2P could
465 not. A heterologous IM boost to IM GRAd with adjuvanted S-2P at week 4 conferred additional
466 protection in the lung, but this was not statistically significant, while heterologous AE GRAd
467 prime with an IM S-2P boost did not yield a meaningful protective benefit to the IM route in the
468 lung. The mRNA boost 16 weeks before challenge enhanced protection in the lung, but this was
469 limited to the single dose of GRAd and the S-2P+S-2P groups. In contrast, the AE prime with
470 GRAd proved most beneficial in terms of protective efficacy in the nasal passage. Neither the
471 single IM GRAd nor the IM S-2P+S-2P were effective at curtailing BA.5 in the nose, while the
472 IM GRAd+S-2P and GRAd(AE)+S-2P began clearing the virus by day 4 and 2, respectively,
473 demonstrating rapid clearance in the nose can be achieved even 60 weeks after immunization.
474 The mRNA boost had its most pronounced effect on the GRAd(AE)+S-2P group, accelerating
475 clearance of the virus and clearing it completely by day 4. Altogether, the protection data
476 demonstrate that GRAd is a suitable vaccine platform against severe disease from SARS-CoV-2,
477 and when combined with AE delivery may help curtail its transmission.

478
479 Serologically, all our vaccine regimens efficiently induced systemic binding antibody responses
480 to the vaccine-matched SARS-CoV-2 WA-1 strain, as well as BA.1 and BA.5 variants that lasted

481 for at least 63 weeks, even in the absence of the mRNA boost. Serum antibodies in all groups
482 also efficiently neutralized the WA-1 strain, however, neutralizing activity against BA.1 and
483 BA.5 weakened significantly in the GRAd and S-2P+S-2P groups over time, while the median
484 BA.5 titer in the GRAd+S-2P and GRAd(AE)+S-2P remained stable over the 63 weeks. The
485 mRNA boost rescued low BA.5 neutralizing antibody titers in some groups, but the titers began
486 to wane shortly thereafter, suggesting a limited benefit of continuous boosting if the primary
487 immunization or immunization series is inadequate. In addition, all immunization strategies
488 efficiently induced durable mucosal IgG in the upper and lower airway to WA-1, BA.1 and
489 BA.5. In contrast, IgA was more prevalent in the BAL of GRAd(AE)+S-2P NHP and remained
490 elevated over 61 weeks. Surprisingly, nasal IgA was only slightly higher in the GRAd(AE)+S-2P
491 NHP compared to the other groups, suggesting that IgA may not be playing a major role in
492 protection against SARS-CoV-2. Indeed, while selective IgA deficiency is a common primary
493 immunodeficiency disorder,⁶⁰ it remains unclear whether this is a risk factor of SARS-CoV-2.⁶¹⁻
494 ⁶³ Thus, despite all our immunization strategies inducing systemic and mucosal binding and
495 neutralizing antibody responses, the heterologous primary vaccination strategies were superior,
496 and AE delivery of GRAd conferred the additional benefit of mucosal humoral immune
497 stimulation.

498

499 All our immunization strategies induced S-specific memory CD4⁺ T cells, and except for in the
500 S-2P+S-2P group, memory CD8⁺ T cells in the blood and the lung. Like immunization with
501 other SARS-CoV-2 vaccines, the memory S-specific T cell response in our immunization
502 regimens skewed toward the T_h1 phenotype, expressing IFN γ , TNF and IL-2.^{27,64,65} In the lung,
503 the T_h1 CD4⁺ T cells peaked at approximately week 6 and mostly contracted to basal levels by

504 week 61 in all groups except in the NHP that received GRAd(AE)+S-2P, suggesting that priming
505 the mucosa with GRAd resulted in the generation of robust and long-lived T cells in the lung, an
506 observation that was not reproduced in the blood, highlighting the importance of directly
507 stimulating the lung mucosa.⁶⁶ Indeed, IM mRNA and viral-vectored, including GRAd, SARS-
508 CoV-2 vaccines induce weak, if any, S-specific CD4+ and CD8+ T cell responses in the airways
509 of NHP.⁶⁷ In our study, the mRNA dose did not boost the CD4+ T cell responses in any group,
510 again suggesting there may be a limited benefit of periodic IM boosters if the primary
511 immunization did not stimulate them in the first place. Memory S-specific CD8+ T cells that
512 expressed IFN γ , TNF and IL-2 were also more prevalent in the lung of GRAd(AE)+S-2P NHP,
513 but this population contracted through week 61, in contrast to the CD4+ T cell population.
514 Finally, we found similar kinetics in the T_{fh} populations in the GRAd(AE)+S-2P group, an
515 important observation as previous studies suggest they contribute to long-term immunity and are
516 associated with protection against respiratory disease.⁶⁸⁻⁷¹ Together, the data suggest that AE
517 delivery of GRAd can stimulate robust, antigen-specific long-lived memory CD4+ T cells in the
518 mucosa, a clear advantage as mucosal immune responses at the site of infection are essential.⁷²
519
520 Antigen-specific B cells that bound S of multiple SARS-CoV-2 variants, including WA-1, BA.1
521 (data not shown), BA.5, and BQ.1.1 were also observed in all our immunization strategies. While
522 most of the B cells were dual specific for WA-1 and BA.5, we observed a notable loss of dual
523 specific WA-1 and BQ.1.1 B cells, and this loss was accompanied by a relative increase in WA-1
524 only specific B cells, suggesting that the WA-1 imprint on immune memory may continue to
525 weaken against new SARS-CoV-2 variants and may be difficult to overcome.³ However, it
526 remains unknown how a matched variant boost would affect the B cell specificities in this study.

527 Nevertheless, the relative proportion of cross-reactive B cells remained stable for over a year,
528 and while the mRNA boost was able to increase the relative proportion of these cross-reactive B
529 cells in some groups, the effect appears to have been only transient. Although the mRNA boost
530 did expand the B cell frequency to a greater extent in the GRAd and GRAd+S-2P groups
531 compared to the S-2P+S-2P and GRAd(AE)+S-2P groups, a contraction quickly followed, a
532 phenomenon that appears to be more substantial in NHP than in humans.⁷³ The differences we
533 observed in B cell frequencies between the GRAd+S-2P and GRAd(AE)+S-2P, a change in only
534 GRAd priming via IM or AE, led us to explore whether this alteration affected epitope
535 specificities to S. The fact that we observed differences in epitope targeting by only changing the
536 delivery of GRAd from IM to AE, and that epitopes targeted by AE delivery appear to be more
537 conserved, suggests that the mechanism of antigen presentation that occurs when antigens are
538 delivered to the lung differs from when delivered to the lymph nodes via the musculature. This is
539 entirely plausible given the anatomical differences between muscle and lung immune cells, and
540 the lymph nodes each tissue drains to.^{74,75} Thus, delivery of the immunizing agent to the
541 anatomical site in which the pathogen causes disease may provide greater immune fidelity.
542
543 In summary, GRAd based vaccines encoding S-2P were highly immunogenic and protective
544 against SARS-CoV-2 BA.5 in macaques and would have likely been effective against earlier
545 variants. The efficacy and immunogenicity of GRAd was improved via heterologous boost with
546 S-2P, while protection with S-2P+S-2P was inadequate. Boosting with mRNA yielded transient
547 increases in systemic and mucosal antibody binding and neutralizing responses and overall B cell
548 frequencies, but it did not have a meaningful impact on T cell responses. Our data support the

549 further development of the GRAd platform for use as a prime only or as part of a prime and
550 boost combination with other approved SARS-CoV-2 vaccines.

551

552 **Limitations of the study**

553 In our study, the immunogens (GRAd viral vector and S-2P protein) were derived from the
554 ancestral Wuhan-Hu-1/USA-WA1/2020, while the NHP were challenged with the SARS-CoV-2
555 BA.5, a significant shift from vaccine insert to challenge virus. While we detected binding and
556 neutralizing antibody responses to BA.5, it is possible that GRAd efficacy could be improved if
557 the insert was matched to the challenge virus. In that vein, T cell responses reported in this study
558 were measured against WA-1, and it is possible that antigenic differences between WA-1 and
559 BA.5 could have resulted in weaker BA.5-specific T cell responses. Thus, Omicron sublineage-
560 specific T cell responses should be evaluated in future studies. Furthermore, we did not evaluate
561 the immunogenicity and efficacy of a single dose of AE GRAd, and while the S-2P boost likely
562 contributed to the observed protection in the GRAd(AE)+S-2P group, we would likely have
563 observed similar humoral and cellular responses and protection in the absence of a boost in this
564 group. Finally, while we evaluated the efficacy against BA.5, it was subsequently displaced by
565 BQ.1.1 and it by XBB.1.5. It is unknown how our immunogens and vaccination strategies would
566 fare upon challenge from currently circulating Omicron sub-lineage variants, but like bivalent
567 mRNA vaccines, viral-vectors could be formulated as a mixture of viruses that encode S from
568 various SARS-CoV-2 variants.

569

570 **Methods**

571

572 **Resource availability**

573 **Lead contact**

574 Further information and requests for resources should be directed to and will be fulfilled by the
575 lead contacts, Robert A. Seder (rseder@mail.nih.gov) Nancy J. Sullivan (njsull@bu.edu).

576

577 **Materials availability**

578 This study did not generate new unique reagents.

579

580 **Data and code availability**

- 581
- All data reported in this paper will be shared by the lead contact upon request.
- 582
- This paper does not report original code.
- 583
- Any additional information required to reanalyze the data reported in this paper is
- 584 available from the lead contact upon request.

585

586 **Experimental model and subject details**

587 **Rhesus macaque model and immunizations**

588 All experiments were conducted according to NIH regulations and standards on the humane care
589 and use of laboratory animals as well as the Animal Care and Use Committees of the NIH
590 Vaccine Research Center and BIOQUAL, Inc. (Rockville, Maryland). All studies were
591 conducted at BIOQUAL, Inc. Forty, four- to nine-year-old rhesus macaques of Indian origin
592 were stratified into five groups of eight based on sex, age, and weight. Group one was
593 immunized with 5×10^{10} GRAd32-Gag at week 0 and placebo (phosphate-buffered saline - PBS)
594 at week 4. This group served as the control. Group two was immunized with 5×10^{10} GRAd32-S-

595 2P at week 0 and placebo at week 4. Group three was immunized 5 µg adjuvanted S-2P (750 µg
596 alum (aluminum hydroxide) and 1500 µg CpG 1018 (Dynavax Technologies); the same
597 adjuvants were used when applicable) at week 0 and week 4. Group four was immunized with
598 5×10^{10} GRAd32-S-2P at week 0 and with 5 µg adjuvanted S-2P at week 4. Group five was
599 immunized with 5×10^{10} GRAd32-S-2P delivered via aerosol (AE) at week 0 and with 5 µg
600 adjuvanted S-2P at week 4. AE was delivered in a 2 ml volume via a pediatric silicon face mask
601 (PARI SMARTMASK[®] Baby/Kids) attached to an Investigational eFlow Nebulizer System
602 (PARI Respiratory Equipment, Inc., Midlothian, VA, USA) that delivered 4 µM particles into the
603 lung, as previously described.⁷⁶ At week 48 (~ 44 weeks after the second immunization), the
604 eight macaques in each group were subdivided into two groups of 4 (except group one) and
605 boosted with 30 µg BNT162b2. The week 0 and week 4 immunizations were delivered
606 intramuscularly in 1 mL diluted in PBS (except AE GRAd32-S-2P) into the right deltoid, while
607 the week 48 immunizations were delivered intramuscularly in 1 mL diluted in PBS into the right
608 quadriceps.

609

610 **Method details**

611 **Cells and viruses**

612 VeroE6-TMPRSS2 cells were generated at the Vaccine Research Center, NIH, Bethesda, MD.
613 Viruses were propagated in Vero-TMPRSS2 cells to generate viral stocks. Viral titers were
614 determined by focus-forming assay on VeroE6-TMPRSS2 cells. Viral stocks were stored at -
615 80°C until use.

616

617 **GRAd32 vectors expressing SARS-CoV-2 S-2P**

618 The GRAd32 vector was isolated, amplified, classified and constructed as a vector as previously
619 described in detail.¹⁷ The GRAd32 vector expressing SARS-CoV-2 pre-fusion stabilized Spike
620 (S-2P) was generated as previously described.¹⁷ Briefly, the SARS-CoV-2 S-2P gene was
621 generated by subcloning a human codon-optimized version of the SARS-CoV-2 S into a shuttle
622 plasmid between the AscI and PacI restriction sites. Two mutations were introduced to convert
623 the 986 lysine and 987 valine (KV) amino acids (aa) into prolines (PP or 2P) to stabilize the
624 protein in its pre-fusion state.⁷⁷ A hemagglutinin (HA) tag was fused downstream of the last
625 SARS-CoV-2 S protein aa (Threonine1273) flanked at its 5' and 3' side by a Glycine and a
626 Serine, respectively, to facilitate antigen expression detection. A minimal Kozak sequence (5'-
627 CCACC-3') was placed immediately upstream of the start codon to enable efficient initiation of
628 translation. The cassette encoding for the SARS-CoV-2 S-2P was inserted by homologous
629 recombination in the E1 locus of the GRAd32 vector. All cloning PCR amplifications were
630 performed using the Q5 High-Fidelity DNA Polymerase (New England Biolabs) according to
631 standard procedures. The GRAd32 S-2P vector was expanded in a 2 L Bioreactor (Biostat B
632 DCU; Sartorius). The titer of virus contained in the bulk cell lysates was quantified by qPCR.
633 Extensive purification of GRAd-S-2P vector was obtained by applying an orthogonal
634 chromatographic method.

635

636 **Expression and purification of SARS-CoV-2 S-2P**

637 SARS-CoV-2 S-2P protein (S2P7471) was produced as previously described.⁷⁸ Briefly, S2P7471
638 was expressed and purified from the CHO-DG44 cell line. S2P7471 was clarified through
639 centrifugation and Satopore XLG 0.8/0.2 filters. S2P7471 was concentrated and buffer
640 exchanged by tangential flow filtration into 1x PBS, purified via Nickle NTA nitrilotriacetic acid

641 chromatography, and purified by Superose 6 size-exclusion chromatography (SEC). Finally,
642 S2P7471 was cleaved by HRV3C protease, and the cleaved product was loaded onto a Superose
643 6 SEC column. Peak fractions of S2P7471 from the SEC were pooled, concentrated using SPIN-
644 X UF spin filters, spiked to 5% sucrose and sterile filtered. S2P7471 was concentrated to 0.607
645 mg/mL, flash-frozen in liquid nitrogen and maintained at -80°C until use.

646

647 **Sequencing of BA.5 virus stock**

648 NEBNext Ultra II RNA Prep reagents and multiplex oligos (New England Biolabs) were used to
649 prepare Illumina-ready libraries, which were sequenced on a NextSeq 2000 sequencer (Illumina).
650 Demultiplexed sequence reads were analyzed in the CLC Genomics Workbench v.22.0.2 by (1)
651 trimming for quality, length, and adaptor sequence, (2) mapping to the Wuhan-Hu-1 SARS-
652 CoV-2 reference (GenBank no. NC_045512), (3) improving the mapping by local realignment in
653 areas containing insertions and deletions (indels), and (4) generating both a sample consensus
654 sequence and a list of variants. Default settings were used for all tools.

655

656 **Viral challenge**

657 Macaques were challenged at week 64 with a total dose of 8×10^5 PFUs of SARS-CoV-2 BA.5
658 kindly provided by M. Suthar (Emory). The viral inoculum was administered as 6×10^5 PFUs in
659 3 mL intratracheally and 2×10^5 PFUs in 1 mL intranasally in a volume of 0.5 mL into each
660 nostril.

661

662 **Serum and mucosal antibody titers**

663 Quantification of antibodies in the blood and mucosa was performed using multiplex
664 electrochemiluminescence serology assays by Meso Scale Discovery Inc. (MSD) as previously
665 described.⁷⁹ Briefly, total IgG and IgA antigen-specific antibodies to variant SARS-CoV-2 S-
666 were determined by MSD V-Plex SARS-CoV-2 Panel 24 (K15575U, K15577U), Panel 27
667 (K15606U, K15608U) and Spike Panel 1 Kit (K15651U, K15653U) for S according to
668 manufacturer's instructions, except 25µl of sample and detection antibody were used per well.
669 Heat inactivated plasma was initially diluted 1:1000 and 1:5000 using Diluent 100. BAL fluid
670 and nasal washes were concentrated 10-fold with Amicon Ultra centrifugal filter devices
671 (Millipore Sigma). Concentrated samples were diluted 1:10 and 1:100 using Diluent 100.
672 Arbitrary units per milliliter (AU/mL) were calculated for each sample using the MSD reference
673 standard curve. For each sample, the data reported was for diluted samples that returned results
674 between the upper and lower limits of quantification.

675

676 **Lentiviral pseudovirus neutralization**

677 Neutralizing antibodies in serum or plasma were measured in a validated pseudovirus-based
678 assay as a function of reductions in luciferase reporter gene expression after a single round of
679 infection with SARS-CoV-2 spike-pseudotyped viruses in 293T/ACE2 cells (293T cell line
680 stably overexpressing the human ACE2 cell surface receptor protein, obtained from Drs. Mike
681 Farzan and Huihui Mu at Scripps) as previously described.^{57,80} SARS-CoV-2 Spike-pseudotyped
682 virus was prepared by transfection in 293T/17 cells (human embryonic kidney cells in origin;
683 obtained from American Type Culture Collection, cat. No. CRL-11268) using a lentivirus
684 backbone vector, a spike-expression plasmid encoding S protein from Wuhan-Hu-1 strain
685 (GenBank no. MN908947.3) with a p.Asp614Gly mutation, a TMPRSS2 expression plasmid,

686 and a firefly Luc reporter plasmid. For pseudovirus encoding the S from B.1.1.529 (BA.1) and
687 BA.5, the plasmid was altered via site-directed mutagenesis to match the S sequence to the
688 corresponding variant sequence as previously described.^{39,67} A pre-titrated dose of pseudovirus
689 was incubated with eight serial 5-fold dilutions of serum samples (1:20 start dilution) in
690 duplicate in 96-well 384-well flat-bottom tissue culture plates (Thermo Fisher, cat. no. 12-565-
691 344) for 1 hr at 37°C before adding 293T/ACE2 cells. One set of 14 wells received cells + virus
692 (virus control) and another set of 14 wells received cells only (background control),
693 corresponding to technical replicates. Luminescence was measured after 66-72 hr of incubation
694 using Britelite-Plus luciferase reagent (Perkin Elmer, cat. no. 6066769). Neutralization titers are
695 the inhibitory dilution of serum samples at which relative luminescence units (RLUs) were
696 reduced by 50% (ID₅₀) compared to virus control wells after subtracting background RLUs.
697 Serum samples were heat-inactivated for 30-45 min at 56°C before assay.

698

699 **B cell probe binding**

700 Kinetics of S-specific memory B cells responses were determined as previously described.³³
701 Briefly, cryopreserved PBMC were thawed and stained with the following antibodies
702 (monoclonal unless indicated): IgD FITC (goat polyclonal, Southern Biotech), IgM PerCP-Cy5.5
703 (clone G20-127, BD Biosciences), IgA Dylight 405 (goat polyclonal, Jackson Immunoresearch
704 Inc), CD20 BV570 (clone 2H7, Biolegend), CD27 BV650 (clone O323, Biolegend), CD14
705 BV785 (clone M5E2, Biolegend), CD16 BUV496 (clone 3G8, BD Biosciences), CD4 BUV737
706 (clone SK3, BD Biosciences), CD19 APC (clone J3-119, Beckman), IgG Alexa 700 (clone G18-
707 145, BD Biosciences), CD3 APC-Cy7 (clone SP34-2, BD Biosciences), CD38 PE (clone
708 OKT10, Caprico Biotechnologies), CD21 PE-Cy5 (clone B-ly4, BD Biosciences), and CXCR5

709 PE-Cy7 (clone MU5UBEE, Thermo Fisher Scientific). Stained cells were then incubated with
710 streptavidin-BV605 (BD Biosciences) labeled BA.1 S-2P, streptavidin-BUV661 (BD
711 Biosciences) labeled WA-1 S-2P and streptavidin-BUV395 (BD Biosciences) labeled BA.5 or
712 BQ.1.1 S-2P for 30 minutes at 4°C (protected from light). Cells were washed and fixed in 0.5%
713 formaldehyde (Tousimis Research Corp) before data acquisition. Aqua live/dead fixable dead
714 cell stain kit (Thermo Fisher Scientific) was used to exclude dead cells. All antibodies were
715 previously titrated to determine the optimal concentration. Samples were acquired on a BD
716 FACSymphony cytometer and analyzed using FlowJo version 10.7.2 (BD, Ashland, OR).

717

718 **Intracellular cytokine staining**

719 Intracellular cytokine staining was performed as previously described.^{33,81,82} Briefly,
720 cryopreserved PBMC and BAL cells were thawed and rested overnight in a 37°C/5% CO₂
721 incubator. The following morning, cells were stimulated with SARS-CoV-2 S protein (S1 and
722 S2, matched to vaccine insert) peptide pools (JPT Peptides) at a final concentration of 2 µg/ml in
723 the presence of 3 mM monensin for 6 h. The S1 and S2 peptide pools were comprised of 158 and
724 157 individual peptides, respectively, as 15 mers overlapping by 11 amino acids in 100%
725 DMSO. Negative controls received an equal concentration of DMSO instead of peptides (final
726 concentration of 0.5 %). The following monoclonal antibodies were used: CD3 APC-Cy7 (clone
727 SP34-2, BD Biosciences), CD4 PE-Cy5.5 (clone S3.5, Invitrogen), CD8 BV570 (clone RPA-T8,
728 BioLegend), CD45RA PE-Cy5 (clone 5H9, BD Biosciences), CCR7 BV650 (clone G043H7,
729 BioLegend), CXCR5 PE (clone MU5UBEE, Thermo Fisher), PD-1 BUV737 (clone EH12.1, BD
730 Biosciences), ICOS PE-Cy7 (clone C398.4A, BioLegend), CD69 ECD (clone TP1.55.3,
731 Beckman Coulter), IFN γ Ax700 (clone B27, BioLegend), IL-2 BV750 (clone MQ1-17H12, BD

732 Biosciences), IL-4 BB700 (clone MP4-25D2, BD Biosciences), TNF-FITC (clone Mab11, BD
733 Biosciences), IL-13 BV421 (clone JES10-5A2, BD Biosciences), IL-17 BV605 (clone BL168,
734 BioLegend), IL-21 Ax647 (clone 3A3-N2.1, BD Biosciences), and CD154 BV785 (clone 24-31,
735 BioLegend). Aqua live/dead fixable dead cell stain kit (Thermo Fisher Scientific) was used to
736 exclude dead cells. All antibodies were previously titrated to determine the optimal
737 concentration. Samples were acquired on a BD FACSymphony flow cytometer and analyzed
738 using FlowJo version 10.8.0 (BD, Ashland, OR).

739

740 **Subgenomic RNA quantification**

741 sgRNA was isolated and quantified by researchers blinded to vaccine status as described,²⁷ with
742 the sole exception of the use of a new probe listed below. Briefly, total RNA was extracted from
743 BAL fluid and nasal swabs using RNazol BD column kit (Molecular Research Center). PCR
744 reactions were conducted with TaqMan Fast Virus 1-Step Master Mix (Applied Biosystems),
745 forward primer in the 5' leader region and gene-specific probes and reverse primers as follows:
746 sgLeadSARSCoV2_F: 5'-CGATCTCTTGATAGATCTGTTCTC-3'; N gene: N2_P: 5'-FAM-
747 CGATCAAAACAACGTCGGCCCC-BHQ1-3', wtN_R: 5'-GGTGAACCAAGACGCAGTAT-
748 3'. Amplifications were performed with a QuantStudio 6 Pro Real-Time PCR System (Applied
749 Biosystems). The assay lower LOD was 50 copies per reaction.

750

751 **Median Tissue Culture Infectious Dose (TCID₅₀) assay**

752 TCID₅₀ was quantified as previously described.⁸³ Briefly, 25,000 Vero-TMPRSS2 cells were
753 plated per well in DMEM+10% FBS + gentamycin and incubated at 37 °C, 5% CO₂ overnight.
754 The following day, BAL samples were serially diluted, and the plates were incubated at 37 °C,

755 5.0% CO₂ for four days. Positive (virus stock of known infectious titer in the assay) and negative
756 (medium only) control wells were included in each assay setup. The cell monolayers were
757 visually inspected for cytopathic effect. TCID₅₀ values were calculated using the Reed–Muench
758 formula.

759

760 **Histopathology and immunohistochemistry**

761 Routine histopathology and detection of SARS-CoV-2 virus antigen via immunohistochemistry
762 was performed as previously described.⁸³ Briefly, 8 to 9 days and 14 to 15 days following BA.5
763 challenge animals were euthanized, and lung tissue was processed and stained with hematoxylin
764 and eosin for pathological analysis or with a rabbit polyclonal anti-SARS-CoV-2 antibody
765 (GeneTex, GTX135357) at a dilution of 1:2000 for detection of SARS-CoV-2. On days 8 and 9,
766 the left caudal, right middle and right caudal lung lobes were evaluated, whereas on days 14 and
767 15, the left cranial, right cranial, and right middle lung lobes were evaluated. Tissue sections
768 were analyzed by a blinded board-certified veterinary pathologist using an Olympus BX51 light
769 microscope. Photomicrographs were taken on an Olympus DP73 camera.

770

771 **Epitope mapping**

772 Serum antibody epitope mapping competition assays were performed as previously
773 described.^{39,83} Briefly, primary amine coupling was used to immobilize anti-histidine antibody
774 on a Series S Sensor Chip CM5 (Cytiva) via His capture kit (Cytiva). His-tagged SARS-CoV-2
775 S-2P was then captured on the sensor surface. Following this, NHP sera (diluted 1:50) was
776 flowed over both active and reference sensor surfaces. Active and reference sensor surfaces were
777 regenerated between each analysis cycle. Human IgG monoclonal antibodies (mAb) used for

778 these analyses include: S2-specific mAbs: S652-112 and S2P6, NTD-specific mAbs: 4-8, S652-
779 118, N3C, and 5-7, RBD-specific mAbs B1-182, CB6, A20-29.1, A19-46.1, LY-COV555, A19-
780 61.1, S309, A23-97.1, A19-30.1, A23-80.1, and CR3022, and SD1-specific mAb A19-36.1.
781 Negative control antibody or competitor mAb was injected over both active and reference
782 surfaces.

783

784 For analysis, sensorgrams were aligned to Y (Response Units) = 0, using Biacore 8K Insights
785 Evaluation Software (Cytiva) beginning at the serum association phase. Relative “analyte
786 binding late” report points (RU) were collected and used to calculate percent competition (% C)
787 using the following formula: $\% C = [1 - (100 * ((RU \text{ in presence of competitor mAb}) / (RU \text{ in}$
788 $\text{presence of negative control mAb})))]$. Results are reported as percent competition.

789

790 **Quantification and statistical analysis**

791 Comparisons between time points or within the same time point within a group are based on
792 unpaired Student’s *t*-tests. Comparisons between groups within the same time points are based
793 on one-way ANOVA with Tukey’s post-hoc test. Binding, neutralizing, and viral assays are log-
794 transformed as appropriate and reported with medians and corresponding interquartile ranges
795 where indicated. Adjustments for multiple comparisons were made when appropriate. All
796 analyses are conducted using GraphPad Prism version 9.5.0 unless otherwise specified. The *p*
797 values are shown in the figure as symbols defined in the figure legends, and the sample *n* is listed
798 in corresponding figure legends. For all data presented, *n*=4 for individual boost cohorts and
799 *n*=4-8 for controls and vaccinated NHP at pre-boost time points. If applicable, ‘ns’ denotes that
800 the indicated comparison was not significant, with $p > 0.05$.

801

802 **Acknowledgments**

803 This project was funded by the Intramural Research Program of the Vaccine Research Center
804 (VRC), National Institutes of Allergy and Infectious Disease (NIAID), National Institutes of
805 Health (NIH). We are grateful to PARI Pharma GmbH for providing the eFlow nebulizer for use
806 in this study. We thank the VRC Production Program (VPP) for providing the WA-1 S-2P
807 protein. VPP contributors include C. Anderson, V. Bhagat, J. Burd, J. Cai, K. Carlton, W.
808 Chuenchor, N. Clbelli, G. Dobrescu, M. Figur, J. Gall, H. Geng, D. Gowetski, K. Gulla, L.
809 Hogan, V. Ivleva, S. Khayat, P. Lei, Y. Li, I. Loukinov, M. Mai, S. Nugent, M. Pratt, E. Reilly,
810 E. Rosales-Zavala, E. Scheideman, A. Shaddeau, A. Thomas, S. Upadhyay, K. Vickery, A.
811 Vinitsky, C. Wang, C. Webber and Y. Yang. We thank Jay Noor from the Translational
812 Research Program at the VRC for assistance with complete blood count tests. We also thank
813 Serge Zouantcha and Elyse Teow for animal care and assistance with procedures and Brandon
814 Narvaez for laboratory support at Bioqual. We thank Robert Coffman, Robert Janssen, Riccardo
815 Manetti and Darren Campbell from Dynavax Technologies for providing CpG 1018 for use in
816 this study.

817

818 **Author contributions**

819 J.I.M, N.J.S., and R.A.S. designed experiments. J.I.M, S.F.A., B.J.F., D.A.W., K.E.F., M.G.,
820 D.R.F., E.L., S.P., J.M., A.M., C.G.L., C.C.H., M.R.B., L.M., A.R.H., S.G., M.E.D.G., M.M.,
821 K.W.B., B.M.N., J.P.M.T., E.M., A.D., K.K., A.C., L.P., A.V.R., D.V., S.Y., Y.L., M.G.L.,
822 H.A., D.A.A., R.W., M.C.N., D.C.D., M.R., N.J.S., and R.A.S. performed, analyzed, and/or
823 supervised experiments. J.I.M., K.E.F., S.F.A., and D.A.W. designed figures. A.C.M.B., M.S.S.,

824 A.L., A.V., S.Co., A.F., A.R., and S.Ca. provided critical reagents. J.I.M. wrote original draft of
825 the manuscript. N.J.S., R.A.S., D.C.D., M.G., D.A.W. assisted with writing and provided
826 feedback. All authors edited the manuscript and provided feedback on research.

827

828 **Declaration of interests**

829 M.R., N.J.S., and D.C.D. are inventors on U.S. Patent Application No. 63/147,419 entitled
830 “Antibodies Targeting the Spike Protein of Coronaviruses”. L.P., A.V.R., D.V., A.C., A.D.,
831 M.G.L., and H.A. are employees of Bioqual, Inc. A.L., A.V., S.Co., A.F., A.R., and S.Ca. are
832 employees of ReiThera Srl. S.Co. and A.F. are shareholders of Keires AG. A.V., S.Co. and A.R.
833 are named inventors of the Patent Application No. 20183515.4 entitled “Gorilla Adenovirus
834 Nucleic Acid- and Amino Acid-Sequences, Vectors Containing Same, and Uses Thereof”. The
835 other authors declare no competing interests.

836

837 **References**

838

839

- 840 1. COVID-19 Dashboard by the Center for Systems Science and Engineering at John
841 Hopkins University. <https://coronavirus.jhu.edu/map.html>.
- 842 2. Barouch, D.H. (2022). Covid-19 Vaccines - Immunity, Variants, Boosters. *N Engl J Med*
843 *387*, 1011-1020. 10.1056/NEJMra2206573.
- 844 3. Offit, P.A. (2023). Bivalent Covid-19 Vaccines - A Cautionary Tale. *N Engl J Med* *388*, 481-
845 483. 10.1056/NEJMp2215780.
- 846 4. Baden, L.R., El Sahly, H.M., Essink, B., Kotloff, K., Frey, S., Novak, R., Diemert, D., Spector,
847 S.A., Roupheal, N., Creech, C.B., et al. (2021). Efficacy and Safety of the mRNA-1273
848 SARS-CoV-2 Vaccine. *N Engl J Med* *384*, 403-416. 10.1056/NEJMoa2035389.
- 849 5. Bergwerk, M., Gonen, T., Lustig, Y., Amit, S., Lipsitch, M., Cohen, C., Mandelboim, M.,
850 Levin, E.G., Rubin, C., Indenbaum, V., et al. (2021). Covid-19 Breakthrough Infections in
851 Vaccinated Health Care Workers. *N Engl J Med* *385*, 1474-1484.
852 10.1056/NEJMoa2109072.

- 853 6. Goldberg, Y., Mandel, M., Bar-On, Y.M., Bodenheimer, O., Freedman, L., Haas, E.J., Milo,
854 R., Alroy-Preis, S., Ash, N., and Huppert, A. (2021). Waning Immunity after the BNT162b2
855 Vaccine in Israel. *N Engl J Med* 385, e85. 10.1056/NEJMoa2114228.
- 856 7. Lyngse, F.P., Kirkeby, C.T., Denwood, M., Christiansen, L.E., Molbak, K., Moller, C.H.,
857 Skov, R.L., Krause, T.G., Rasmussen, M., Sieber, R.N., et al. (2022). Household
858 transmission of SARS-CoV-2 Omicron variant of concern subvariants BA.1 and BA.2 in
859 Denmark. *Nat Commun* 13, 5760. 10.1038/s41467-022-33498-0.
- 860 8. DiPiazza, A.T., Graham, B.S., and Ruckwardt, T.J. (2021). T cell immunity to SARS-CoV-2
861 following natural infection and vaccination. *Biochem Biophys Res Commun* 538, 211-
862 217. 10.1016/j.bbrc.2020.10.060.
- 863 9. Sadarangani, M., Marchant, A., and Kollmann, T.R. (2021). Immunological mechanisms
864 of vaccine-induced protection against COVID-19 in humans. *Nat Rev Immunol* 21, 475-
865 484. 10.1038/s41577-021-00578-z.
- 866 10. Gupta, R.K., and Topol, E.J. (2021). COVID-19 vaccine breakthrough infections. *Science*
867 374, 1561-1562. 10.1126/science.abl8487.
- 868 11. Siddle, K.J., Krasilnikova, L.A., Moreno, G.K., Schaffner, S.F., Vostok, J., Fitzgerald, N.A.,
869 Lemieux, J.E., Barkas, N., Loreth, C., Specht, I., et al. (2022). Transmission from
870 vaccinated individuals in a large SARS-CoV-2 Delta variant outbreak. *Cell* 185, 485-492
871 e410. 10.1016/j.cell.2021.12.027.
- 872 12. Lin, D.Y., Gu, Y., Xu, Y., Wheeler, B., Young, H., Sunny, S.K., Moore, Z., and Zeng, D.
873 (2022). Association of Primary and Booster Vaccination and Prior Infection With SARS-
874 CoV-2 Infection and Severe COVID-19 Outcomes. *JAMA* 328, 1415-1426.
875 10.1001/jama.2022.17876.
- 876 13. Iwasaki, A. (2016). Exploiting Mucosal Immunity for Antiviral Vaccines. *Annu Rev*
877 *Immunol* 34, 575-608. 10.1146/annurev-immunol-032414-112315.
- 878 14. Ku, M.W., Bourguine, M., Authie, P., Lopez, J., Nemirov, K., Moncoq, F., Noirat, A., Vesin,
879 B., Nevo, F., Blanc, C., et al. (2021). Intranasal vaccination with a lentiviral vector
880 protects against SARS-CoV-2 in preclinical animal models. *Cell Host Microbe* 29, 236-249
881 e236. 10.1016/j.chom.2020.12.010.
- 882 15. Hassan, A.O., Kafai, N.M., Dmitriev, I.P., Fox, J.M., Smith, B.K., Harvey, I.B., Chen, R.E.,
883 Winkler, E.S., Wessel, A.W., Case, J.B., et al. (2020). A Single-Dose Intranasal ChAd
884 Vaccine Protects Upper and Lower Respiratory Tracts against SARS-CoV-2. *Cell* 183, 169-
885 184 e113. 10.1016/j.cell.2020.08.026.
- 886 16. Feng, L., Wang, Q., Shan, C., Yang, C., Feng, Y., Wu, J., Liu, X., Zhou, Y., Jiang, R., Hu, P., et
887 al. (2020). An adenovirus-vectored COVID-19 vaccine confers protection from SARS-
888 COV-2 challenge in rhesus macaques. *Nat Commun* 11, 4207. 10.1038/s41467-020-
889 18077-5.
- 890 17. Capone, S., Raggioli, A., Gentile, M., Battella, S., Lahm, A., Sommella, A., Contino, A.M.,
891 Urbanowicz, R.A., Scala, R., Barra, F., et al. (2021). Immunogenicity of a new gorilla
892 adenovirus vaccine candidate for COVID-19. *Mol Ther* 29, 2412-2423.
893 10.1016/j.ymthe.2021.04.022.
- 894 18. Vitelli, A., Folgori, A., Scarselli, E., Colloca, S., Capone, S., and Nicosia, A. (2017).
895 Chimpanzee adenoviral vectors as vaccines - challenges to move the technology into the
896 fast lane. *Expert Rev Vaccines* 16, 1241-1252. 10.1080/14760584.2017.1394842.

- 897 19. Green, C.A., Scarselli, E., Sande, C.J., Thompson, A.J., de Lara, C.M., Taylor, K.S.,
898 Haworth, K., Del Sorbo, M., Angus, B., Siani, L., et al. (2015). Chimpanzee adenovirus-
899 and MVA-vectored respiratory syncytial virus vaccine is safe and immunogenic in adults.
900 *Sci Transl Med* 7, 300ra126. [10.1126/scitranslmed.aac5745](https://doi.org/10.1126/scitranslmed.aac5745).
- 901 20. Colloca, S., Barnes, E., Folgori, A., Ammendola, V., Capone, S., Cirillo, A., Siani, L.,
902 Naddeo, M., Grazioli, F., Esposito, M.L., et al. (2012). Vaccine vectors derived from a
903 large collection of simian adenoviruses induce potent cellular immunity across multiple
904 species. *Sci Transl Med* 4, 115ra112. [10.1126/scitranslmed.3002925](https://doi.org/10.1126/scitranslmed.3002925).
- 905 21. Borthwick, N., Ahmed, T., Ondondo, B., Hayes, P., Rose, A., Ebrahimsa, U., Hayton, E.J.,
906 Black, A., Bridgeman, A., Rosario, M., et al. (2014). Vaccine-elicited human T cells
907 recognizing conserved protein regions inhibit HIV-1. *Mol Ther* 22, 464-475.
908 [10.1038/mt.2013.248](https://doi.org/10.1038/mt.2013.248).
- 909 22. Folegatti, P.M., Ewer, K.J., Aley, P.K., Angus, B., Becker, S., Belij-Rammerstorfer, S.,
910 Bellamy, D., Bibi, S., Bittaye, M., Clutterbuck, E.A., et al. (2020). Safety and
911 immunogenicity of the ChAdOx1 nCoV-19 vaccine against SARS-CoV-2: a preliminary
912 report of a phase 1/2, single-blind, randomised controlled trial. *Lancet* 396, 467-478.
913 [10.1016/S0140-6736\(20\)31604-4](https://doi.org/10.1016/S0140-6736(20)31604-4).
- 914 23. Barros-Martins, J., Hammerschmidt, S.I., Cossmann, A., Odak, I., Stankov, M.V., Morillas
915 Ramos, G., Dopfer-Jablonka, A., Heidemann, A., Ritter, C., Friedrichsen, M., et al. (2021).
916 Immune responses against SARS-CoV-2 variants after heterologous and homologous
917 ChAdOx1 nCoV-19/BNT162b2 vaccination. *Nat Med* 27, 1525-1529. [10.1038/s41591-021-01449-9](https://doi.org/10.1038/s41591-021-01449-9).
- 919 24. Schmidt, T., Klemis, V., Schub, D., Mihm, J., Hielscher, F., Marx, S., Abu-Omar, A., Ziegler,
920 L., Guckelmuus, C., Urschel, R., et al. (2021). Immunogenicity and reactogenicity of
921 heterologous ChAdOx1 nCoV-19/mRNA vaccination. *Nat Med* 27, 1530-1535.
922 [10.1038/s41591-021-01464-w](https://doi.org/10.1038/s41591-021-01464-w).
- 923 25. Tan, S.H.X., Pung, R., Wang, L.F., Lye, D.C., Ong, B., Cook, A.R., and Tan, K.B. (2022).
924 Association of Homologous and Heterologous Vaccine Boosters With COVID-19
925 Incidence and Severity in Singapore. *JAMA* 327, 1181-1182. [10.1001/jama.2022.1922](https://doi.org/10.1001/jama.2022.1922).
- 926 26. Costa Clemens, S.A., Weckx, L., Clemens, R., Almeida Mendes, A.V., Ramos Souza, A.,
927 Silveira, M.B.V., da Guarda, S.N.F., de Nobrega, M.M., de Moraes Pinto, M.I., Gonzalez,
928 I.G.S., et al. (2022). Heterologous versus homologous COVID-19 booster vaccination in
929 previous recipients of two doses of CoronaVac COVID-19 vaccine in Brazil (RHH-001): a
930 phase 4, non-inferiority, single blind, randomised study. *Lancet* 399, 521-529.
931 [10.1016/S0140-6736\(22\)00094-0](https://doi.org/10.1016/S0140-6736(22)00094-0).
- 932 27. Corbett, K.S., Nason, M.C., Flach, B., Gagne, M., O'Connell, S., Johnston, T.S., Shah, S.N.,
933 Edara, V.V., Floyd, K., Lai, L., et al. (2021). Immune correlates of protection by mRNA-
934 1273 vaccine against SARS-CoV-2 in nonhuman primates. *Science* 373, eabj0299.
935 [10.1126/science.abj0299](https://doi.org/10.1126/science.abj0299).
- 936 28. Gilbert, P.B., Donis, R.O., Koup, R.A., Fong, Y., Plotkin, S.A., and Follmann, D. (2022). A
937 Covid-19 Milestone Attained - A Correlate of Protection for Vaccines. *N Engl J Med* 387,
938 2203-2206. [10.1056/NEJMp2211314](https://doi.org/10.1056/NEJMp2211314).
- 939 29. Kim, D., Lee, J.Y., Yang, J.S., Kim, J.W., Kim, V.N., and Chang, H. (2020). The Architecture
940 of SARS-CoV-2 Transcriptome. *Cell* 181, 914-921 e910. [10.1016/j.cell.2020.04.011](https://doi.org/10.1016/j.cell.2020.04.011).

- 941 30. Zou, L., Ruan, F., Huang, M., Liang, L., Huang, H., Hong, Z., Yu, J., Kang, M., Song, Y., Xia,
942 J., et al. (2020). SARS-CoV-2 Viral Load in Upper Respiratory Specimens of Infected
943 Patients. *N Engl J Med* 382, 1177-1179. 10.1056/NEJMc2001737.
- 944 31. Lavelle, E.C., and Ward, R.W. (2022). Mucosal vaccines - fortifying the frontiers. *Nat Rev*
945 *Immunol* 22, 236-250. 10.1038/s41577-021-00583-2.
- 946 32. Hachmann, N.P., Miller, J., Collier, A.Y., Ventura, J.D., Yu, J., Rowe, M., Bondzie, E.A.,
947 Powers, O., Surve, N., Hall, K., and Barouch, D.H. (2022). Neutralization Escape by SARS-
948 CoV-2 Omicron Subvariants BA.2.12.1, BA.4, and BA.5. *N Engl J Med* 387, 86-88.
949 10.1056/NEJMc2206576.
- 950 33. Gagne, M., Moliva, J.I., Foulds, K.E., Andrew, S.F., Flynn, B.J., Werner, A.P., Wagner, D.A.,
951 Teng, I.T., Lin, B.C., Moore, C., et al. (2022). mRNA-1273 or mRNA-Omicron boost in
952 vaccinated macaques elicits similar B cell expansion, neutralizing responses, and
953 protection from Omicron. *Cell* 185, 1556-1571 e1518. 10.1016/j.cell.2022.03.038.
- 954 34. Jackson, L.A., Anderson, E.J., Roupheal, N.G., Roberts, P.C., Makhene, M., Coler, R.N.,
955 McCullough, M.P., Chappell, J.D., Denison, M.R., Stevens, L.J., et al. (2020). An mRNA
956 Vaccine against SARS-CoV-2 - Preliminary Report. *N Engl J Med* 383, 1920-1931.
957 10.1056/NEJMoa2022483.
- 958 35. Johnston, R.J., Poholek, A.C., DiToro, D., Yusuf, I., Eto, D., Barnett, B., Dent, A.L., Craft, J.,
959 and Crotty, S. (2009). Bcl6 and Blimp-1 are reciprocal and antagonistic regulators of T
960 follicular helper cell differentiation. *Science* 325, 1006-1010. 10.1126/science.1175870.
- 961 36. Nurieva, R.I., Chung, Y., Martinez, G.J., Yang, X.O., Tanaka, S., Matskevitch, T.D., Wang,
962 Y.H., and Dong, C. (2009). Bcl6 mediates the development of T follicular helper cells.
963 *Science* 325, 1001-1005. 10.1126/science.1176676.
- 964 37. Tangye, S.G., Ferguson, A., Avery, D.T., Ma, C.S., and Hodgkin, P.D. (2002). Isotype
965 switching by human B cells is division-associated and regulated by cytokines. *J Immunol*
966 169, 4298-4306. 10.4049/jimmunol.169.8.4298.
- 967 38. Koup, R.A., and Douek, D.C. (2011). Vaccine design for CD8 T lymphocyte responses.
968 *Cold Spring Harb Perspect Med* 1, a007252. 10.1101/cshperspect.a007252.
- 969 39. Corbett, K.S., Gagne, M., Wagner, D.A., S, O.C., Narpala, S.R., Flebbe, D.R., Andrew, S.F.,
970 Davis, R.L., Flynn, B., Johnston, T.S., et al. (2021). Protection against SARS-CoV-2 Beta
971 variant in mRNA-1273 vaccine-boosted nonhuman primates. *Science* 374, 1343-1353.
972 10.1126/science.abl8912.
- 973 40. Wang, L., Zhou, T., Zhang, Y., Yang, E.S., Schramm, C.A., Shi, W., Pegu, A., Oloniniyi, O.K.,
974 Henry, A.R., Darko, S., et al. (2021). Ultrapotent antibodies against diverse and highly
975 transmissible SARS-CoV-2 variants. *Science* 373. 10.1126/science.abh1766.
- 976 41. Barnes, C.O., Jette, C.A., Abernathy, M.E., Dam, K.A., Esswein, S.R., Gristick, H.B.,
977 Malyutin, A.G., Sharaf, N.G., Huey-Tubman, K.E., Lee, Y.E., et al. (2020). SARS-CoV-2
978 neutralizing antibody structures inform therapeutic strategies. *Nature* 588, 682-687.
979 10.1038/s41586-020-2852-1.
- 980 42. Yuan, M., Wu, N.C., Zhu, X., Lee, C.D., So, R.T.Y., Lv, H., Mok, C.K.P., and Wilson, I.A.
981 (2020). A highly conserved cryptic epitope in the receptor binding domains of SARS-CoV-
982 2 and SARS-CoV. *Science* 368, 630-633. 10.1126/science.abb7269.
- 983 43. Afkhami, S., D'Agostino, M.R., Zhang, A., Stacey, H.D., Marzok, A., Kang, A., Singh, R.,
984 Bavananthasivam, J., Ye, G., Luo, X., et al. (2022). Respiratory mucosal delivery of next-

- 985 generation COVID-19 vaccine provides robust protection against both ancestral and
986 variant strains of SARS-CoV-2. *Cell* *185*, 896-915 e819. 10.1016/j.cell.2022.02.005.
- 987 44. Jeyanathan, V., Afkhami, S., D'Agostino, M.R., Zganiacz, A., Feng, X., Miller, M.S.,
988 Jeyanathan, M., Thompson, M.R., and Xing, Z. (2022). Differential Biodistribution of
989 Adenoviral-Vectored Vaccine Following Intranasal and Endotracheal Deliveries Leads to
990 Different Immune Outcomes. *Front Immunol* *13*, 860399. 10.3389/fimmu.2022.860399.
- 991 45. Lanini, S., Capone, S., Antinori, A., Milleri, S., Nicastrì, E., Camerini, R., Agrati, C.,
992 Castilletti, C., Mori, F., Sacchi, A., et al. (2022). GRAd-COV2, a gorilla adenovirus-based
993 candidate vaccine against COVID-19, is safe and immunogenic in younger and older
994 adults. *Sci Transl Med* *14*, eabj1996. 10.1126/scitranslmed.abj1996.
- 995 46. Capone, S., Fusco, F.M., Milleri, S., Borrè, S., Carbonara, S., Lo Caputo, S., Leone, S., Gori,
996 G., Maggi, P., Cascio, A., et al. (2022). GRAd-COV2 vaccine provides potent and durable
997 immunity in randomised placebo-controlled phase 2 trial (COVITAR). medRxiv,
998 2022.2010.2008.22280836. 10.1101/2022.10.08.22280836.
- 999 47. Sadoff, J., Gray, G., Vandebosch, A., Cárdenas, V., Shukarev, G., Grinsztejn, B., Goepfert,
1000 P.A., Truyers, C., Fennema, H., Spiessens, B., et al. (2021). Safety and Efficacy of Single-
1001 Dose Ad26.COV2.S Vaccine against Covid-19. *N Engl J Med* *384*, 2187-2201.
1002 10.1056/NEJMoa2101544.
- 1003 48. Logunov, D.Y., Dolzhikova, I.V., Zubkova, O.V., Tukhvatullin, A.I., Shcheblyakov, D.V.,
1004 Dzhharullaeva, A.S., Grousova, D.M., Erokhova, A.S., Kovyrshina, A.V., Botikov, A.G., et al.
1005 (2020). Safety and immunogenicity of an rAd26 and rAd5 vector-based heterologous
1006 prime-boost COVID-19 vaccine in two formulations: two open, non-randomised phase
1007 1/2 studies from Russia. *Lancet* *396*, 887-897. 10.1016/S0140-6736(20)31866-3.
- 1008 49. Zhu, F.C., Guan, X.H., Li, Y.H., Huang, J.Y., Jiang, T., Hou, L.H., Li, J.X., Yang, B.F., Wang, L.,
1009 Wang, W.J., et al. (2020). Immunogenicity and safety of a recombinant adenovirus type-
1010 5-vectored COVID-19 vaccine in healthy adults aged 18 years or older: a randomised,
1011 double-blind, placebo-controlled, phase 2 trial. *Lancet* *396*, 479-488. 10.1016/S0140-
1012 6736(20)31605-6.
- 1013 50. Zhu, F.C., Li, Y.H., Guan, X.H., Hou, L.H., Wang, W.J., Li, J.X., Wu, S.P., Wang, B.S., Wang,
1014 Z., Wang, L., et al. (2020). Safety, tolerability, and immunogenicity of a recombinant
1015 adenovirus type-5 vectored COVID-19 vaccine: a dose-escalation, open-label, non-
1016 randomised, first-in-human trial. *Lancet* *395*, 1845-1854. 10.1016/S0140-
1017 6736(20)31208-3.
- 1018 51. Polack, F.P., Thomas, S.J., Kitchin, N., Absalon, J., Gurtman, A., Lockhart, S., Perez, J.L.,
1019 Perez Marc, G., Moreira, E.D., Zerbini, C., et al. (2020). Safety and Efficacy of the
1020 BNT162b2 mRNA Covid-19 Vaccine. *N Engl J Med* *383*, 2603-2615.
1021 10.1056/NEJMoa2034577.
- 1022 52. Keech, C., Albert, G., Cho, I., Robertson, A., Reed, P., Neal, S., Plested, J.S., Zhu, M.,
1023 Cloney-Clark, S., Zhou, H., et al. (2020). Phase 1-2 Trial of a SARS-CoV-2 Recombinant
1024 Spike Protein Nanoparticle Vaccine. *N Engl J Med* *383*, 2320-2332.
1025 10.1056/NEJMoa2026920.
- 1026 53. Agrati, C., Castilletti, C., Battella, S., Cimini, E., Matusali, G., Sommella, A., Sacchi, A.,
1027 Colavita, F., Contino, A.M., Bordoni, V., et al. (2022). Safety and immune response

- 1028 kinetics of GRAd-COV2 vaccine: phase 1 clinical trial results. *NPJ Vaccines* 7, 111.
1029 10.1038/s41541-022-00531-8.
- 1030 54. Anderson, E.J., Roupheal, N.G., Widge, A.T., Jackson, L.A., Roberts, P.C., Makhene, M.,
1031 Chappell, J.D., Denison, M.R., Stevens, L.J., Pruijssers, A.J., et al. (2020). Safety and
1032 Immunogenicity of SARS-CoV-2 mRNA-1273 Vaccine in Older Adults. *N Engl J Med* 383,
1033 2427-2438. 10.1056/NEJMoa2028436.
- 1034 55. Walsh, E.E., Frenck, R.W., Jr., Falsey, A.R., Kitchin, N., Absalon, J., Gurtman, A., Lockhart,
1035 S., Neuzil, K., Mulligan, M.J., Bailey, R., et al. (2020). Safety and Immunogenicity of Two
1036 RNA-Based Covid-19 Vaccine Candidates. *N Engl J Med* 383, 2439-2450.
1037 10.1056/NEJMoa2027906.
- 1038 56. Sadoff, J., Le Gars, M., Shukarev, G., Heerwegh, D., Truyers, C., de Groot, A.M., Stoop, J.,
1039 Tete, S., Van Damme, W., Leroux-Roels, I., et al. (2021). Interim Results of a Phase 1-2a
1040 Trial of Ad26.COV2.S Covid-19 Vaccine. *N Engl J Med* 384, 1824-1835.
1041 10.1056/NEJMoa2034201.
- 1042 57. Gilbert, P.B., Montefiori, D.C., McDermott, A.B., Fong, Y., Benkeser, D., Deng, W., Zhou,
1043 H., Houchens, C.R., Martins, K., Jayashankar, L., et al. (2022). Immune correlates analysis
1044 of the mRNA-1273 COVID-19 vaccine efficacy clinical trial. *Science* 375, 43-50.
1045 10.1126/science.abm3425.
- 1046 58. Goldblatt, D., Fiore-Gartland, A., Johnson, M., Hunt, A., Bengt, C., Zavadzka, D., Snipe,
1047 H.D., Brown, J.S., Workman, L., Zar, H.J., et al. (2022). Towards a population-based
1048 threshold of protection for COVID-19 vaccines. *Vaccine* 40, 306-315.
1049 10.1016/j.vaccine.2021.12.006.
- 1050 59. Agrati, C., Capone, S., Castilletti, C., Cimini, E., Matusali, G., Meschi, S., Tartaglia, E.,
1051 Camerini, R., Lanini, S., Milleri, S., et al. (2021). Strong immunogenicity of heterologous
1052 prime-boost immunizations with the experimental vaccine GRAd-COV2 and BNT162b2
1053 or ChAdOx1-nCOV19. *NPJ Vaccines* 6, 131. 10.1038/s41541-021-00394-5.
- 1054 60. Ameratunga, R., Woon, S.T., Steele, R., Lehnert, K., Leung, E., Edwards, E.S.J., and
1055 Brooks, A.E.S. (2021). Common Variable Immunodeficiency Disorders as a Model for
1056 Assessing COVID-19 Vaccine Responses in Immunocompromised Patients. *Front*
1057 *Immunol* 12, 798389. 10.3389/fimmu.2021.798389.
- 1058 61. Milito, C., Lougaris, V., Giardino, G., Punziano, A., Vultaggio, A., Carrabba, M., Cinetto, F.,
1059 Scarpa, R., Delle Piane, R.M., Baselli, L., et al. (2021). Clinical outcome, incidence, and
1060 SARS-CoV-2 infection-fatality rates in Italian patients with inborn errors of immunity. *J*
1061 *Allergy Clin Immunol Pract* 9, 2904-2906 e2902. 10.1016/j.jaip.2021.04.017.
- 1062 62. Colkesen, F., Kandemir, B., Arslan, S., Colkesen, F., Yildiz, E., Korkmaz, C., Vatansev, H.,
1063 Evcen, R., Aykan, F.S., Kilinc, M., et al. (2022). Relationship between Selective IgA
1064 Deficiency and COVID-19 Prognosis. *Jpn J Infect Dis* 75, 228-233.
1065 10.7883/yoken.JJID.2021.281.
- 1066 63. Barzegar-Amini, M., Mahmoudi, M., Dadgarmoghaddam, M., Farzad, F., Najafabadi,
1067 A.Q., and Jabbari-Azad, F. (2022). Comparison of Serum Total IgA Levels in Severe and
1068 Mild COVID-19 Patients and Control Group. *J Clin Immunol* 42, 10-18. 10.1007/s10875-
1069 021-01149-6.
- 1070 64. Joyce, M.G., King, H.A.D., Elakhal-Naouar, I., Ahmed, A., Peachman, K.K., Macedo
1071 Cincotta, C., Subra, C., Chen, R.E., Thomas, P.V., Chen, W.H., et al. (2022). A SARS-CoV-2

- 1072 ferritin nanoparticle vaccine elicits protective immune responses in nonhuman
1073 primates. *Sci Transl Med* 14, eabi5735. 10.1126/scitranslmed.abi5735.
- 1074 65. Bos, R., Rutten, L., van der Lubbe, J.E.M., Bakkers, M.J.G., Hardenberg, G., Wegmann, F.,
1075 Zuijdsgeest, D., de Wilde, A.H., Koornneef, A., Verwilligen, A., et al. (2020). Ad26 vector-
1076 based COVID-19 vaccine encoding a prefusion-stabilized SARS-CoV-2 Spike immunogen
1077 induces potent humoral and cellular immune responses. *NPJ Vaccines* 5, 91.
1078 10.1038/s41541-020-00243-x.
- 1079 66. Bolton, D.L., Song, K., Tomaras, G.D., Rao, S., and Roederer, M. (2017). Unique cellular
1080 and humoral immunogenicity profiles generated by aerosol, intranasal, or parenteral
1081 vaccination in rhesus macaques. *Vaccine* 35, 639-646. 10.1016/j.vaccine.2016.12.008.
- 1082 67. Corbett, K.S., Werner, A.P., Connell, S.O., Gagne, M., Lai, L., Moliva, J.I., Flynn, B., Choi,
1083 A., Koch, M., Foulds, K.E., et al. (2021). mRNA-1273 protects against SARS-CoV-2 beta
1084 infection in nonhuman primates. *Nat Immunol* 22, 1306-1315. 10.1038/s41590-021-
1085 01021-0.
- 1086 68. Szabo, P.A., Dogra, P., Gray, J.I., Wells, S.B., Connors, T.J., Weisberg, S.P., Krupska, I.,
1087 Matsumoto, R., Poon, M.M.L., Idzikowski, E., et al. (2021). Longitudinal profiling of
1088 respiratory and systemic immune responses reveals myeloid cell-driven lung
1089 inflammation in severe COVID-19. *Immunity* 54, 797-814 e796.
1090 10.1016/j.immuni.2021.03.005.
- 1091 69. Tan, A.T., Linster, M., Tan, C.W., Le Bert, N., Chia, W.N., Kunasegaran, K., Zhuang, Y.,
1092 Tham, C.Y.L., Chia, A., Smith, G.J.D., et al. (2021). Early induction of functional SARS-CoV-
1093 2-specific T cells associates with rapid viral clearance and mild disease in COVID-19
1094 patients. *Cell Rep* 34, 108728. 10.1016/j.celrep.2021.108728.
- 1095 70. Kohlmeier, J.E., Miller, S.C., and Woodland, D.L. (2007). Cutting edge: Antigen is not
1096 required for the activation and maintenance of virus-specific memory CD8+ T cells in the
1097 lung airways. *J Immunol* 178, 4721-4725. 10.4049/jimmunol.178.8.4721.
- 1098 71. Auladell, M., Jia, X., Hensen, L., Chua, B., Fox, A., Nguyen, T.H.O., Doherty, P.C., and
1099 Kedzierska, K. (2019). Recalling the Future: Immunological Memory Toward
1100 Unpredictable Influenza Viruses. *Front Immunol* 10, 1400. 10.3389/fimmu.2019.01400.
- 1101 72. Sette, A., and Crotty, S. (2021). Adaptive immunity to SARS-CoV-2 and COVID-19. *Cell*
1102 184, 861-880. 10.1016/j.cell.2021.01.007.
- 1103 73. Goel, R.R., Painter, M.M., Apostolidis, S.A., Mathew, D., Meng, W., Rosenfeld, A.M.,
1104 Lundgreen, K.A., Reynaldi, A., Khoury, D.S., Pattekar, A., et al. (2021). mRNA vaccines
1105 induce durable immune memory to SARS-CoV-2 and variants of concern. *Science* 374,
1106 abm0829. 10.1126/science.abm0829.
- 1107 74. Kawasaki, T., Ikegawa, M., and Kawai, T. (2022). Antigen Presentation in the Lung. *Front*
1108 *Immunol* 13, 860915. 10.3389/fimmu.2022.860915.
- 1109 75. Rijkers, G.T., Weterings, N., Obregon-Henao, A., Lepolder, M., Dutt, T.S., van Overveld,
1110 F.J., and Henao-Tamayo, M. (2021). Antigen Presentation of mRNA-Based and Virus-
1111 Vectored SARS-CoV-2 Vaccines. *Vaccines (Basel)* 9. 10.3390/vaccines9080848.
- 1112 76. Darrah, P.A., DiFazio, R.M., Maiello, P., Gideon, H.P., Myers, A.J., Rodgers, M.A.,
1113 Hackney, J.A., Lindenstrom, T., Evans, T., Scanga, C.A., et al. (2019). Boosting BCG with
1114 proteins or rAd5 does not enhance protection against tuberculosis in rhesus macaques.
1115 *NPJ Vaccines* 4, 21. 10.1038/s41541-019-0113-9.

- 1116 77. Pallesen, J., Wang, N., Corbett, K.S., Wrapp, D., Kirchdoerfer, R.N., Turner, H.L., Cottrell,
1117 C.A., Becker, M.M., Wang, L., Shi, W., et al. (2017). Immunogenicity and structures of a
1118 rationally designed prefusion MERS-CoV spike antigen. *Proc Natl Acad Sci U S A* *114*,
1119 E7348-E7357. [10.1073/pnas.1707304114](https://doi.org/10.1073/pnas.1707304114).
- 1120 78. Cibelli, N., Arias, G., Figur, M., Khayat, S.S., Leach, K., Loukinov, I., Shadrack, W.,
1121 Chuenchor, W., Tsybovsky, Y., Vaccine Production Program Analytical, D., et al. (2022).
1122 Advances in purification of SARS-CoV-2 spike ectodomain protein using high-throughput
1123 screening and non-affinity methods. *Sci Rep* *12*, 4458. [10.1038/s41598-022-07485-w](https://doi.org/10.1038/s41598-022-07485-w).
- 1124 79. Corbett, K.S., Flynn, B., Foulds, K.E., Francica, J.R., Boyoglu-Barnum, S., Werner, A.P.,
1125 Flach, B., O'Connell, S., Bock, K.W., Minai, M., et al. (2020). Evaluation of the mRNA-
1126 1273 Vaccine against SARS-CoV-2 in Nonhuman Primates. *N Engl J Med* *383*, 1544-1555.
1127 [10.1056/NEJMoa2024671](https://doi.org/10.1056/NEJMoa2024671).
- 1128 80. Shen, X., Tang, H., McDanal, C., Wagh, K., Fischer, W., Theiler, J., Yoon, H., Li, D., Haynes,
1129 B.F., Sanders, K.O., et al. (2021). SARS-CoV-2 variant B.1.1.7 is susceptible to neutralizing
1130 antibodies elicited by ancestral spike vaccines. *Cell Host Microbe* *29*, 529-539 e523.
1131 [10.1016/j.chom.2021.03.002](https://doi.org/10.1016/j.chom.2021.03.002).
- 1132 81. Donaldson, M.M., Kao, S.F., and Foulds, K.E. (2019). OMIP-052: An 18-Color Panel for
1133 Measuring Th1, Th2, Th17, and Tfh Responses in Rhesus Macaques. *Cytometry A* *95*,
1134 261-263. [10.1002/cyto.a.23670](https://doi.org/10.1002/cyto.a.23670).
- 1135 82. Marcus, H., Thompson, E., Zhou, Y., Bailey, M., Donaldson, M.M., Stanley, D.A., Asiedu,
1136 C., Foulds, K.E., Roederer, M., Moliva, J.I., and Sullivan, N.J. (2021). Ebola-GP DNA Prime
1137 rAd5-GP Boost: Influence of Prime Frequency and Prime/Boost Time Interval on the
1138 Immune Response in Non-human Primates. *Front Immunol* *12*, 627688.
1139 [10.3389/fimmu.2021.627688](https://doi.org/10.3389/fimmu.2021.627688).
- 1140 83. Gagne, M., Corbett, K.S., Flynn, B.J., Foulds, K.E., Wagner, D.A., Andrew, S.F., Todd, J.M.,
1141 Honeycutt, C.C., McCormick, L., Nurmukhambetova, S.T., et al. (2022). Protection from
1142 SARS-CoV-2 Delta one year after mRNA-1273 vaccination in rhesus macaques coincides
1143 with anamnestic antibody response in the lung. *Cell* *185*, 113-130 e115.
1144 [10.1016/j.cell.2021.12.002](https://doi.org/10.1016/j.cell.2021.12.002).
- 1145

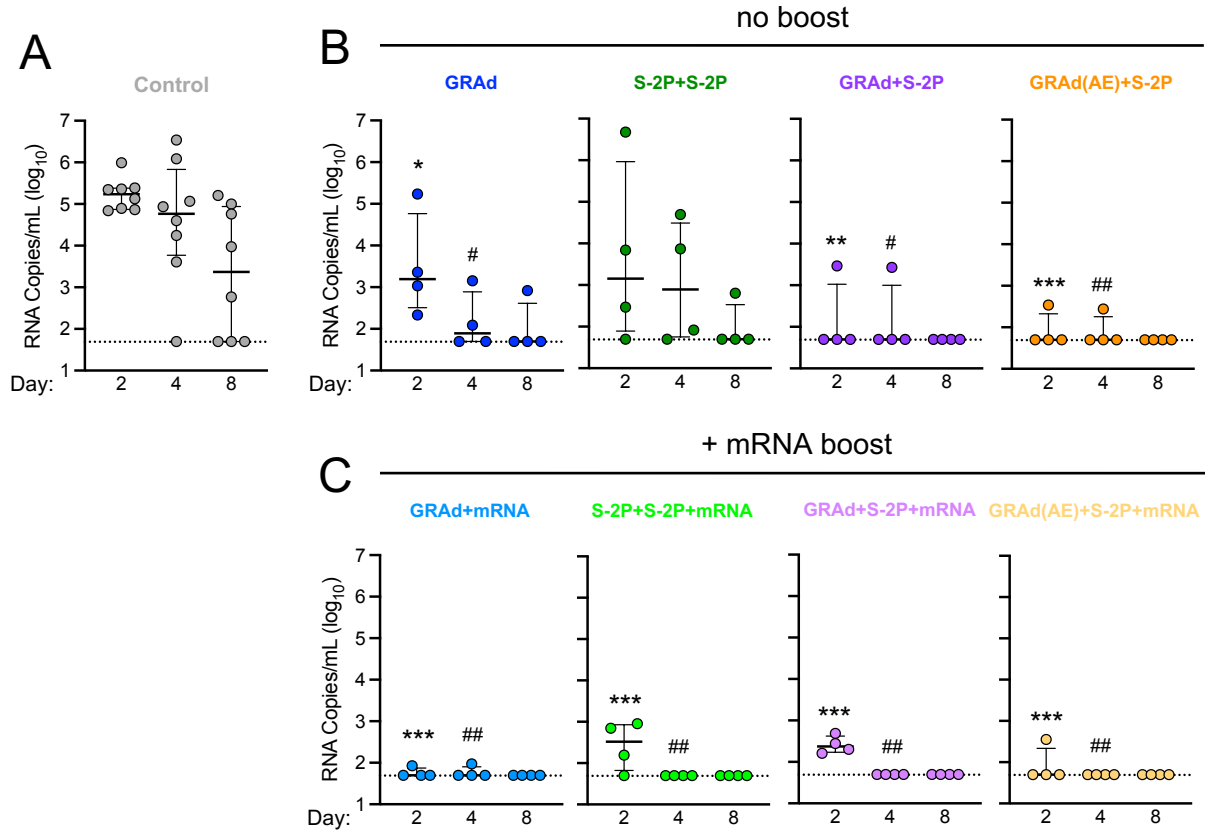


Figure 1

Figure 1. GRAd confers durable protection against BA.5 in the lower airway

(A–C) BAL was collected at days 2, 4 and 8 following challenge with 8×10^5 PFU BA.5.

(A) BA.5 sgRNA_N copy numbers per mL of BAL in control NHP.

(B) BA.5 sgRNA_N copy numbers per mL of BAL in GRAd, S-2P+S-2P, GRAd+S-2P and GRAd(AE)-S-2P NHP.

(C) BA.5 sgRNA_N copy numbers per mL of BAL in GRAd, S-2P+S-2P, GRAd+S-2P and GRAd(AE)-S-2P NHP boosted with mRNA at week 48.

Circles (A–C) indicate individual NHP. Error bars represent interquartile range with the median denoted by a horizontal line. Assay limit of detection indicated by a dotted horizontal line. Statistical analysis shown for corresponding timepoints between control and test group (e.g., ‘*’ symbols denote comparisons at day 2, ‘#’ symbols denote comparison at day 4). *,# $p < 0.05$, **,## $p < 0.01$, *** $p < 0.001$. Eight control NHP and 4 immunized NHP per cohort.

See also Figure S1 for experimental schema, Figure S2 for BA.5 titration in NHP, Figure S3 for viral load and Figure S4 for lung pathology.

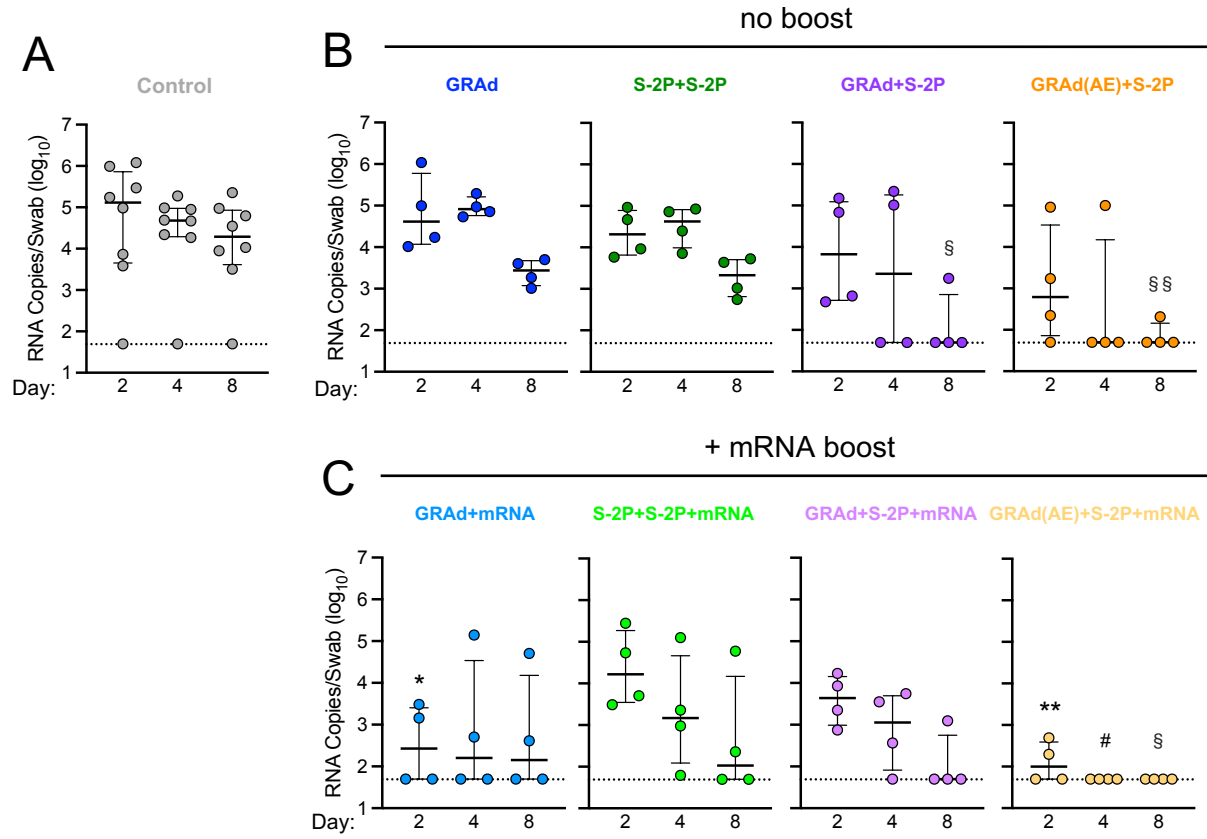


Figure 2

Figure 2. Aerosol delivery of GRAd rapidly protects against BA.5 in the upper airway

(A-C) NS was collected at days 2, 4 and 8 following challenge with 8×10^5 PFU BA.5.

(A) BA.5 sgRNA_N copy numbers per swab in control NHP.

(B) BA.5 sgRNA_N copy numbers per swab in GRAd, S-2P+S-2P, GRAd+S-2P and GRAd(AE)-S-2P NHP.

(C) BA.5 sgRNA_N copy numbers per swab in GRAd, S-2P+S-2P, GRAd+S-2P and GRAd(AE)-S-2P NHP boosted with mRNA at week 48.

Circles (A–C) indicate individual NHP. Error bars represent interquartile range with the median denoted by a horizontal line. Assay limit of detection indicated by a dotted horizontal line. Statistical analysis shown for corresponding timepoints between control and test group (*e.g.*, ‘*’ symbols denote comparison at day 2, ‘#’ symbols denote comparison at day 4, ‘\$’ symbols denote comparison at day 8). *, #, \$ $p < 0.05$, **, §§ $p < 0.01$. Eight control NHP and 4 immunized NHP per cohort.

See also Figure S1 for experimental schema, Figure S2 for BA.5 titration in NHP and Figure S3 for viral load.

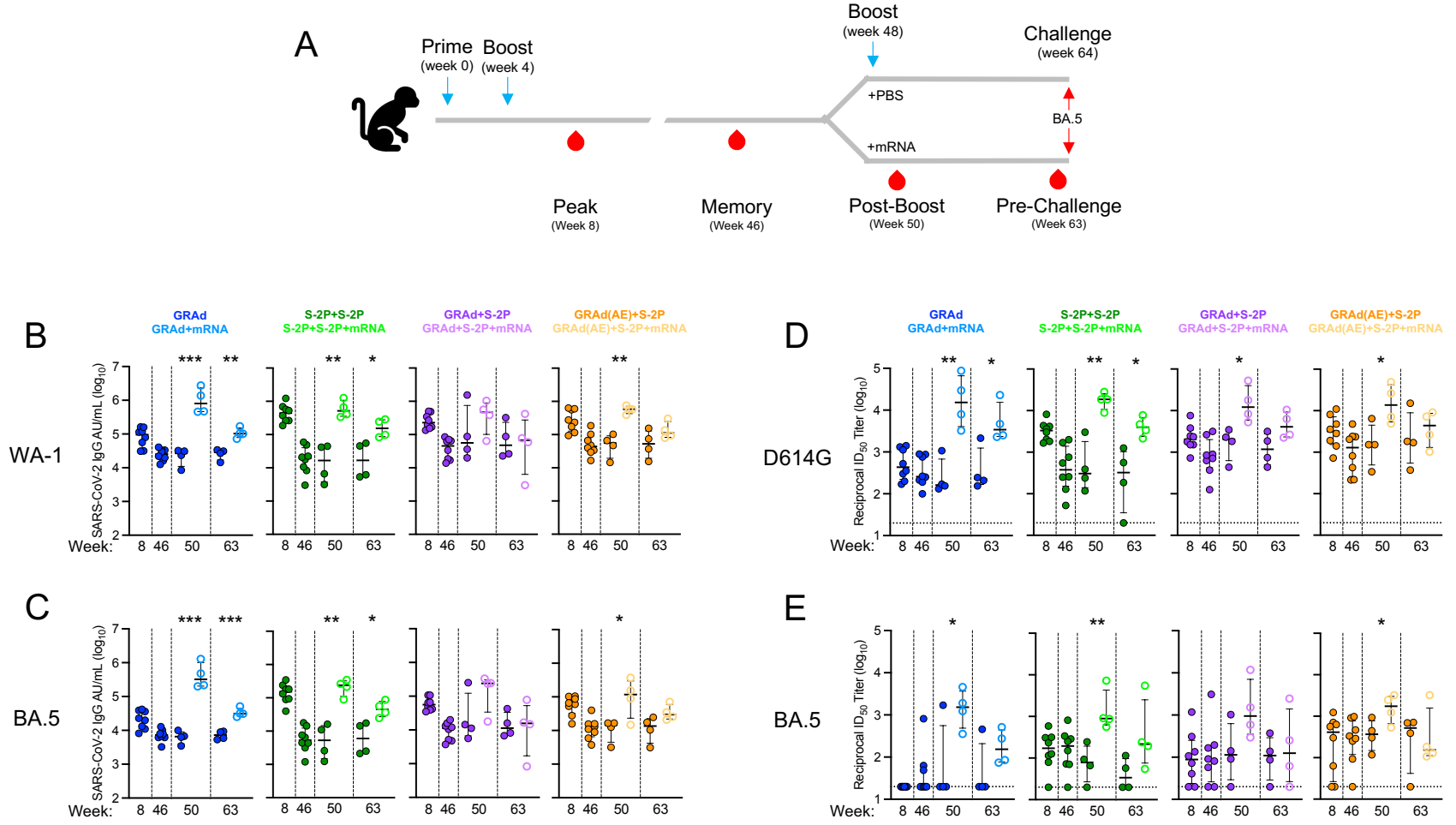


Figure 3

Figure 3. GRAd immunization strategies generate durable antibody responses to SARS-CoV-2 variants that can be boosted with mRNA.

(A) Sera were collected at week 8, 46, 50 and 63.

(B and C) IgG-binding titers to (B) ancestral WA-1 S and (C) BA.5 S expressed in AU/mL.

(D and E) Neutralizing titers to (D) ancestral D614G lentiviral pseudovirus and (E) BA.5 lentiviral pseudovirus expressed as the reciprocal ID₅₀.

Circles (B–D) represent individual NHP. Error bars represent the interquartile range with the median denoted by a horizontal black line. Assay limit of detection indicated by a horizontal dotted line which may fall below the depicted range. Vertical dashed lines are for visualization purposes only. Eight immunized NHP, split into 2 cohorts of 4 NHP post mRNA boost. Statistical analysis shown for corresponding timepoints between mRNA boosted and non-boosted cohorts. * $p < 0.05$, ** $p < 0.01$, *** $p < 0.001$. Eight immunized NHP at week 8 and 46, 4 immunized NHP at week 50 and 63.

See also Figure S1 for experimental schema, Figure S5 for neutralization responses to D614G at week 2 and 4, Figure S6 for binding and neutralizing responses to BA.1 before and following challenge, and Figure S7 for binding and neutralizing responses to WA-1/D614G and BA.5 following challenge.

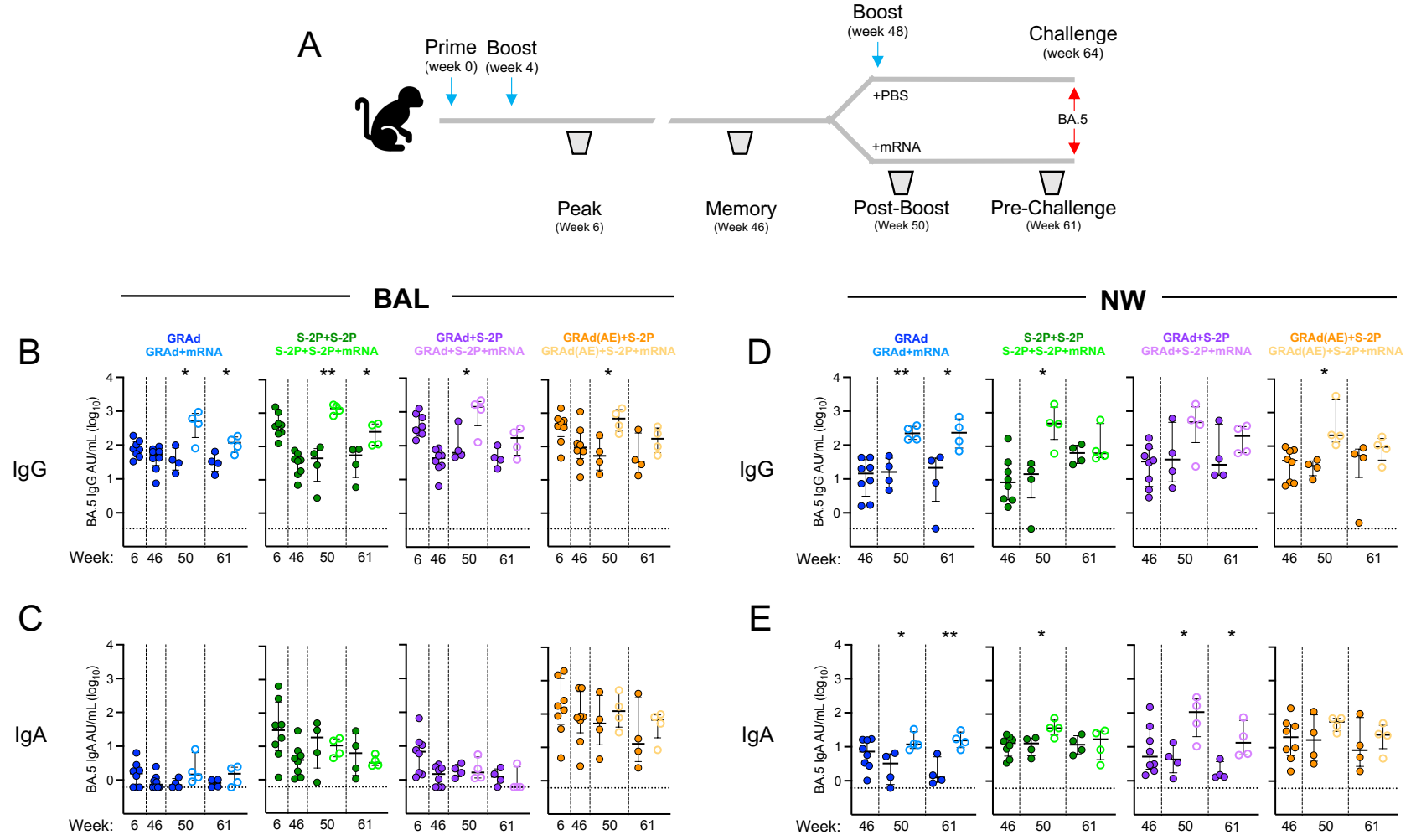


Figure 4

Figure 4. GRAd immunization strategies generate durable IgG and IgA responses to BA.5 in the lower and upper airway mucosa.

(A) BAL (B and C) was collected at week 6, 46, 50 and 61 and NW (D and E) was collected at week 46, 50, and 61.

(A and B) IgG (B) and IgA (C) antibody binding titers to BA.5 expressed in AU/mL in BAL.

(C and D) IgG (D) and IgA (E) antibody binding titers to BA.5 expressed in AU/mL in NW.

Circles (B–E) represent individual NHP. Error bars represent the interquartile range with the median denoted by a horizontal black line. Assay limit of detection indicated by a horizontal dotted line. Vertical dashed lines are for visualization purposes only. Eight vaccinated NHP, split into 2 cohorts of 4 NHP post mRNA boost. Statistical analysis shown for corresponding timepoints between mRNA boosted and non-boosted cohorts. * $p < 0.05$, ** $p < 0.01$. Eight immunized NHP at week 6 and 46, 4 immunized NHP at week 50 and 61.

See also Figure S1 for experimental schema, Figure S8 for WA-1 and BA.1 IgG and IgA BAL and NW binding titers prior to challenge, Figure S9 for IgG and IgA binding titers in BAL following challenge and Figure S10 for IgG and IgA binding titers in NW following challenge.

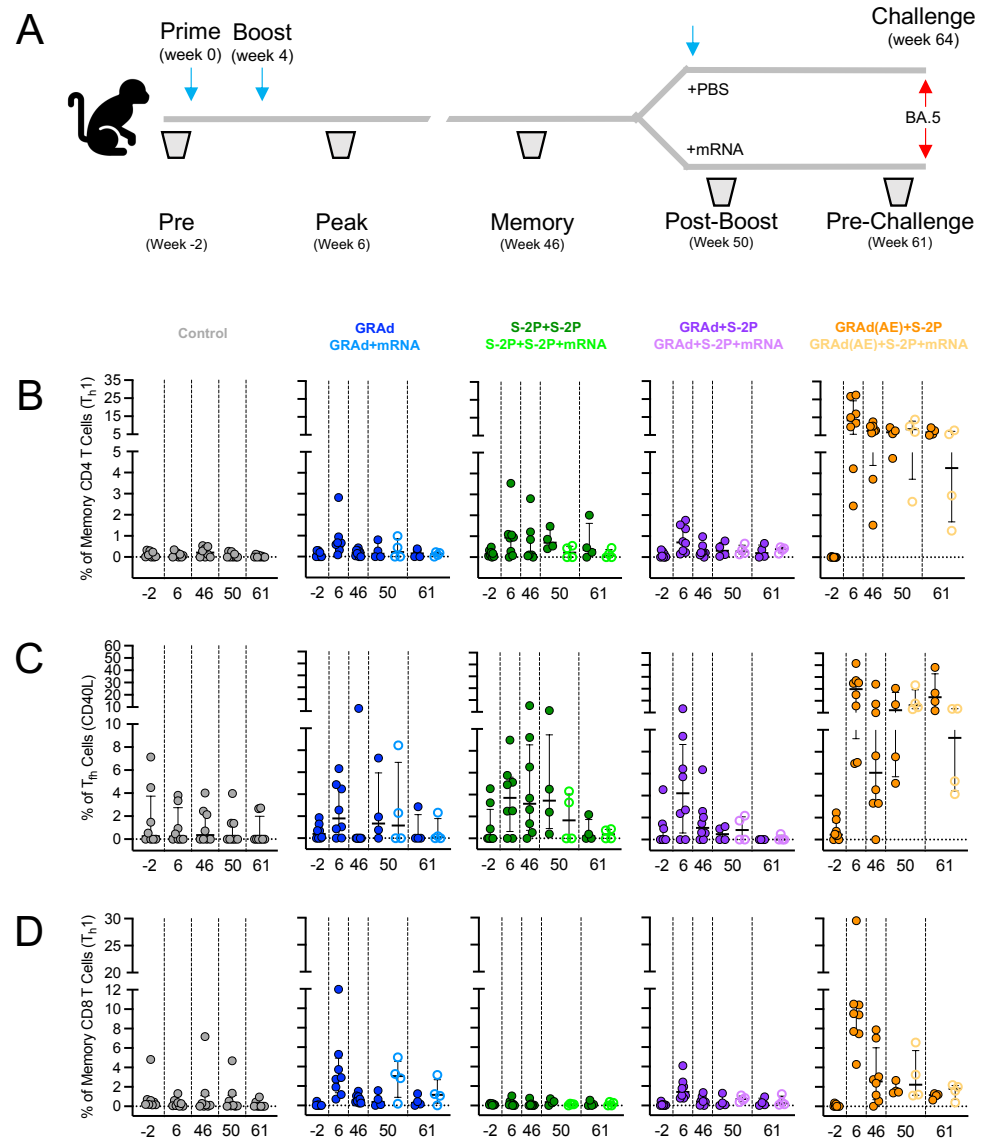


Figure 5

Figure 5. AE GRAd generates potent year-long S-specific T cell responses in the lung.

(A) BAL cells were collected at week -2, 6, 46, 50 and 61.

(B–D) Cells were stimulated with SARS-CoV-2 S1 and S2 peptide pools (WA-1) and then measured by intracellular cytokine staining.

(A) Percentage of memory CD4⁺ T cells with T_h1 markers (IL-2, TNF, or IFN γ) following stimulation.

(B) Percentage of T_{fh} cells that express CD40L.

(C) Percentage of CD8 T cells expressing IL-2, TNF, or IFN γ .

Circles in (B–D) indicate individual NHP. Error bars represent the interquartile range with the median denoted by a horizontal black line. Dotted lines set at 0%. Reported percentages may be negative due to background subtraction and may extend below the range of the y-axis. Eight vaccinated NHP, split into 2 cohorts of 4 NHP post mRNA boost. Eight control NHP, 8 immunized NHP at week 6 and 46, 4 immunized NHP at week 50 and 61.

See also Figure S1 for experimental schema, Figure S11 for T cell gating strategy, Figure S12 for T_h2 and T_{fh} (IL-21) responses in BAL prior to and following challenges, Figure S13 for CD4⁺ T_h1, T_{fh} (CD40L) and CD8⁺ T cell responses following challenge and Figure S14 for T cell responses in blood.

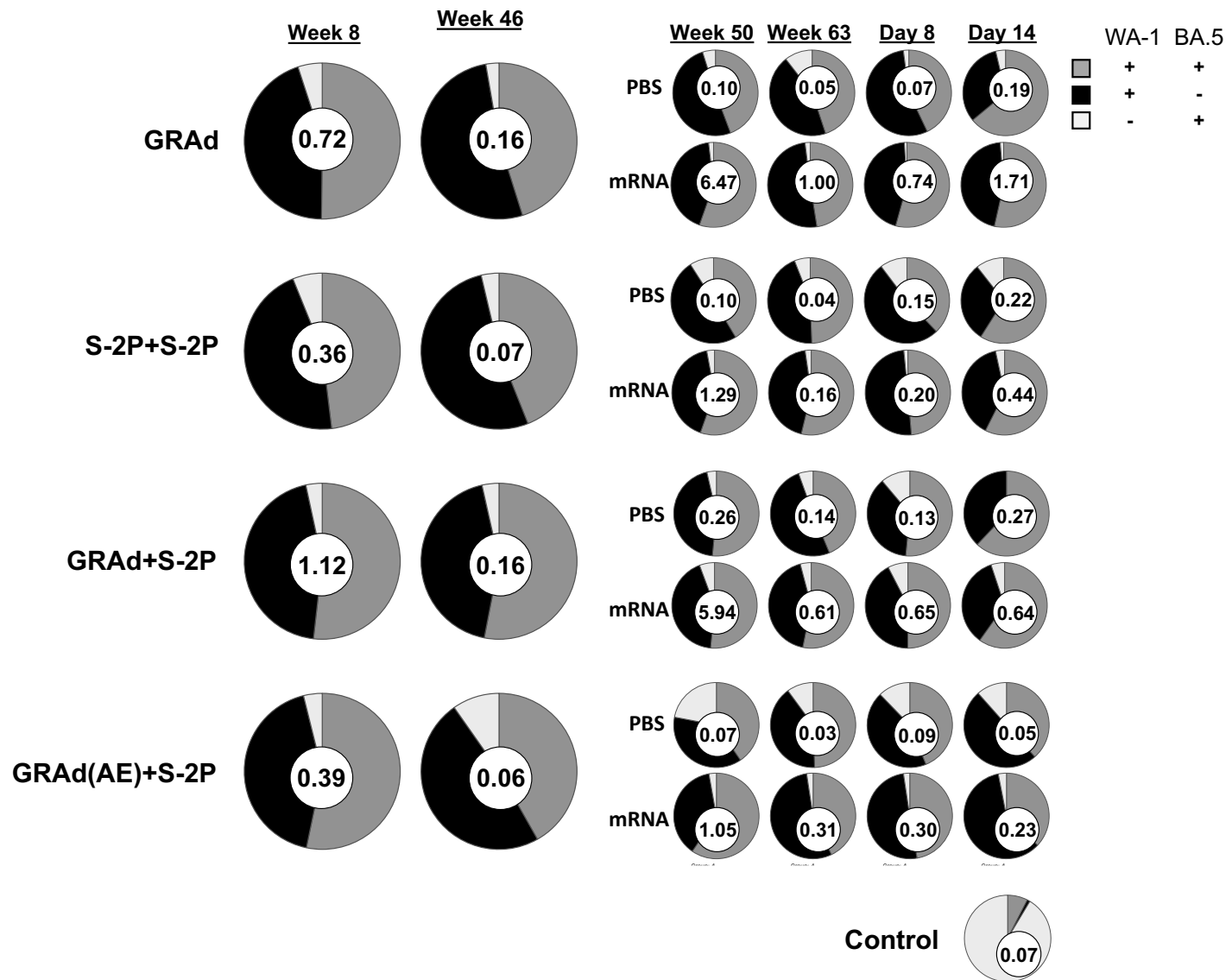


Figure 6

Figure 6: Cross-reactive S-specific memory B cells are generated following immunization.

Pie charts indicate the frequency (numbered circle at the center) and proportion of total S-2P-binding memory B cells that are dual specific for WA-1 and BA.5 (dark gray), specific for WA-1 (black), or specific for BA.5 (light gray) for all NHP in each group and timepoint in the blood at week 8, 46, 50 and 63 post-immunization, and days 8 and 14 post-challenge. Seven or eight NHP per group at week 8 and 46, 3-4 NHP per group at week 50 and 63, and day 8, 1-2 NHP at day 14.

See also Figure S1 for experimental schema, Figure S15 for B cell gating strategy and Figure S16 for WA-1 and BQ.1.1 cross-reactive B cell responses in blood.

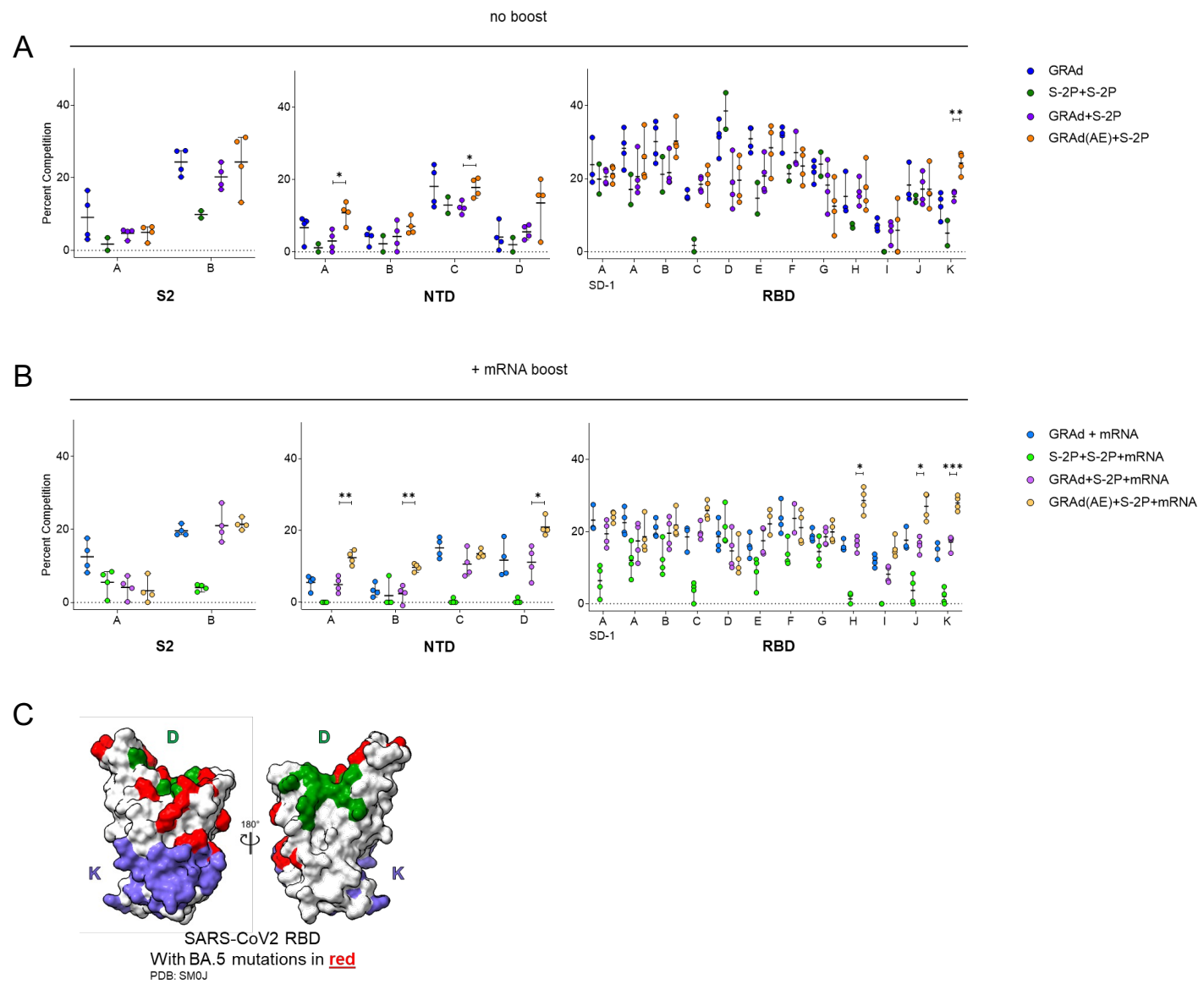


Figure 7

Figure 7: Priming with IM or AE GRAd alters serum antibody epitope profile in presence or absence of mRNA boost

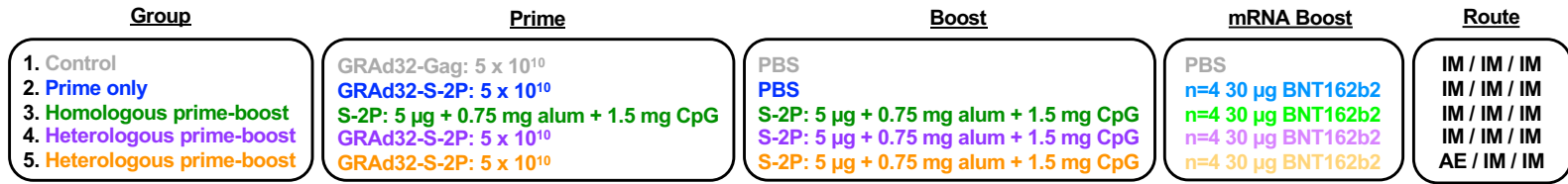
(A and B) Relative serum reactivity was measured as percent of total measured serum antibody S-2P binding competed by single monoclonal antibodies (mAbs) targeting S2, NTD, and RBD epitopes on WA-1 S-2P. Relative serum reactivity was evaluated in NHPs receiving no additional boost at week 63 (panel A) or mRNA boost (panel B).

Circles in (A and B) indicate individual NHP. Error bars represent the range with the median denoted by a horizontal black line. Eight vaccinated NHP, split into 2 cohorts of 4 NHP post mRNA boost. Statistical analysis shown for percentage of competition of binding to indicated epitopes at week 63 between “GRAd(AE)+S2P” and “GRAd+S2P” groups. * $p < 0.05$, ** $p < 0.01$, *** $p < 0.001$.

(C) Footprints of site D (A19-46.1) and Site K (CR3022) defining mAbs indicate areas of binding on SARS-CoV-2 RBD with BA.5 mutations highlighted in red.

See also Figure S1 for experimental schema.

A



B

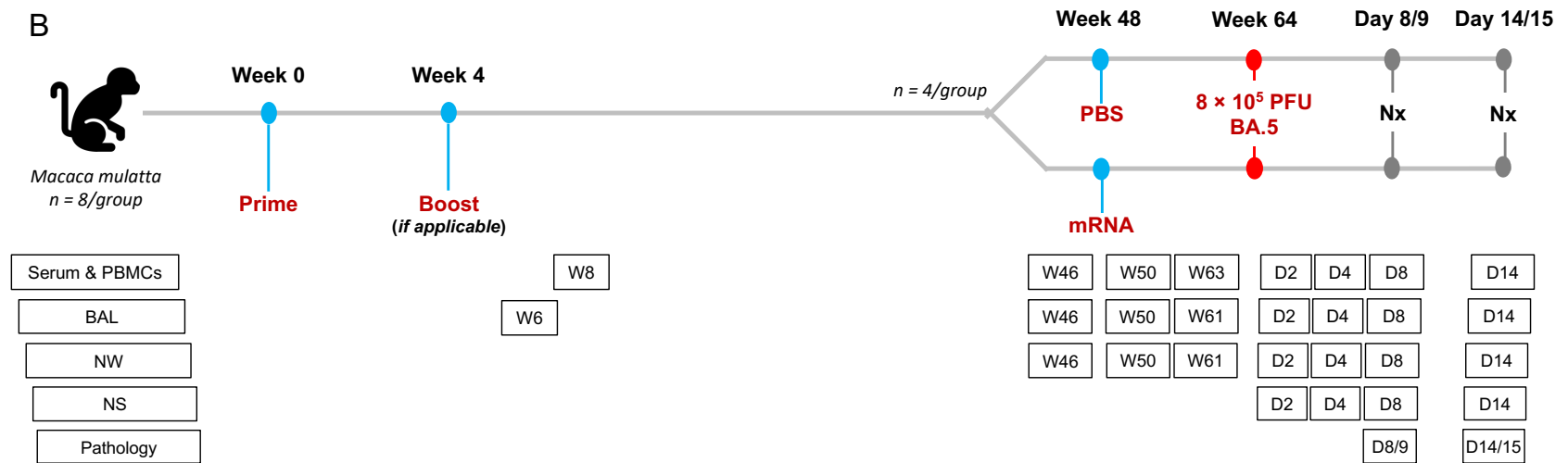


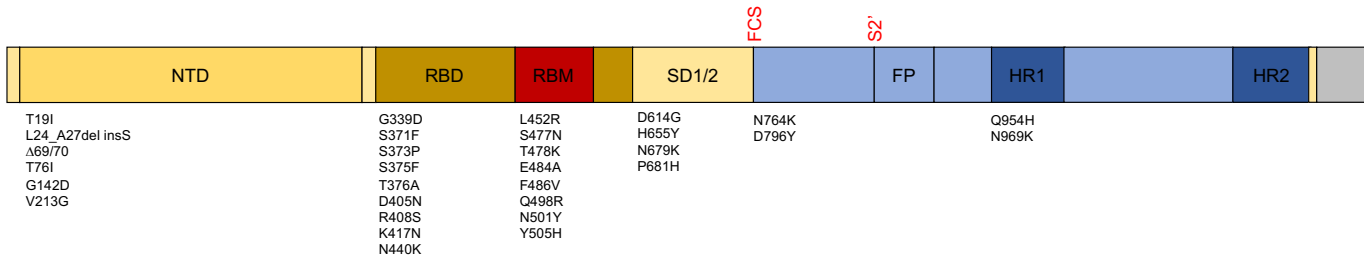
Figure S1

Figure S1. Experimental groups, timeline and sampling schedule, related to Figure 1.

(A) Eight NHP per group were immunized with a variety of different SARS-CoV-2 immunogens. Group one was immunized with 5×10^{10} GRAd32-Gag. This group served as the control. Group two was immunized with 5×10^{10} GRAd32-S-2P. Group three was immunized with 5 μ g adjuvanted S-2P (750 μ g alum and 1500 μ g CpG 1018; the same adjuvants were used when applicable). Group four was immunized with 5×10^{10} GRAd32-S-2P and with 5 μ g adjuvanted S-2P. Group five was immunized with 5×10^{10} GRAd32-S-2P delivered via aerosol (AE) and with 5 μ g adjuvanted S-2P. Phosphate buffered saline (PBS) was used as the placebo control as listed.

(B) NHP were primed with the selected immunogen at week 0, and boosted, if applicable, at week 4. At week 48 (44 weeks after the second immunization or 48 weeks after prime only), the eight macaques in each group were subdivided into two groups of 4 (except control group) and immunized with 30 μ g BNT162b2 (mRNA encoding S-2P). The week 0 and week 4 immunizations were delivered intramuscularly (IM) in 1 mL diluted in PBS (except aerosol GRAd32-S-2P) into the right deltoid, while the week 48 immunizations were delivered intramuscularly in 1 mL diluted in PBS into the right quadriceps. At week 64, all NHP were challenged with 8×10^5 PFU of BA.5. Samples were collected as listed. Abbreviations: BAL – Bronchoalveolar lavage, NW – nasal wash, NS – nasal swab, Nx – necropsy.

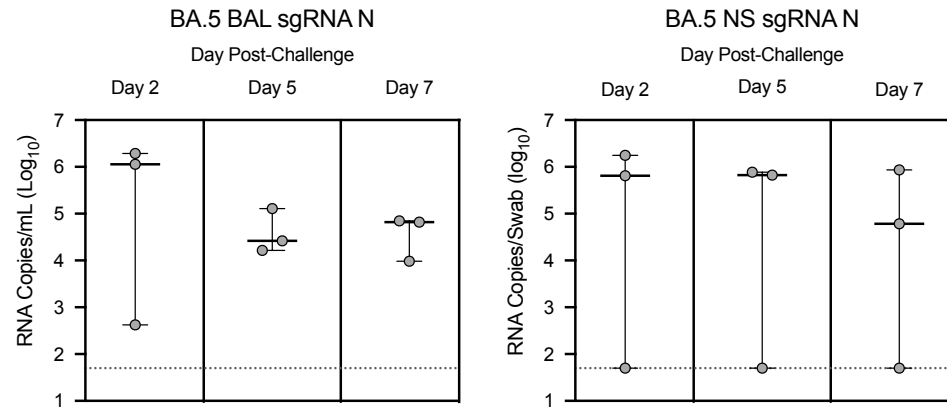
A



B

Gene	Amino acid change
ORF1ab	G82_M85del insV
ORF1ab	H83fs
ORF1ab	S135R
ORF1ab	L204F
ORF1ab	T842I
ORF1ab	G1307S
ORF1ab	L3027F
ORF1ab	T3090I
ORF1ab	T3255I
ORF1ab	P3395H
ORF1ab	L3606fs
ORF1ab	D3675/3676/3677
ORF1ab	L3829F
ORF1ab	P4715L
ORF1ab	R5716C
ORF1ab	I5967V
ORF1ab	T6564I
ORF3a	L106fs
ORF3a	T223I
E	T9I
E	Δ14
M	D3N
M	Q19E
M	A63T
N	P13L
N	Δ31/32/33
N	R203_G204del insKR
N	S413R

C



D

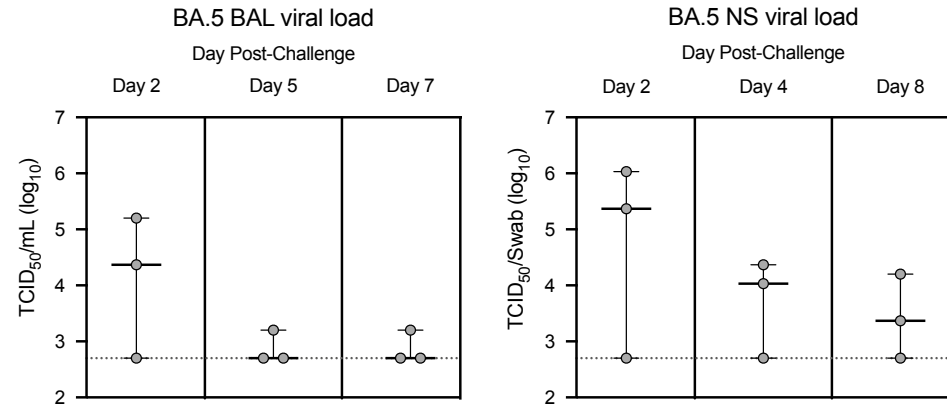


Figure S2

Figure S2. BA.5 challenge stock sequence and titration in NHP, related to Figure 1.

(A and B) BA.5 stock was sequenced and aligned with Wuhan-Hu-1.

(A) S gene only. Amino acid replacements listed above graphic. NTD, N-terminal domain; RBD, receptor binding domain; RBM, receptor binding motif; FP, fusion peptide; HR1, heptad repeat 1; HR2, heptad repeat 2; FCS, furin cleavage site; S2', S2' site.

(B) Whole genome.

(C–D) BA.5 stock was confirmed to be virulent in NHP. Circles indicate individual NHP. Error bars represent interquartile range with the median denoted by a dotted horizontal line. Assay limit of detection indicated by a horizontal dotted line.

(C) BA.5 sgRNA_N copy numbers per mL of BAL or per swab in naïve NHP.

(D) BA.5 TCID₅₀ per mL of BAL or per swab in naïve NHP.

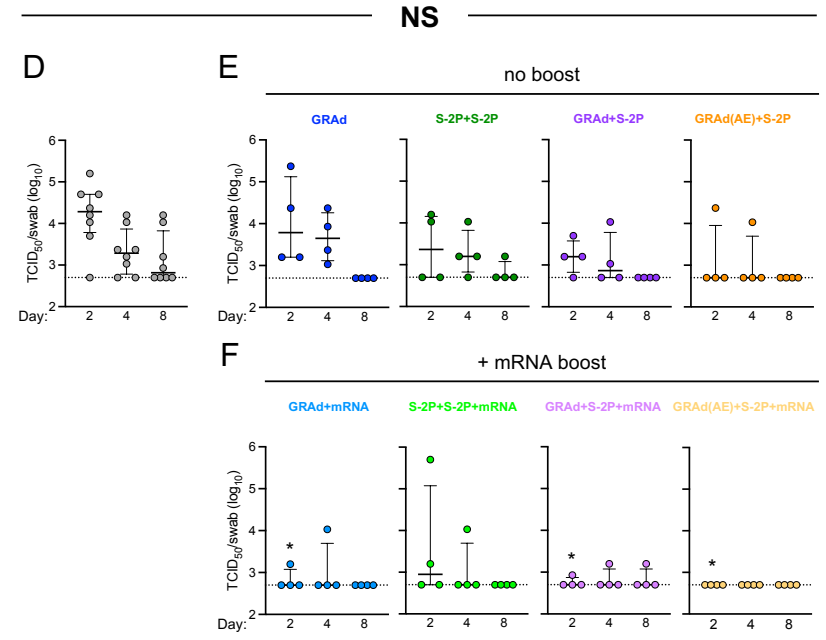
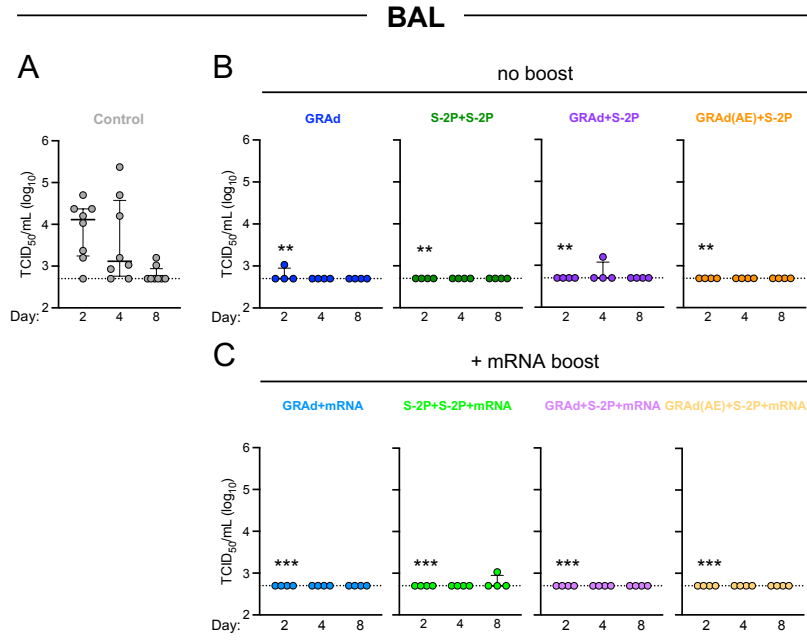


Figure S3

Figure S3. GRAd confers durable protection against BA.5 in the upper and lower airway, related to Figure 1 and 2.

(A–F) BAL and NS was collected at days 2, 4 and 8 following challenge with 8×10^5 PFU BA.5.

(A) BA.5 TCID₅₀ per mL in control NHP.

(B) BA.5 TCID₅₀ per mL in GRAd, S-2P+S-2P, GRAd+S-2P and GRAd(AE)-S-2P NHP.

(C) BA.5 TCID₅₀ per mL in GRAd, S-2P+S-2P, GRAd+S-2P and GRAd(AE)-S-2P NHP boosted with mRNA at week 48.

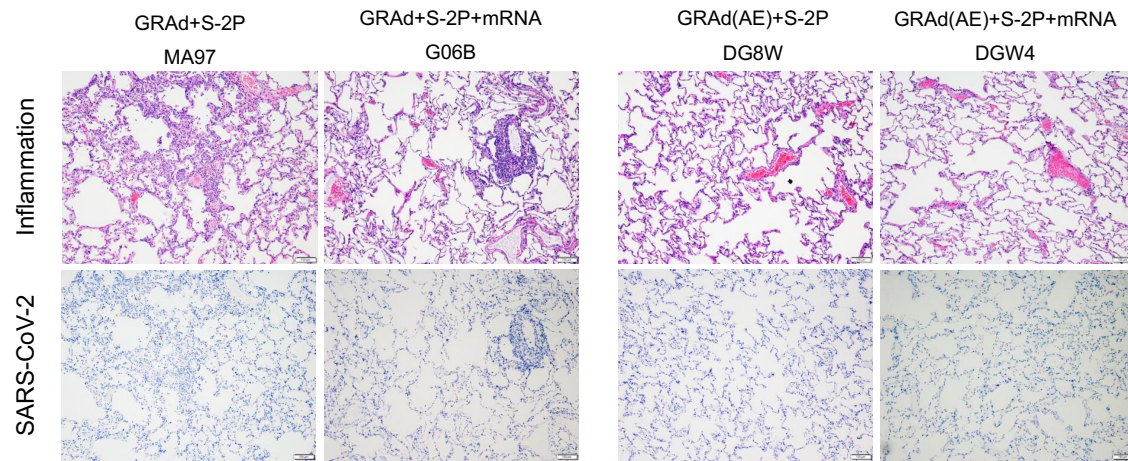
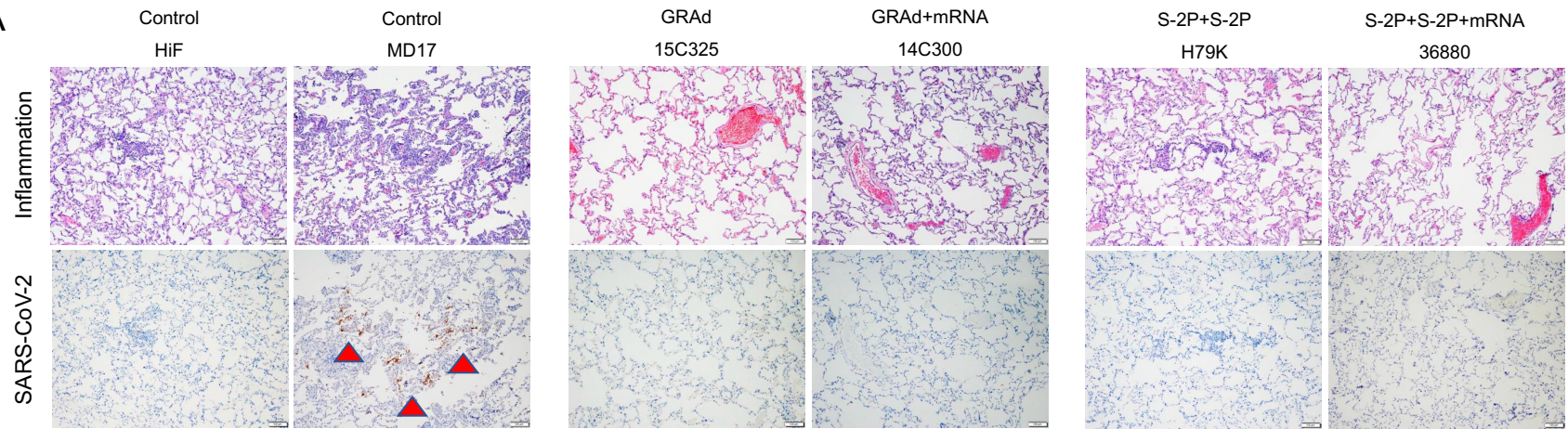
(D) BA.5 TCID₅₀ per swab in control NHP.

(E) BA.5 TCID₅₀ per swab in GRAd, S-2P+S-2P, GRAd+S-2P and GRAd(AE)-S-2P NHP.

(F) BA.5 TCID₅₀ per swab in GRAd, S-2P+S-2P, GRAd+S-2P and GRAd(AE)-S-2P NHP boosted with mRNA at week 48.

Circles (A–F) indicate individual NHP. Error bars represent interquartile range with the median denoted by a horizontal line. Assay limit of detection indicated by a dotted horizontal line. Statistical analysis shown for corresponding timepoints between control and test group (e.g., ‘*’ symbols denote comparisons at day 2). * $p < 0.05$, ** $p < 0.01$, *** $p < 0.001$. Eight control NHP and 4 immunized NHP per cohort.

A



B

			SARS-CoV-2			Inflammation						SARS-CoV-2			Inflammation		
Group	Nx	ID	Lc	Rmid	Rc	Lc	Rmid	Rc	Group	Nx	ID	Lc	Rmid	Rc	Lc	Rmid	Rc
GRAd	8	H64X	-	-	-	+	+	-	GRAd	14	H62F	-	-	-	-	+	+/-
	9	15C325	-	-	-	-	-	-		15	36887	-	-	-	-	-	-
S-2P+S-2P	8	G25K	-	-	-	-	-	+	S-2P+S-2P	14	36290	-	-	-	-	+	-
	9	H79K	-	-	-	+	-	+/-		15	0HG	-	-	-	-	-	-
GRAd+S-2P	9	MA97	-	-	-	+++	-	+	GRAd+S-2P	14	36282	-	-	-	-	-	-
	9	H83N	-	-	-	-	-	++		15	37893	-	-	-	+/-	++	+
GRAd(AE)+S-2P	8	DHGK	-	-	-	+/-	-	+	GRAd(AE)+S-2P	14	DGW7	-	-	-	+	-	-
	9	DG8W	-	-	-	-	+/-	-		15	36331	-	-	-	+/-	+/-	-
GRAd+mRNA	8	14C300	-	-	-	-	-	-	GRAd+mRNA	14	0H5	-	-	-	-	-	-
	9	LV84	-	-	-	++	+/-	-		15	MH63	-	-	-	-	-	-
S-2P+S-2P+mRNA	8	36880	-	-	-	-	-	-	S-2P+S-2P+mRNA	14	MG68	-	-	-	+/-	-	-
	9	MB39	-	-	-	-	-	++		15	14C315	-	-	-	+	+/-	+/-
GRAd+S-2P+mRNA	8	G06B	-	-	-	-	-	+/-	GRAd+S-2P+mRNA	14	H73T	-	-	-	-	-	-
	8	MA83	-	-	-	+/-	-	-		15	HD4	-	-	-	+/-	-	-
GRAd(AE)+S-2P+mRNA	8	DGW4	-	-	-	-	-	-	GRAd(AE)+S-2P+mRNA	14	DGR7	-	-	-	+/-	+/-	-
	9	DHGX	-	-	-	++	+/-	++		15	DGC8	-	-	-	-	-	+
Controls	8	MD17	-	+	+	-	++	++	Controls	14	36890	-	-	-	-	+	-
	8	H83X	-	-	-	+/-	++	+/-		14	H46Y	-	-	-	+	-	+/-
	9	HiF	-	+/-	-	+	++	+/-		15	0J2	-	-	-	-	+/-	-
	9	31930	+/-	-	-	+++	-	-		15	MA74	-	-	-	-	-	-

Figure S4

Figure S4. Viral antigen and pathology in the lung after challenge, related to Figure 1.

(A and B) 2 NHP per group were euthanized on day 8 or 9 and 14 or 15 following challenge and tissue sections taken from the lung.

(A) Top: Hematoxylin and eosin stain illustrating the extent of inflammation and cellular infiltrates. Bottom: Representative images indicating detection of SARS-CoV-2 N antigen by immunohistochemistry with a polyclonal anti-N antibody. Antigen-positive foci are marked by a red arrow. Images at 10x magnification with black bars for scale (100 μ m).

(B) SARS-CoV-2 antigen and inflammation scores in the left caudal lobe (Lc), right middle lobe (Rmid), and right caudal lobe (Rc) of the lung at days 8 or 9, and the left cranial lobe (Lc), right middle lobe (Rmid), and right cranial lobe (Rc) of the lung at days 14 or 15. Antigen scoring legend: – no antigen detected; +/- rare to occasional foci; + occasional to multiple foci; ++ multiple to numerous foci; +++ numerous foci. Inflammation scoring legend: – absent to minimal inflammation; +/- minimal to mild inflammation; + mild to moderate inflammation; ++ moderate-to-severe inflammation; +++ severe inflammation. Horizontal rows correspond to individual NHP.

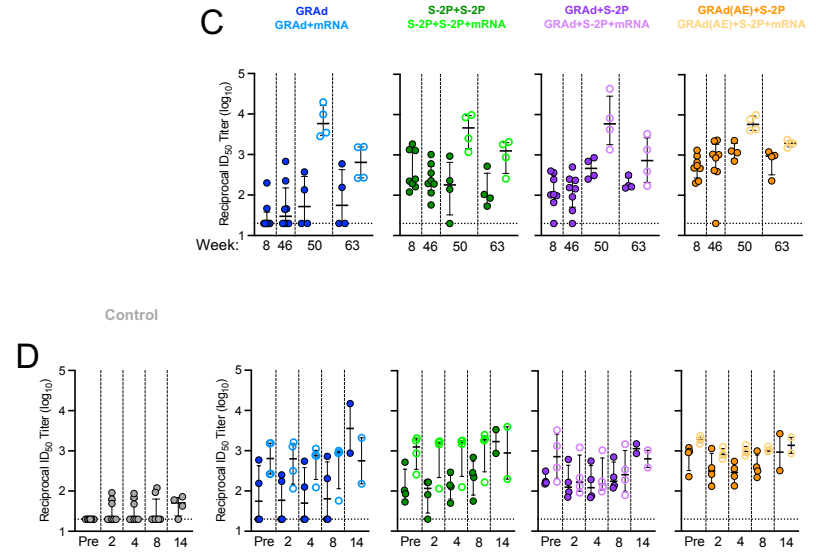
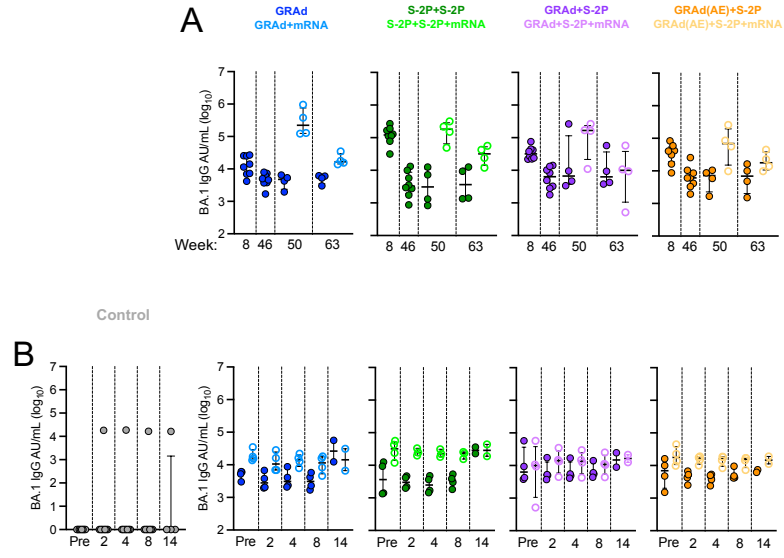


Figure S5

Figure S5. BA.1 binding and neutralization titers in serum pre-challenge and post-challenge, related to Figure 3.

(A and C) Sera were collected at week 8, 46, 50 and 63.

(B and D) Sera were collected at days 2, 4, 8 and 14 following challenge with BA.5.

(A) IgG-binding titers to BA.1 S expressed in AU/mL pre-challenge.

(B) IgG-binding titers to BA.1 S expressed in AU/mL post-challenge.

(C) Neutralizing titers to BA.1 lentiviral pseudovirus expressed as the reciprocal ID₅₀ pre-challenge.

(D) Neutralizing titers to BA.1 lentiviral pseudovirus expressed as the reciprocal ID₅₀ post-challenge.

Circles (A–D) represent individual NHP. Error bars represent the interquartile range with the median denoted by a horizontal black line. Assay limit of detection indicated by a horizontal dotted line which may fall below the depicted range. Vertical dashed lines are for visualization purposes only. Eight immunized NHP, split into 2 cohorts of 4 NHP post mRNA boost. Eight control NHP (4 at day 14), 8 immunized NHP at week 8 and 46, 4 immunized NHP at week 50 and 63, 4 immunized NHP at days 2, 4 and 8, and 2 immunized NHP at day 14.

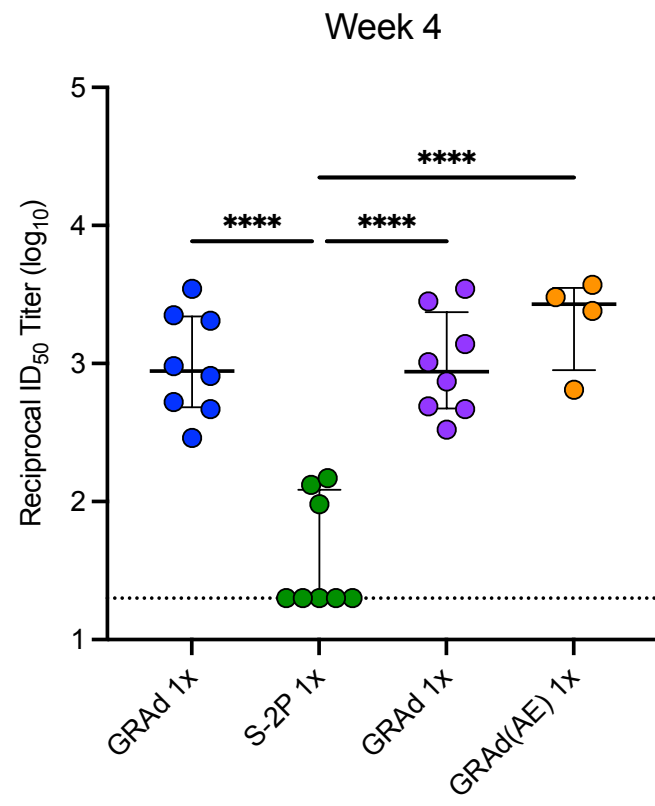
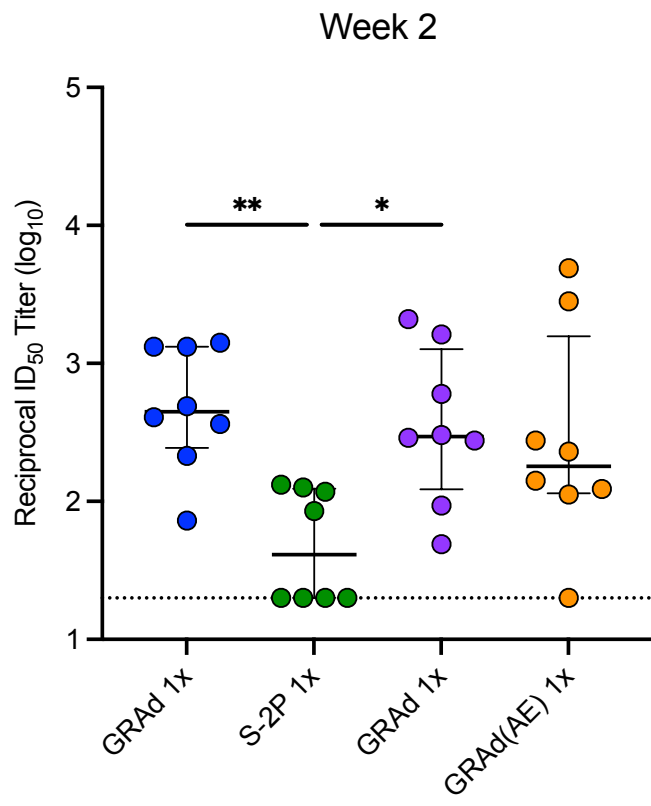


Figure S6

Figure S6. D614G neutralization titers in serum at week 2 and 4, related to Figure 3.

Sera were collected at week 2 and 4. Neutralizing titers to ancestral D614G lentiviral pseudovirus expressed as the reciprocal ID₅₀.

Circles represent individual NHP. Error bars represent the interquartile range with the median denoted by a horizontal black line. Assay limit of detection indicated by a horizontal dotted line. Eight immunized NHP (except for week 4 GRAd(AE) 1x, only 4 out of the 8 NHP were not bled at this timepoint due to blood sampling limits). Statistical analysis shown for corresponding timepoint between groups. * $p < 0.05$, ** $p < 0.01$, **** $p < 0.0001$.

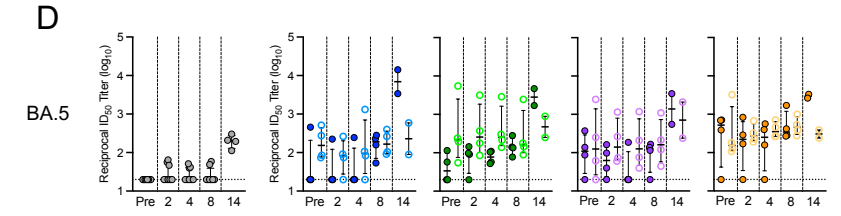
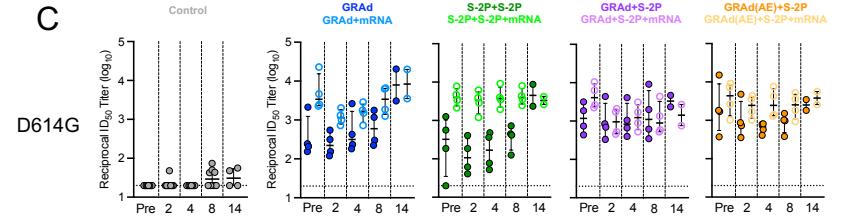
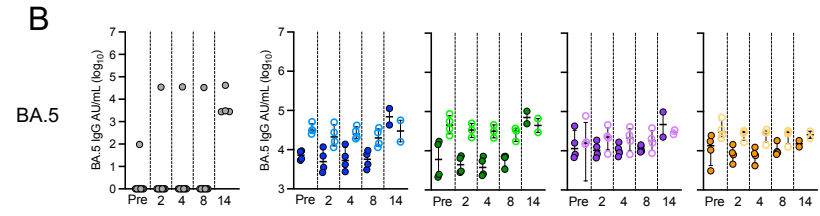
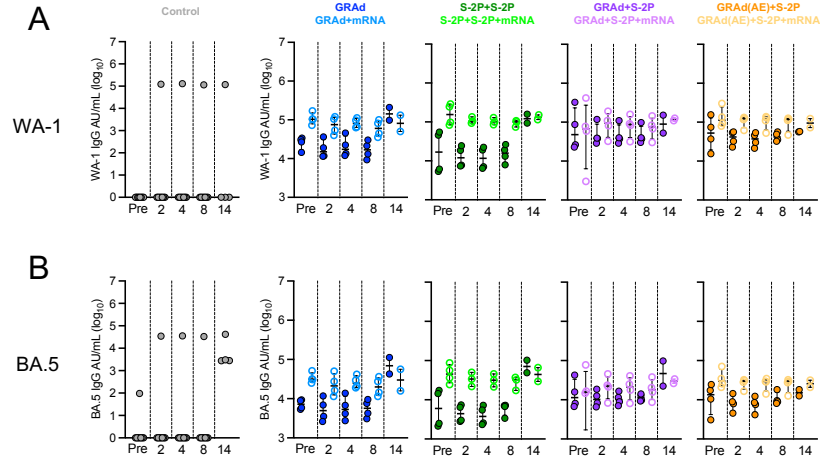


Figure S7

Figure S7. WA-1 or D614G and BA.5 binding and neutralization titers in serum following challenge, related to Figure 3.

(A–D) Sera were collected at days 2, 4, 8 and 14 following challenge with BA.5.

(A and B) IgG-binding titers to WA-1 and BA.5 S expressed in AU/mL post-challenge.

(C and D) Neutralizing titers to WA-1 and BA.5 lentiviral pseudovirus expressed as the reciprocal ID₅₀ post-challenge.

Circles (A–D) represent individual NHP. Error bars represent the interquartile range with the median denoted by a horizontal black line. Assay limit of detection indicated by a horizontal dotted line which may fall below the depicted range. Vertical dashed lines are for visualization purposes only. Eight immunized NHP, split into 2 cohorts of 4 NHP post mRNA boost. Eight control NHP (4 at day 14), 8 immunized NHP at week 8 and 46, 4 immunized NHP at week 50 and 63, 4 immunized NHP at days 2, 4 and 8, and 2 immunized NHP at day 14.

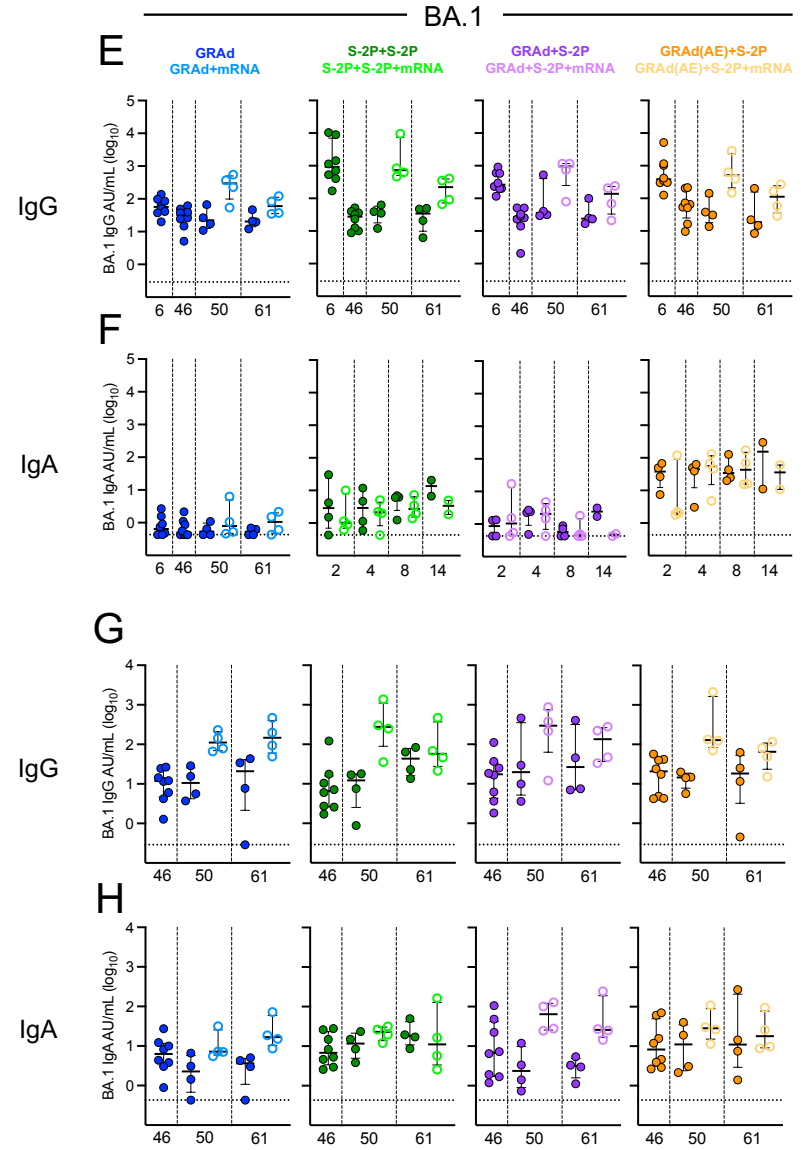
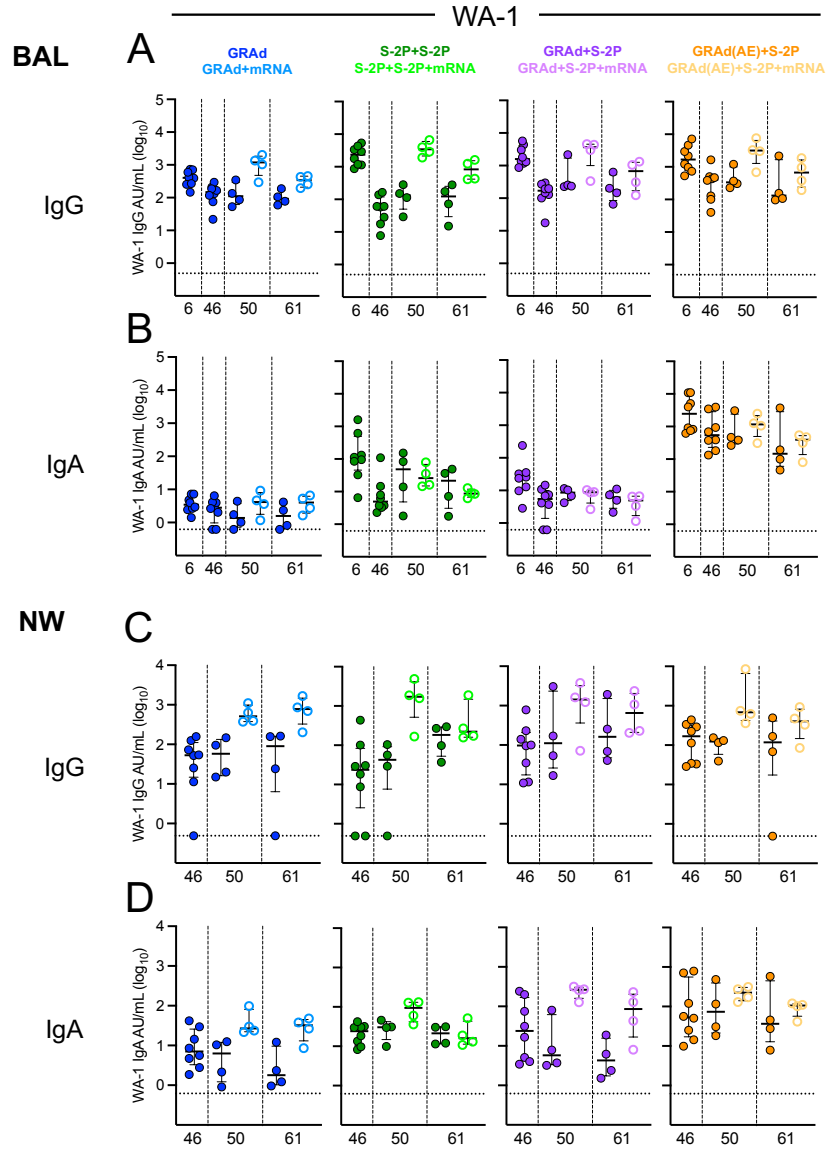


Figure S8

Figure S8. WA-1 and BA.1 IgG and IgA binding titers in BAL and NW prior to challenge, related to Figure 4.

(A–H) BAL (A and B) was collected at week 6, 46, 50 and 61 and NW (C and D) was collected at week 46, 50, and 61.

(A and B) IgG (A) and IgA (B) antibody binding titers to WA-1 expressed in AU/mL in BAL.

(C and D) IgG (C) and IgA (D) antibody binding titers to WA-1 expressed in AU/mL in NW.

(E and F) IgG (A) and IgA (B) antibody binding titers to BA.1 expressed in AU/mL in BAL.

(G and H) IgG (C) and IgA (D) antibody binding titers to BA.1 expressed in AU/mL in NW.

Circles (A–G) represent individual NHP. Error bars represent the interquartile range with the median denoted by a horizontal black line. Assay limit of detection indicated by a horizontal dotted. Vertical dashed lines are for visualization purposes only. Eight vaccinated NHP, split into 2 cohorts of 4 NHP post mRNA boost. Eight immunized NHP at week 6 and 46, 4 immunized NHP at week 50 and 61.

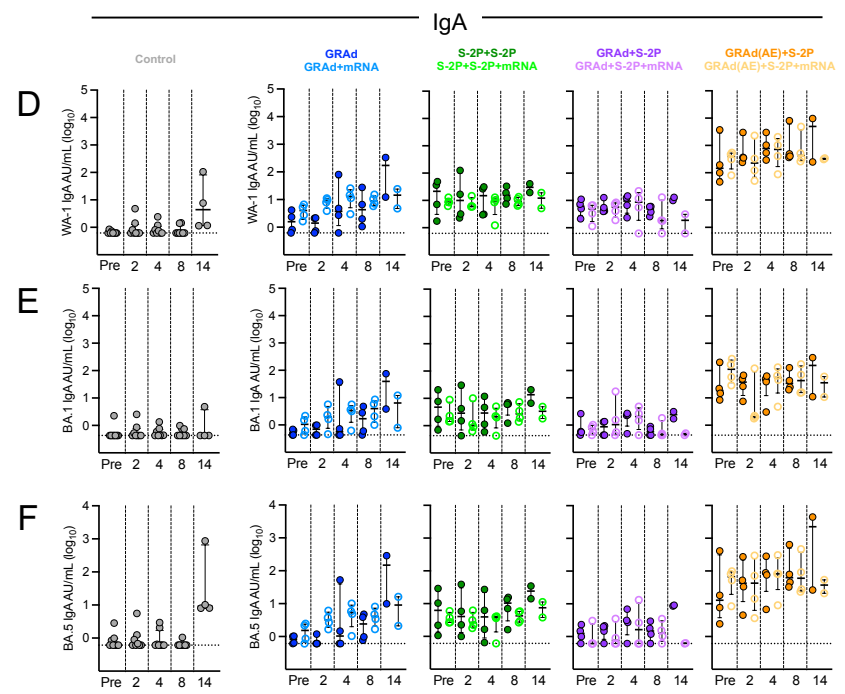
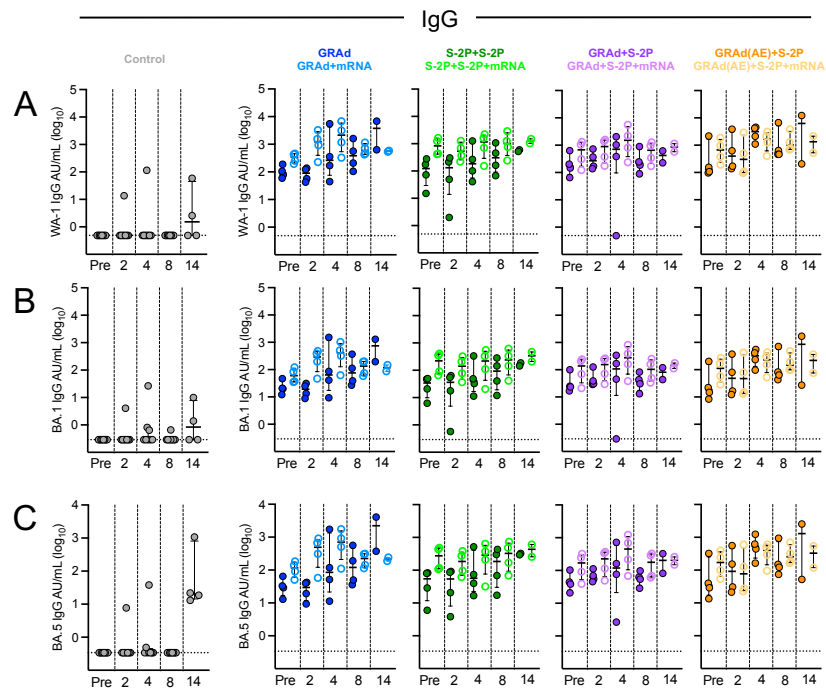


Figure S9

Figure S9. IgG and IgA binding titers in BAL following challenge, related to Figure 4.

(A–F) BAL was collected at days 2, 4, 8 and 14 following challenge.

(A–C) IgG antibody binding titers to WA-1 (A), BA.1 (B) and BA.5 (C) expressed in AU/mL in BAL.

(D–F) IgA antibody binding titers to WA-1 (A), BA.1 (B) and BA.5 (C) expressed in AU/mL in BAL.

Circles (A–F) represent individual NHP. Error bars represent the interquartile range with the median denoted by a horizontal black line. Assay limit of detection indicated by a horizontal dotted line. Vertical dashed lines are for visualization purposes only. Eight vaccinated NHP, split into 2 cohorts of 4 NHP post mRNA boost. Eight control NHP (4 at day 14), 4 immunized NHP at days 2, 4 and 8, 2 immunized NHP at day 14. For reference, the week 61 BAL IgG or IgA titer was included in the graphs as “pre”.

Figure S10. IgG and IgA binding titers in NW following challenge, related to Figure 4.

(A–F) NW was collected at days 2, 4, 8 and 14 following challenge.

(A–C) IgG antibody binding titers to WA-1 (A), BA.1 (B) and BA.5 (C) expressed in AU/mL in NW.

(D–F) IgA antibody binding titers to WA-1 (A), BA.1 (B) and BA.5 (C) expressed in AU/mL in NW.

Circles (A–F) represent individual NHP. Error bars represent the interquartile range with the median denoted by a horizontal black line. Assay limit of detection indicated by a horizontal dotted line. Vertical dashed lines are for visualization purposes only. Eight vaccinated NHP, split into 2 cohorts of 4 NHP post mRNA boost. Eight control NHP (4 at day 14), 4 immunized NHP at days 2, 4 and 8, 2 immunized NHP at day 14. For reference, the week 61 NW IgG or IgA titer was included in the graphs as “pre”.

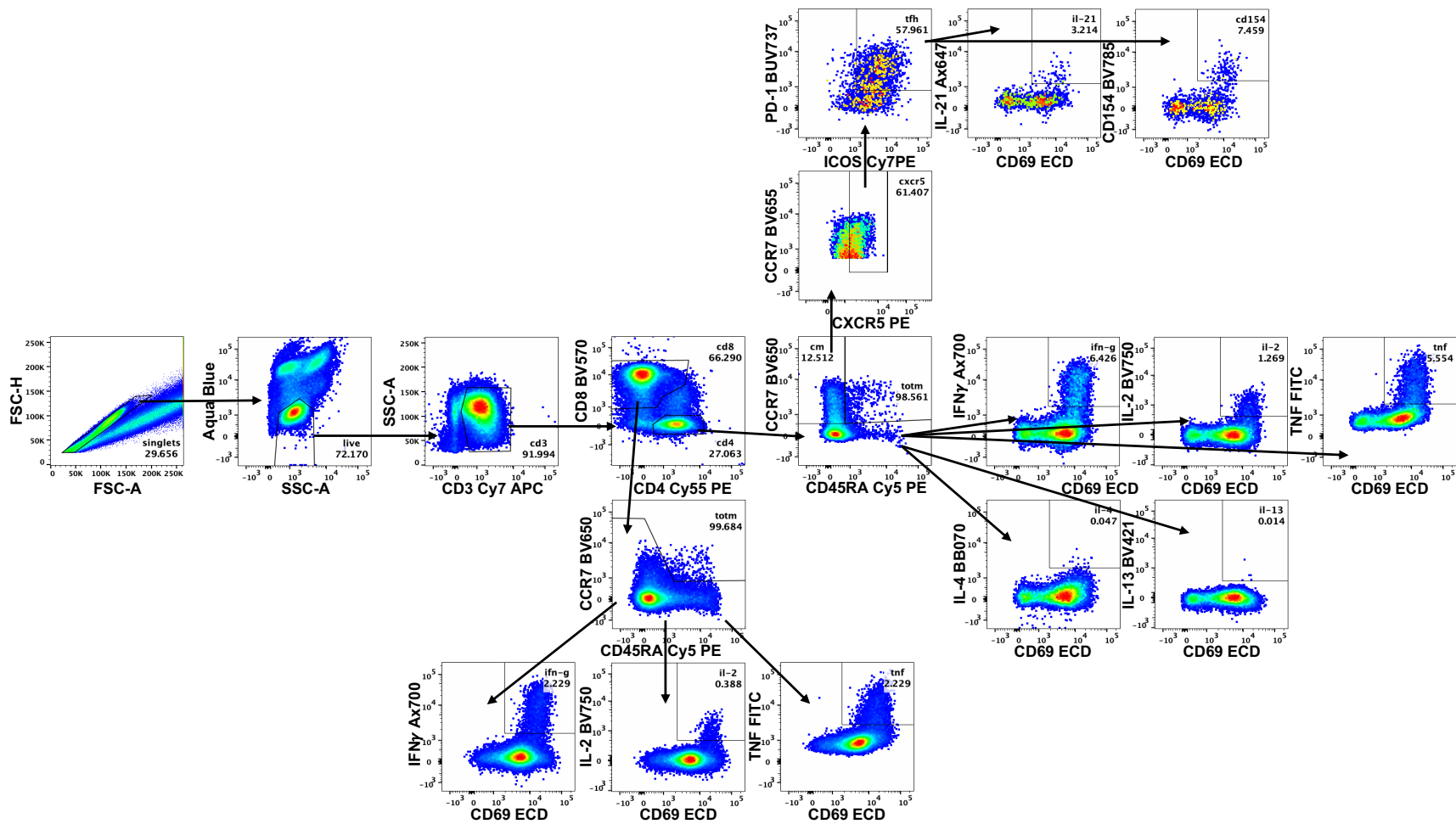


Figure S11

Figure S11. T cell gating strategy, related to Figure 5.

Representative flow cytometry plots showing gating strategy for T cells in Figures 5, S11 and S12. Cells were gated as singlets and live cells on forward and side scatter and a live/dead aqua blue stain. CD3⁺ events were gated as CD4⁺ or CD8⁺ T cells. Total memory CD8⁺ T cells were selected based on expression of CCR7 and CD45RA, and SARS-CoV-2 S-specific memory CD8⁺ T cells were gated according to co-expression of CD69 and IL-2, TNF or IFN γ . The CD4⁺ events were defined as naive, total memory, or central memory according to expression of CCR7 and CD45RA, and CD4⁺ cells with a T_h1 phenotype were defined as memory cells that co-expressed CD69 and IL-2, TNF or IFN γ . CD4⁺ cells with a T_h2 phenotype were defined as memory cells that co-expressed CD69 and IL-4 or IL-13. T_{fh} cells were defined as central memory CD4⁺ T cells that expressed CXCR5, ICOS, and PD-1. T_{fh} cells were further characterized as IL-21⁺ and CD69⁺ or CD40L⁺ (CD154) and CD69⁺.

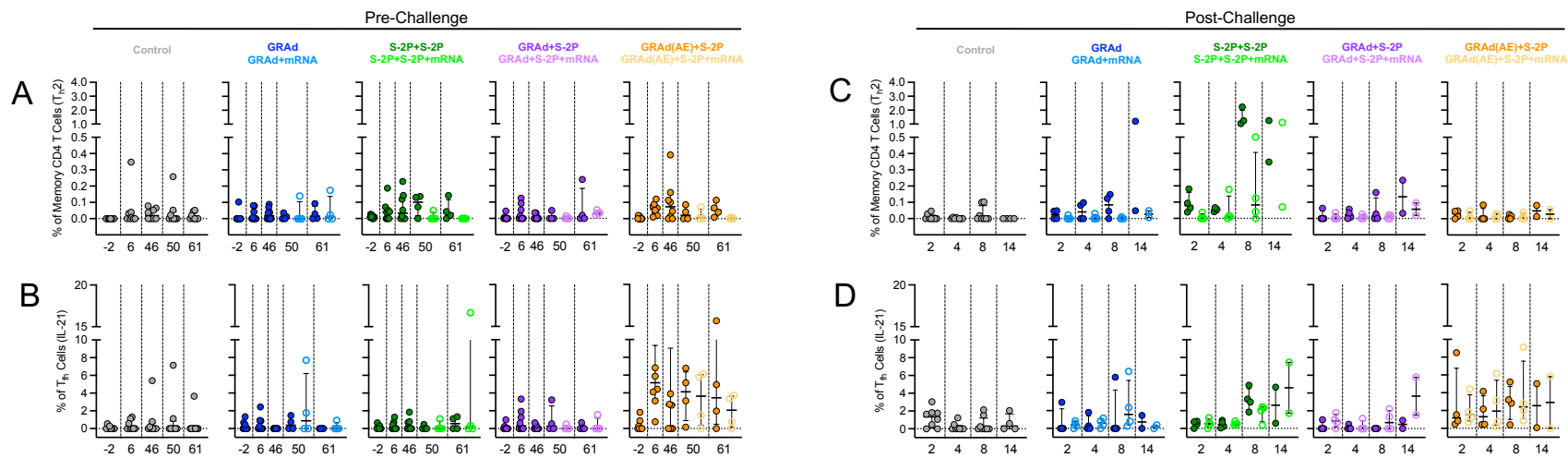


Figure S12

Figure S12. T_h2 and IL-21+ T_{fh} cells in BAL, related to Figure 5.

(A–B) BAL was collected at week -2, 6, 46, 50 and 61. Cells were stimulated with SARS-CoV-2 S1 and S2 peptide pools (WA1) and then measured by intracellular cytokine staining.

(C–D) BAL was collected at days 2, 4, 8, 50 and 14 following challenge. Cells were stimulated with SARS-CoV-2 S1 and S2 peptide pools (WA-1) and then measured by intracellular cytokine staining.

(A, C) Percentage of memory CD4+ T cells with T_h2 markers (IL-4 or IL-13) following stimulation.

(B, D) Percentage of T_{fh} cells that express IL-21.

Circles in (A–D) indicate individual NHP. Error bars represent the interquartile range with the median denoted by a horizontal black line. Dotted lines set at 0%. Reported percentages may be negative due to background subtraction and may extend below the range of the y axis. Eight vaccinated NHP, split into 2 cohorts of 4 NHP post mRNA boost. Eight control NHP at days 2, 4 and 8, four at day 14.

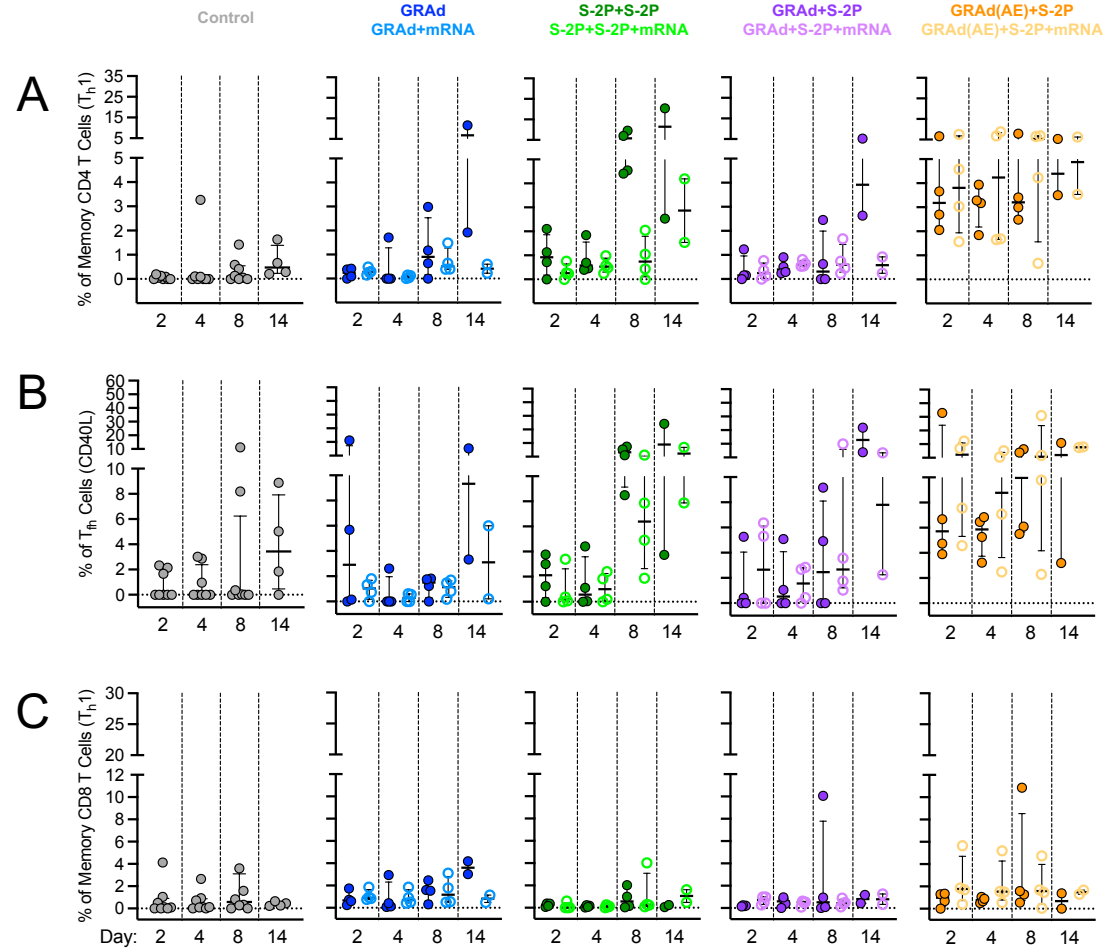


Figure S13

Figure S13. T cell in BAL following challenge, related to Figure 5.

(A–C) BAL was collected at days 2, 4, 8 and 14 following challenge. Cells were stimulated with SARS-CoV-2 S1 and S2 peptide pools (WA-1) and then measured by intracellular cytokine staining.

(A) Percentage of memory CD4⁺ T cells with Th1 markers (IL-2, TNF, or IFN γ).

(B) Percentage of T_{fh} cells that express CD40L.

(C) Percentage of CD8 T cells expressing IL-2, TNF, or IFN γ .

Circles in (A–D) indicate individual NHP. Error bars represent the interquartile range with the median denoted by a horizontal black line. Dotted lines set at 0%. Reported percentages may be negative due to background subtraction and may extend below the range of the y axis. Eight vaccinated NHP, split into 2 cohorts of 4 NHP post mRNA boost. Eight control NHP (4 at day 14), 4 immunized NHP at days 2, 4 and 8, 2 immunized NHP at day 14.

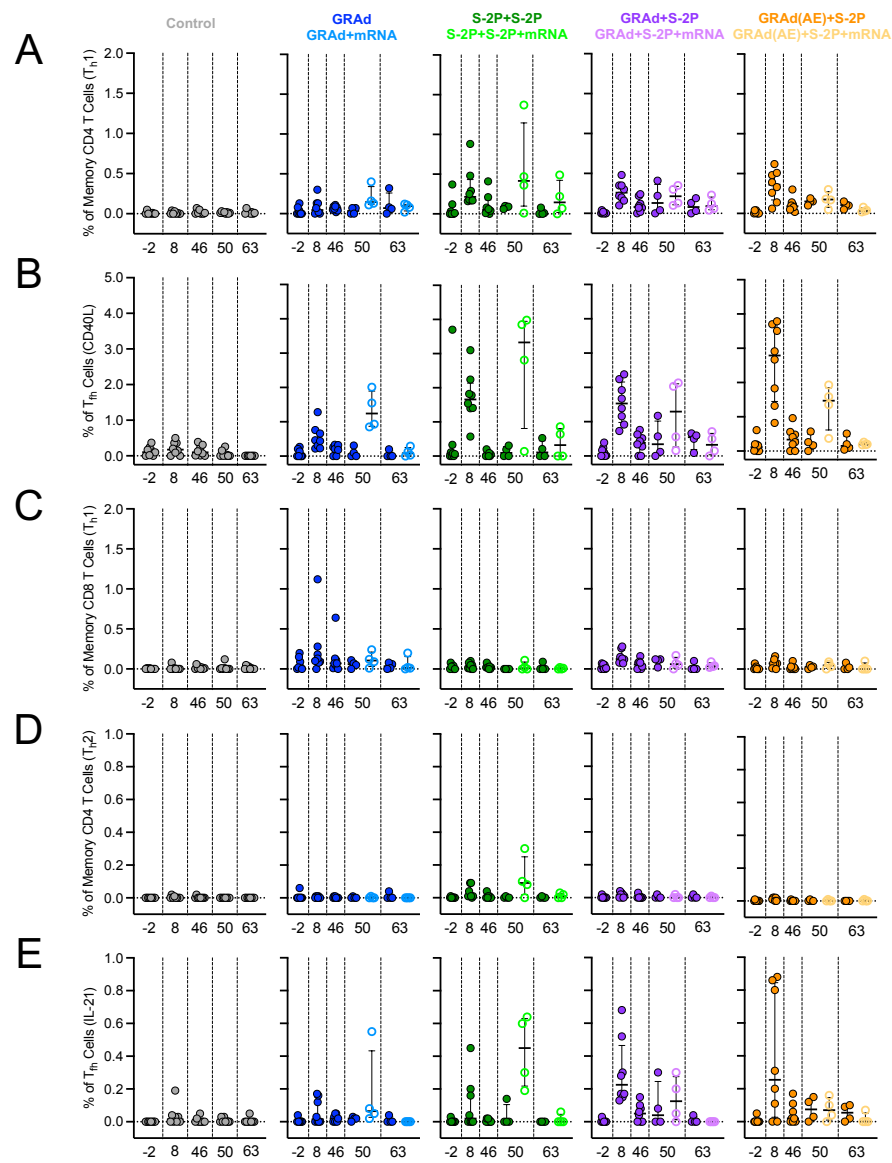


Figure S14

Figure S14. T cell in blood prior to challenge, related to Figure 5.

(A–E) Peripheral blood mononuclear cells (PBMCs) were collected at week -2, 8, 46, 50 and 63. Cells were stimulated with SARS-CoV-2 S1 and S2 peptide pools (WA-1) and then measured by intracellular cytokine staining.

(A) Percentage of memory CD4⁺ T cells with Th1 markers (IL-2, TNF, or IFN γ).

(B) Percentage of T_{fh} cells that express CD40L.

(C) Percentage of CD8 T cells expressing IL-2, TNF, or IFN γ .

(D) Percentage of memory CD4⁺ T cells with T_h2 markers (IL-4 or IL-13).

(E) Percentage of T_{fh} cells that express IL-21.

Circles in (A–E) indicate individual NHP. Error bars represent the interquartile range with the median denoted by a horizontal black line. Dotted lines set at 0%. Reported percentages may be negative due to background subtraction and may extend below the range of the y axis. Eight vaccinated NHP, split into 2 cohorts of 4 NHP post mRNA boost. Eight control NHP at days 2, 4 and 8, four at day 14.

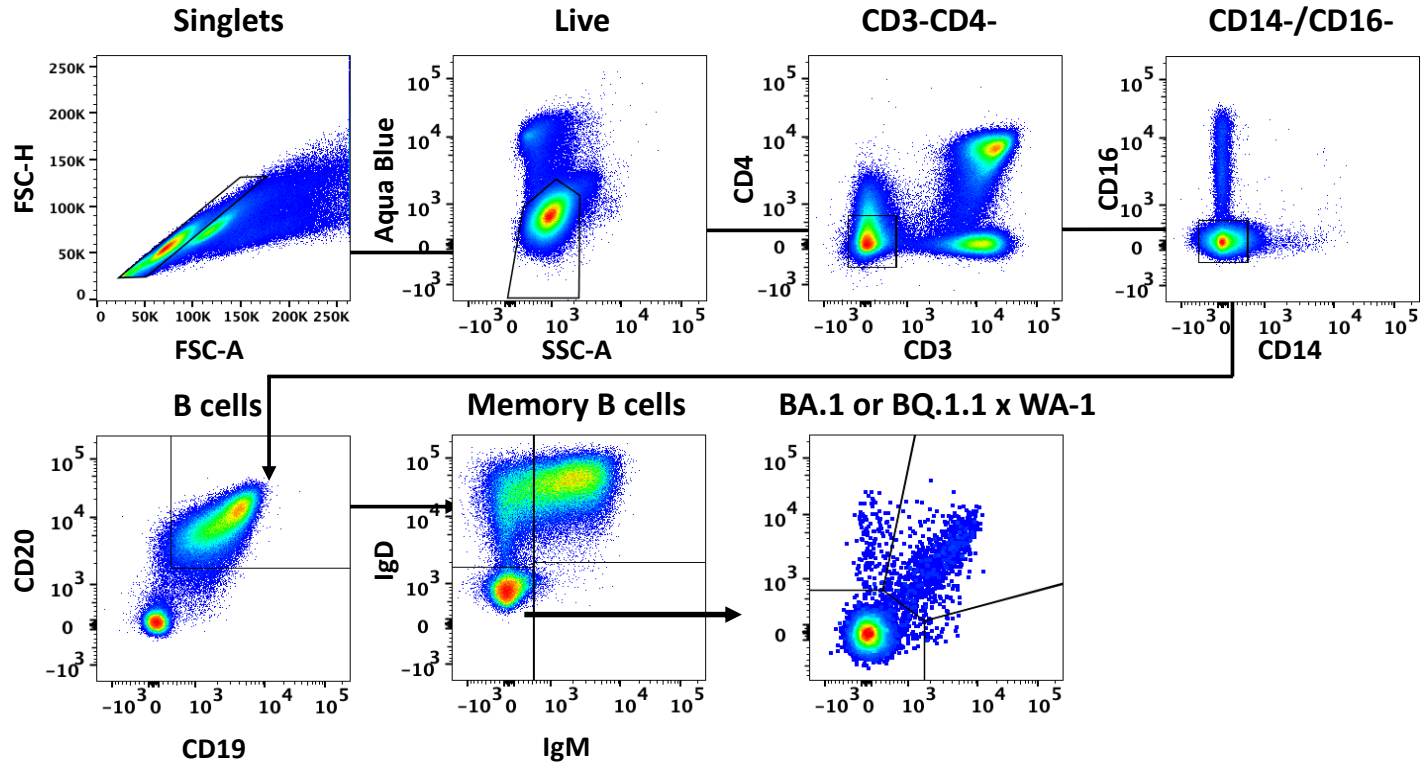


Figure S15

Figure S15. B cell gating strategy, related to Figure 6.

Representative flow cytometry plots showing gating strategy for B cells in Figures 6 and S16. Cells were gated as singlets and live cells on forward and side scatter and a live/dead aqua blue stain. CD3-, CD4-cells were then gated on absence of CD14 and CD16 expression and positive expression of CD20 and CD19. Memory B cells were selected based on lack of IgD or IgM. Finally, memory B cells of variant S-2P (WA-1 and BA.5 or WA-1 and BQ.1.1) probes were used to determine binding specificity.

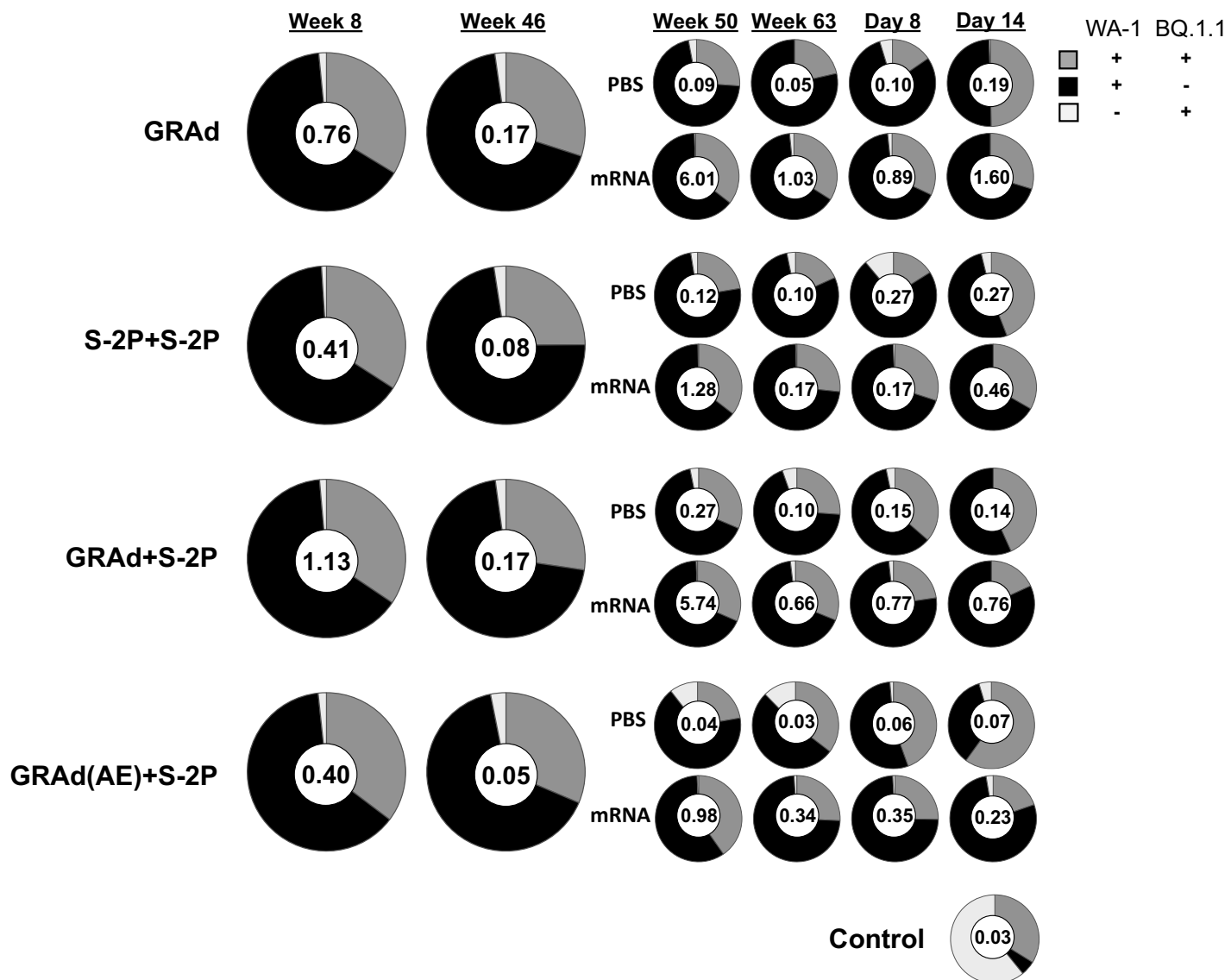


Figure S16

Figure S16: WA-1 and BQ.1.1 cross-reactive S-2P specific memory B cells following immunization, related to Figure 6.

Pie charts indicate the frequency (numbered circle at the center) and proportion of total S-binding memory B cells that are dual specific for WA-1 and BQ.1.1 (dark gray), specific for WA-1 (black), or specific for BQ.1.1 (light gray) for all NHP in each group and timepoint at week 8, 46, 50 and 63 post-immunization, and days 8 and 14 post-challenge. Seven or eight NHP per group at week 8 and 46, 3-4 NHP per group at week 50 and 63, and day 8, 1-2 NHP at day 14.